Journal of Engineering and Technology

of The Open University of Sri Lanka

Volume 10 No. 01 March 2022 ISSN 2279-2627

JET – OUSL | Faculty of Engineering Technology

JET- OUSL

The Journal of Engineering and Technology of the Open University of Sri Lanka is a peer-reviewed journal, published biannually by the Faculty of Engineering Technology of the Open University of Sri Lanka.

Scope
The journal accepts only original research articles based on theoretical and applied research in all aspects of Engineering and Technology specializations.

Research Articles
Articles are full length papers presenting complete description of original research or technological achievements. Statements and opinions expressed in all the articles of this Journal are those of the individual contributors and the Editorial Boards of the Faculty of Engineering Technology of the Open University of Sri Lanka do not hold the responsibility of such statements and opinions.

Peer Review Policy
The practice of peer review is to ensure that only good knowledge is published. It is an unbiased process at the good scholarly publishing and is carried out by all reputable scientific journals. Our referees play a vital role in maintaining the high standards and all manuscripts are peer reviewed following the procedure outlined below.

Initial Manuscript Evaluation
The Editor first evaluates all manuscripts. Manuscripts rejected at this stage are not sufficiently original or are outside the aims and scope of the journal. Those that meet the minimum criteria are normally passed on to at least 2 experts for review.

Type of Peer Review
JET-OUSL employs double blind reviewing, where both the referee and author remain anonymous throughout the process. Referees are matched to the paper according to their expertise preferably from outside of the Open University of Sri Lanka.

Referee Reports
Referees are asked to evaluate whether the manuscript is original, methodologically sound, ethically sound, clearly presented results followed by discussion and conclusions with correct references of preceding relevant work. Referees are provided with a structured form along with the manuscript for constructive comments. Language correction is not part of the peer review process, but referees may suggest corrections to the manuscript.

Printer at The Open University Press
ISSN 2279-2627
Published in March 2022

Journal of Engineering and Technology

of the Open University of Sri Lanka

Volume 10 No. 01 March 2022 ISSN 2279-2627

Editorial / Correspondences

All correspondences including manuscripts for submissions should be addressed to:

Editor in Chief – Journal of Engineering and Technology
Faculty of Engineering Technology
The Open University of Sri Lanka
Nawala, Nugegoda
Sri Lanka
Email: bcliy@ou.ac.lk, Telephone: +94112881111

Contents

Volume 10 No. 01 March 2022 ISSN 2279-2627

Harnessing Geothermal Energy in Sri Lanka: A Feasibility Study

K.G.G.R.R. Abewickrama[1], R.H.G. Sasikala[2*]
[1'2]Department of Electrical and Computer Engineering, The Open University of Sri Lanka, Nawala, Nugeoda, Sri Lanka.

*Corresponding Author: email: rhsas@ou.ac.lk, Tele: +94715186953

Abstract – *Sri Lanka needs advanced technological power generation methods to face future electricity requirements when considering the present energy crisis in the country. As a gift of nature, several hot water springs occur in Sri Lanka, and these are the only geothermal manifestation seen in the country. Geothermal energy resource is one of the renewable resources which is still an unfamiliar energy source for the country. In this research the feasibility of power generation using existing geothermal resources in Sri Lanka is carried out including location selection, capacity estimation, plant design, and economic analysis for a geothermal power plant. Location selection is mainly based on geochemical and geophysical data, and the selected geothermal source must have an exploitable amount of heat at accessible depth. Four areas were analyzed to select the best location which has indicated maximum hot water temperatures from all other hot water spring areas. The volumetric assessment method is used to estimate the power generating capacity in a selected location. This research also includes the design of the plant layout with the most suitable power plant technology. An economic analysis of the power plant has also been presented. Volumetric method results indicate that the reservoir could produce 3.1 MW to 8.3 MW power for 130ºC to 70ºC reinjection temperatures respectively. Economic analysis results obtained that the Levelized cost of the energy lies between 73.34 Rs/kWh to 39.04 Rs/kWh for 130ºC to 70ºC reinjection temperatures.*

Keywords*: Geophysical data, geothermal manifestation, levelized cost of the energy, reinjection temperatures, volumetric assessment*

1 INTRODUCTION

Sri Lanka is facing an energy crisis due to increasing energy demand day by day due to the growth of industrial and household energy requirements. The country's potential for hydroelectric power generation has already been largely exploited. With the ever-growing demand for power and energy in Sri Lanka, the country is increasingly becoming dependent on thermal sources, importing petroleum products mainly from oil-producing countries. These finite resources are rapidly depleting and make a considerable contribution to environmental pollution while increase the unit cost of electricity generation. Hence, an environmentally friendly, pollution-free, renewable energy source is very important to face future energy requirements.

Geothermal energy resources are one of the renewable resources in Sri Lanka which have been manifested as 10 low enthalpy thermal springs along a narrow belt that runs approximately parallel to the Highland complex (HC) and Vijayan complex (VC) lithological boundary. These hot springs are only used for bathing and no economic value from those except some of these places being visited by tourists. Medical bathing is popular at the Mahapelessa spring (Mangala and Wijetilake, 2011; Bandara, et al., 2019).

This research focuses on finding the feasibility of geothermal power generation from an available hot spring in Sri Lanka. The three main factors that should be considered to find the feasibility of power generation are the geothermal source, power generating capacity, and the total cost of the project. A geothermal source must have an exploitable amount of heat at accessible depth and the power generating capacity should be in a feasible range to minimize the total cost of the project. The main objective of this research is to explore the possibility of power generation using existing geothermal reservoirs in the country and find its technical and economic feasibility.

In this study several hot springs in HV and VC lithological boundaries were studied as geothermal sources. Spring temperatures were estimated to find a suitable location while considering other factors for location selection. A volumetric method is proposed to estimate the geothermal energy capacity of the reservoir. Due to the uncertainty inherent in many of the required parameters used in the volumetric method, Monte Carlo simulation was used to define a probability distribution for these variables. Power generation technology and power plant equipment were selected according to estimated power generation capacities, reservoir temperature, and depth. The Levelized Cost of Energy (LCOE) for the estimated power generation was calculated to find the economic feasibility of the project.

2 LITERATURE REVIEW

Until 20th century geothermal resources were used primarily for leisure purposes such as hot springs for geothermal baths. At the beginning of the 20th century, active exploitation of geothermal resources for electricity supply purposes was inaugurated. Successful production of electricity from geothermal heat was first achieved in Larderello, Italy, in 1904. But first commercial use of that technology occurred there in 1913 with the construction of a 250-kW capacity power plant where the generator was powered by the natural steam erupting from the earth.

In the year of 1920, many experimental generators were introduced in Beppu, Japan, and the Geysers, California, but Italy was the world's only industrial producer of geothermal electricity until 1958. In 1985 world second successful geothermal power plant was built in Wairakei in New Zealand which used flash steam technology at first. In 1960, Pacific Gas and Electric began the first successful geothermal electric power station in the United States at the Geysers in California which produced 11 MW.

The first binary cycle power started in Soviet Russia in 1967 and United States in 1981. This technology allows the use of much lower temperature resources than were previously recoverable. In 2006 Chena Hot Springs, Alaska started binary cycle plant which uses very low fluid temperature of 57 °C (135 °F) to generate electricity.

By 2015 more than 80 countries were using geothermal energy, either directly or in conjunction with geothermal heat pumps (GHP), China, Turkey, Iceland, Japan, Hungary, and the United States. The total worldwide installed capacity for direct use in 2015 was about 12635 MW utilizing about 73549 GWh per year (Max, Romanelli and Hussain, 2015 ; Moghtaderi, Zhou and Doroodchi, 2019 ; *Geothermal Power*, anon, 2017; Bertani, 2016 ; Serpen, Korkmaz and Satman, 2008)

3 METHODOLOGY

The literature survey for worldwide projects and geothermal resources in Sri Lanka is a compulsory critical step to finding electricity generation capability using geothermal energy because Sri Lanka is new to this technology. The collection of data to select a

suitable location for the power station and finding the nature of the reservoir is the next step. The capacity of the power plant suitable for the country was determined by suitable plant technology. Then the power plant will be designed, and an economic analysis was done to determine the unit cost.
Relevant data are collected from the Sustainable Energy Authority and the National Institute of Fundamental Studies (NIFS). Lithological information (geophysical and geochemical) about the geothermal potential in Sri Lanka were collected from the department of geology, at the University of Peradeniya to select the best location for a power plant.

A volumetric method was used to estimate the geothermal energy capacity of the reservoir. The volumetric method refers to the calculation of thermal energy in the rock and the fluid which could be extracted based on specified reservoir volume, reservoir temperature, and reference or final temperature. Due to the uncertainty inherent in many of the required parameters used in the volumetric method, Monte Carlo simulation is used to define a probability distribution for these variables. Monté Carlo simulation was done using a Frontier analytic solver to predict the results. Analytic Solver can be used to create and solve Monte Carlo simulation and optimization models in the Microsoft Excel workbook.

4 IDENTIFICATION OF A SUITABLE LOCATION

4.1 The current situation in Sri Lanka

In Sri Lanka, Geothermal Energy has been manifested as 10 low enthalpy thermal springs along a narrow belt that runs approximately parallel to the Highland complex (HC) and Vijayan complex (VC) lithological boundary (Samaranayake, et al., 2015). They are located mostly in the eastern part of Sri Lanka as shown in Fig.1.

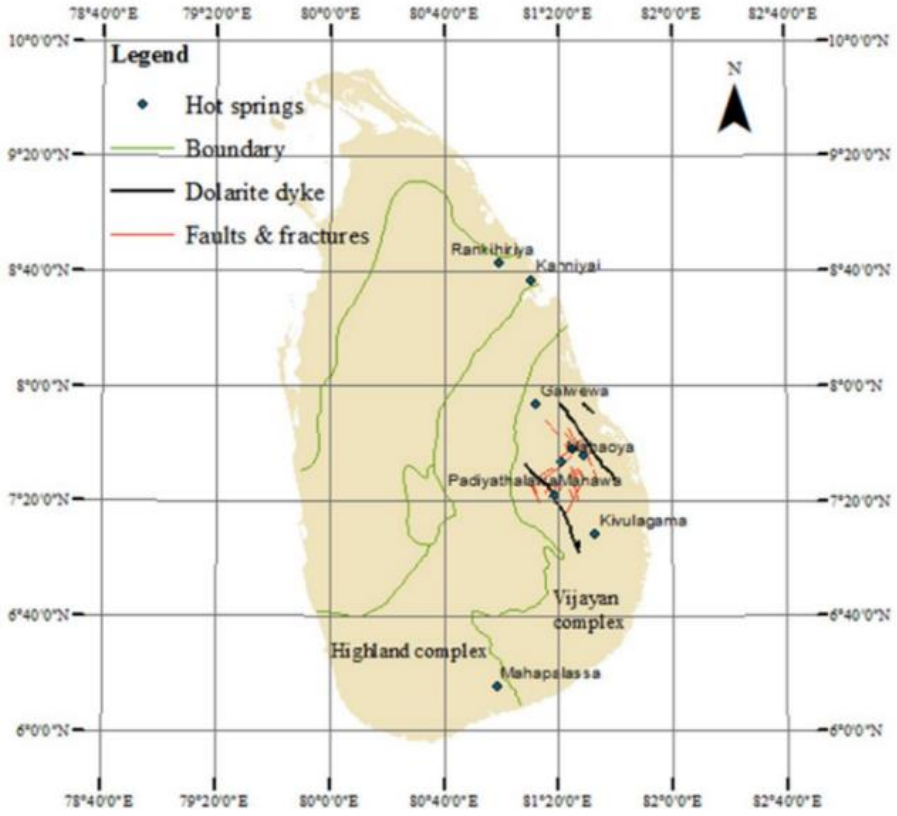

Fig. 1. Locations of hot water springs in Sri Lanka (Samaranayake, et al., 2015)

In the world, generally, locations near places with volcanic activity, places with geysers, and hot water springs are potential geothermal sites. Sri Lanka is situated far away from an active plate boundary, and there is no volcanic region close to Sri Lanka. In Sri Lanka, the only evidence for geothermal energy is hot water springs as shown in Table 1.

Table 1 Hot water springs and temperatures

Hot water spring	Temperature(°C)
Rankihiriya	-
Kanniya	42
Nelumwewa/Galwewa	61
Mutugalwela	-
Kapurella	70
Maha oya	54
Marangala/padiyathalawa	52

Therefore, there should be a possible location close to this HC and VC boundary line to develop a geothermal power plant. Research work by (Mangala and Wijetilake, 2015) and (Samaranayake, et. al.,2015) revealed that geothermometers indicate the subsurface temperature of the geothermal reservoirs could be between 100°C and 140°C. A potential geothermal energy source was estimated in a geothermal belt with a length of 350 km (length of the hot spring belt), a depth of 2 km, and a width of 2 km (Mangala and Wijetilake, 2015; Bandara, et al., 2019).

4.2 Geothermal exploration methods

Geothermal exploration programs utilize a variety of techniques to identify geothermal reservoirs and information that can point to areas of low density, high porosity, high permeability, and subsurface fault lines that can help define well field development. In this research study, observations of two exploration techniques are used to analyze a suitable location. They are geophysical methods (Magnetotelluric (MT) and Transient Electromagnetic (TEM))and geochemical methods.

This study used measurement data taken from previous research work due to unavailability of resources and limitation of the time for site measurements.

MT and TEM observations including figures used in this study are extracted from the thesis of "Mapping geothermal resources in Sri Lanka", presented by Nuwan Buddika Suriyaarchchi, Postgraduate Institute of Science, University of Peradeniya (Suriyaarachchi, 2017).

Chemical geothermometry is a primary tool used to determine subsurface temperatures of geothermal reservoirs. The input parameters for the geothermometer are the chemical analyses of the water samples of hot springs (Franco and Donatini, 2017). Hence, the accuracy of the subsurface temperatures determined by the chemical geothermometers depends on the chemical analyses accuracy. Silica conductive and theoretically based cation geothermometers are the most appropriate geothermometers for estimating reservoir temperatures of Sri Lanka's low enthalpy geothermal systems.

All geothermometer results including figures used in this study were extracted from the research of "An appropriate deep reservoir temperature estimate for thermal spring systems in the crystalline terrain of Sri Lanka; a comparison of geothermometers"

presented by S.M.P.G.S. Kumara and H.A. Dharmagunawardhane (Kumara and Dharmagunawardhane, 2017).

4.3 Selected areas

In this feasibility study, four areas were selected (namely Kapurella, Padiyathalawa, Mahaoya, and Nelumwewa) for the analysis of the most suitable location among the 10 well-known hot spring locations using geophysical and geochemical observations.

4.3.1 Padiyathalawa hot spring area

There is a hot spring complex located in the Padiyatalawa village, also known as Wahawa/Marangala hot springs. Tanks are built in this hot spring to get the hot water out but only a few are being used. The temperature indication of hot water is 50- 60°C (Samaranayake, et. al., 2015).

According to the MT resistivity profile shown in fig 2, there is a high resistive (>1000Ωm) zone in depth from 500 m to 2000 m. There are two low resistivity (800Ωm) zones that appear at 2000m depth below No 7-sounding pointing and 4500m depth below No 2 sounding site. Middle of these low resistive zones, resistivity values drop further below 50 Ωm (Suriyaarachchi, 2017).

The estimated geothermal reservoir temperatures of Padiyathalawa hot spring are based on the Na/K, K/Mg, and Quartz geothermometers. The reservoir temperature is in between 123°C and 184°C (Kumara and Dharmagunawardhane, 2017).

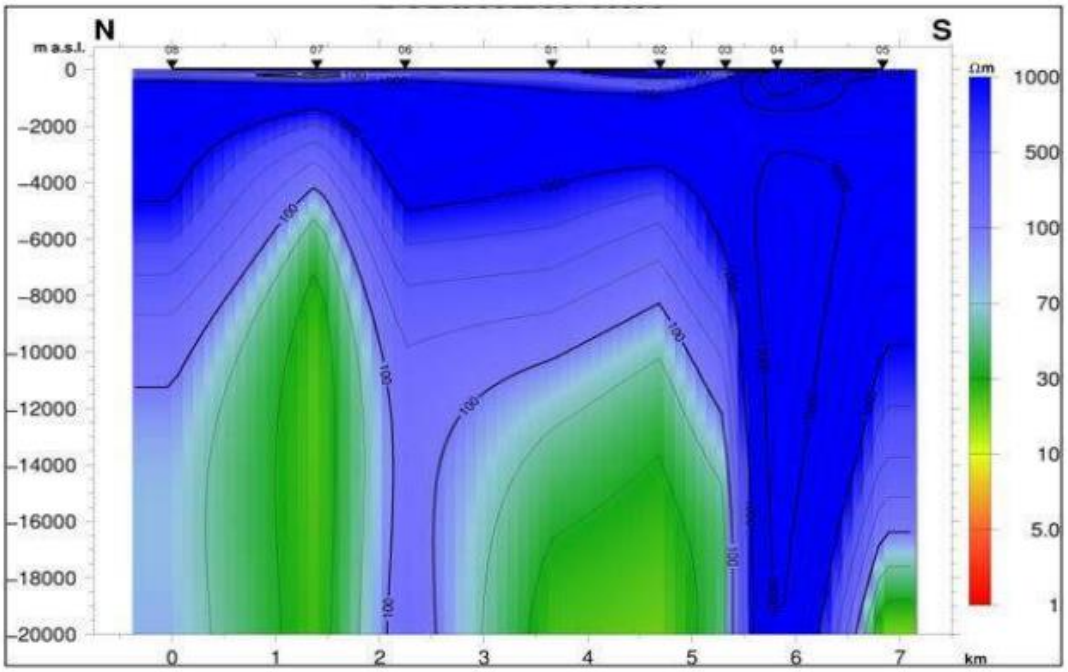

Fig. 2. Resistivity profile up to 20000m depth from MT method, Padiyathalawa hot spring area (Suriyaarachchi, 2017)

4.3.2 Kapurella hot spring area

Kapurella records the highest surface temperature (70 °C) among all Sri Lankan thermal springs. Kapurella hot spring is simply formed along NE to SW direction and the whole area is covered with marshy land vegetation (Ekanayake, et al., n.d.).

According to the MT resistivity profile shown in fig 3, there is a low resistivity zone (600Ωm) that starts to appear below point No 308 and point No 305 at a depth of 1000 m, and it extends further below. The resistivity value of the middle of that zone is 8-30 Ωm. The heat source of the hot spring could be connected to a cooling magmatic source at a depth of 10 Km (Suriyaarachchi, 2017).

The estimated geothermal reservoir temperatures of Kapurella hot springs based on the Na/K, K/Mg, and Quartz geothermometers revealed that reservoir temperature is between 130°C and 203°C (Kumara and Dharmagunawardhane, 2017).

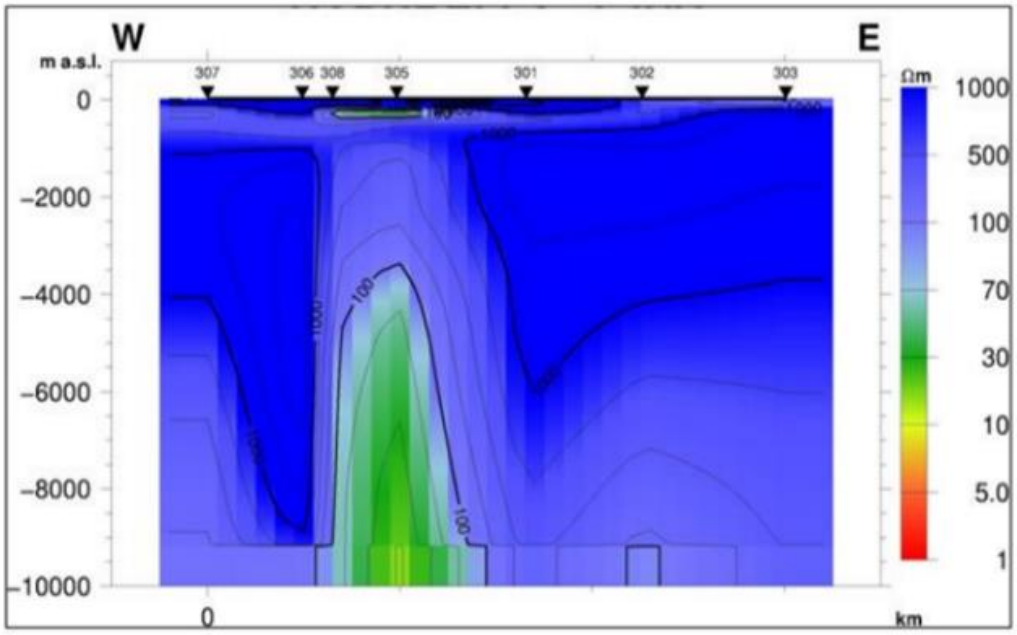

Fig. 3. Resistivity profile up to 10000m depth from MT method, Kapurella hot spring area (Suriyaarachchi, 2017)

4.3.3 Nelumwewa hot spring area

Nelum Wewa Hot spring in Polonnaruwa is the most recent discovery among all other hot springs. The temperature indication of the water is 61°C (Kumara and Dharmagunawardhane, 2014).

According to the TEM resistivity profile shown in fig 4, there are many low resistivity zones under the hot spring area. Because there are two irrigation tanks located close to the thermal water spring. The heat source of the spring is located under the Dimbulagala Mountain as a Hot Dry Rock, and it transfers heat to groundwater through fractures, and it provides a pathway for thermal water to emerge at the surface as the hot spring (Kumara and Dharmagunawardhane, 2014).

The estimated geothermal reservoir temperatures of Nelumwewa hot springs based on the Na/K, K/Mg, and Quartz geothermometers revealed that the reservoir temperature is between 134°C and 204°C (Kumara and Dharmagunawardhane, 2017).

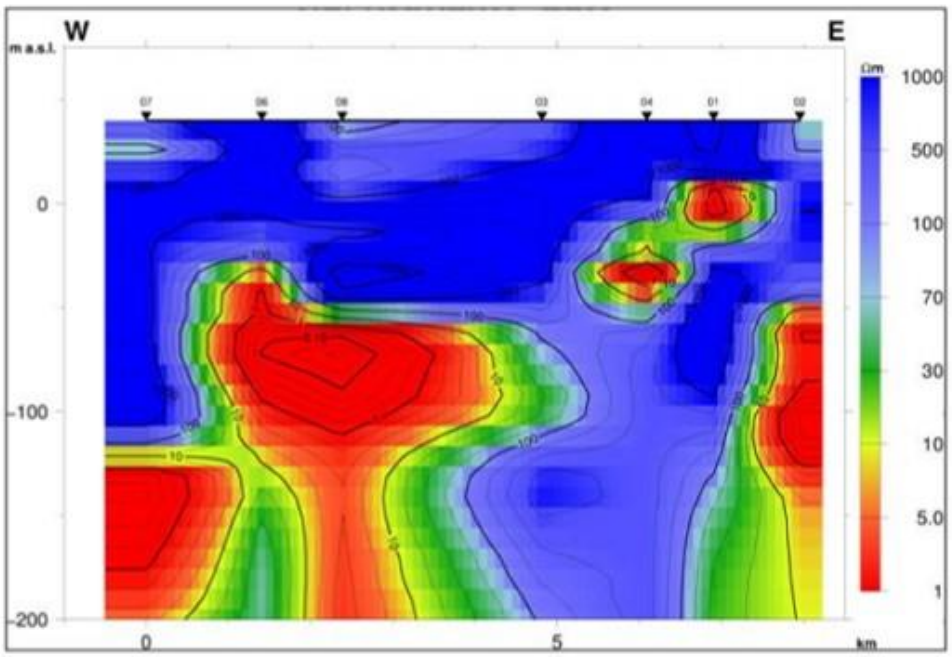

Fig.4. Resistivity profile for shallow depth from TEM method, Nelumwewa hot spring area (Suriyaarachchi, 2017)

4.3.4 Mahaoya hot spring area

There are seven hot water wells in the Maha Oya Hot water spring site. The average temperature of the hottest well is about 58°C while the lowest is 38°C (Kumara and Dharmagunawardhane, 2017). According to the MT resistivity profile shown in fig 5, there is no evidence of very low resistivity that could be holding water or HDR at accessible depth (Hobbs, et al., 2013).

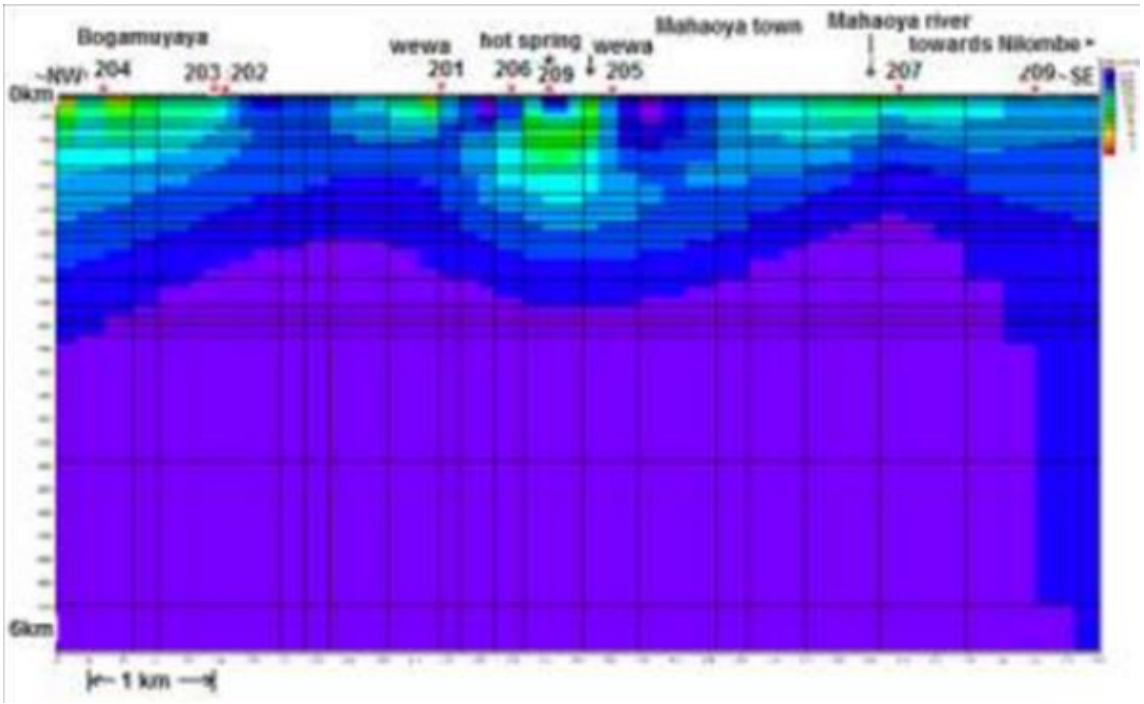

Fig. 5. Resistivity profile up to 6km depth from MT method, Mahaoya hot spring area (Hobbs, et al., 2013)

The estimated geothermal reservoir temperatures of Maha Oya hot springs based on the Na/K, K/Mg, and Quartz geothermometers revealed that the reservoir temperature is between 134°C and 204°C.

4.4 Most suitable location

The temperatures of geothermal reservoirs of the selected four hot springs are appropriate to develop a binary cycle power plant. Temperature, depth to the reservoir and heat amount should also be considered to find the best location. Table 2 shows the details of the locations.

A very low resistivity zone is evidence of a heat source that could be holding thermal water or HDR at accessible depth. In the Padiyathalawa area, the moderately low resistivity zone appears at 2000m depth and the low resistivity 100Ωm region appears at 4500m depth. But this low resistivity region is completely covered by a high resistive zone, and this high resistive layer is spread over the whole profile at a depth from 500m to 2000m.

The heat source of Nelumwewa is located under the Dimbulagala Mountain and it is a Hot Dry Rock which means there is no water, have to inject fresh water into it (Kumara and Dharmagunawardhane, 2017). The water will be heated, and when it comes to the surface, some portion turns into steam. This is called an Enhanced Geothermal System (EGS). The initial cost of EGS power plants is very high and is not suitable for developing countries like Sri Lanka.

Table 2 Details of Selected Locations

Location	Geophysical observation	Average Reservoir temperature(°C)
Padiyathalawa	Low resistivity zones start to appear at depths of 2000m and 4500m, and 100Ωm zone at 4500m.	144
Kapurella	A low resistivity zone starts to appear at depths of 1000m, and a 100Ωm zone at 3500m.	157
Nelumwewa	Heat source located under the Dimbulagala Mountain as a Hot Dry Rock	160
Mahaoya	No evidence of very low resistivity zones at accessible depth.	159

According to the MT resistivity profile, there is no evidence of very low resistivity zones at accessible depth in the Mahaoya hot spring area.

According to the MT resistivity profile of the Kapurella area, there is a low resistivity zone (600Ωm) at the start of 1000m, and it extends further below. The resistivity value of the middle of that zone is 8-30Ωm and there is no very high resistivity zone around the low resistivity region. So, that low resistivity zone should be the geothermal reservoir. Therefore, by considering the above details most suitable location for the geothermal power plant is the Kapurella area. Kapurella has an exploitable amount of heat, comparatively closer to the surface, at about 3 km depth (Suriyaarachchi, 2017).

5 ESTIMATION OF POWER GENERATION CAPACITY

There are several estimating methods used to estimate the energy and electric power generation capacity of geothermal reservoirs which can be grouped into two main categories with no production data and methods integrated with the use of production data (Franco and Donatini, 2017).

In this feasibility study, the volumetric assessment method is used to estimate power capacity. The volumetric method is the primary static modelling method, used in geothermal resource capacity estimation without any down hall data. This method assumes that extract the heat from a specific volume of the geothermal reservoir and cooling it down from an initial temperature (T) to a base temperature (T0). The accessible geothermal heat energy (Q) is computed using the following volumetric equation (Muffler and Cataldi, 1978; Trota, et al., 2019).

$$\mathbf{Q} = \mathbf{Q_r} + \mathbf{Q_w} \qquad (1)$$

$$\mathbf{Q} = \mathbf{Ah(1-\emptyset)C_r\rho_r(T-T_0)} + \mathbf{Ah\emptyset C_w\rho_w(T-T_0)} \qquad (2)$$

Q_r = Stored heat of the rocks in selected volume (J)
Q_w = Stored heat of the water (J)
A = Area of the reservoir (m^2)
h = thickness of the reservoir (m)
$\emptyset$ = Porosity
C_r = Specific heat of rock (Kj/kg°C)
ρ_r = density of rock (kg/m^3)
T = Reservoir Temperature (°C)
T_0 = Base (reference) temperature (°C)
C_w = Specific heat of water (kJ/kg°C)
ρ_w = density of water (kg/m^3)
The power generation capacity or size of the power plant (P) is calculated using the equation (3) shown below (Trota, et al., 2019).

$$\boldsymbol{P} = \frac{\boldsymbol{QR_fC_e}}{\boldsymbol{P_ft}} \qquad (\mathbf{3})$$

P = Power generation capacity (MW)
R_f = Recovery factor
C_e = Conversion efficiency
P_f = Plant factor
t = Time in years

Due to the uncertainty inherent in many of the required parameters used in the volumetric method, Monte Carlo simulation is used to define a probability distribution for these variables. Monte Carlo Simulation is the most tenable method used when a model has uncertain parameters, or a dynamic complex system needs to be analyzed. It is a probabilistic method for modeling risk in a system (Shah, et al, 2018).

In the study, a model analytic solver was used for the Monto Carlo simulation and the Monte Carlo simulation was done to assess the electricity generation potential of the geothermal resource in the country for 30 years. Parameters used for a volumetric assessment are tabulated in Table 3. Those were applied to the Monte Carlo simulation.

Table 3 Input parameters for Monte Carlo volumetric assessment (For reference temp-130°)

Input parameter	Minimum	Most likely	Maximum	Distribution
Area (m^2)		1000000		Fixed
Thickness (m)	1000	2000	3000	Triangular
Porosity (%)	5		10	Constant
Specific heat of rock (kJ/kg°C)		900		Fixed
Specific heat of water (kJ/kg°C)		4370		Fixed
Density of rock (kg/m^3)		2750		Fixed
Density of water (kg/m^3)		900		Fixed
Reservoir Temperature (°C)	130	170	203	Triangular
Reinjection temperature (°C)		70-130		Fixed
Recovery factor (%)	12.5		25	Constant
Conversion efficiency (%)		7.8		Fixed
Plant factor		0.95		Fixed
Number of runs		1000		Fixed

Volumetric equations (2), (3), and parameter values in Table 3 were applied to the Monte Carlo simulation, and the results are shown in Fig.8.

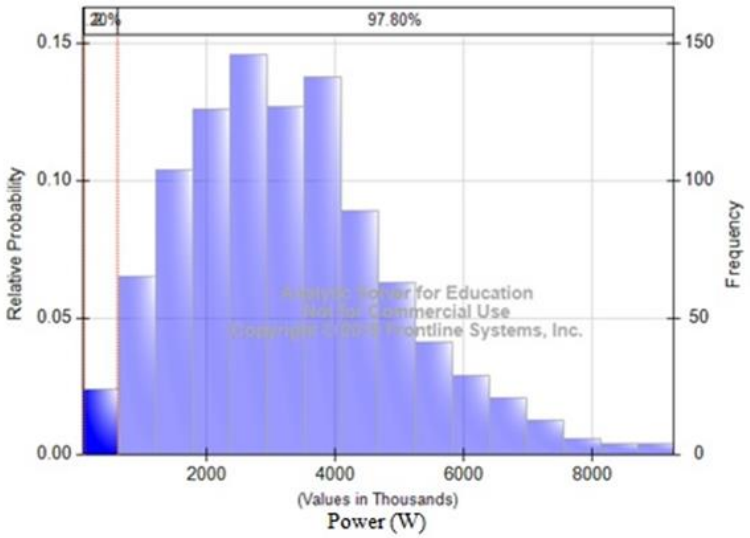

Fig.8. Probability distribution of power

The Monte Carlo simulation results show that the volumetric assessment predicts with the most probable value that the reservoir could produce is 3.2 MW for 30 years with a reference temperature of 130°C. According to the probability distribution shown in Fig. 8, it is most probable that the electrical power production capacity lies between 2.5 MW and 3.1 MW if the recoverable heat is used for 30 years, and this is the minimum power generation capacity for this geothermal field. To find an optimal value, a Monte Carlo simulation was done for eight different values of reference temperatures, and estimated power capacities are shown in Table 4.

Table 4 Estimated power generation for different reference temperatures.

Reference temperature (°C)	Average power (MW)
130	3.1
120	4.0
110	4.8
100	5.6
90	6.5
80	7.3
70	8.3
60	9.1

6 DESIGN OF POWER PLANT

Sri Lanka has low-temperature geothermal resources and due to the unavailability of downhole data, information on the state of geothermal brine is an uncertain parameter. Therefore, a binary cycle system is considered a suitable technology for this type of resource. Because binary cycle power plant is used where geothermal resources are not sufficiently hot to produce steam, or where the source contains minerals or chemical impurities to allow flashing (Mendrinos, Kontoleontos and Karytsas, 2006).

The heat exchangers used in the binary power plants are typically shell and tube exchangers with the geothermal fluid on the tube side of the exchanger and the working fluid on the shell side (Zhang, et al., 2020). A Shell-and-tube heat exchanger is suggested for this research with working fluid on the shell side and cooling water (CW) on the tube side. For cooling purposes, dry cooling systems are not suitable for the Kapurella area since the high ambient temperature and large area requirements. Therefore, a wet cooling system is proposed for the design. The typical temperature difference between the inlet and outlet cooling water is 10°C (Mendrinos, Kontoleontos and Karytsas, 2006).

The heat transfer area of the preheater, evaporator, and condenser can be calculated using the standard formulas. But due to the unavailability of field measured data heat exchanger areas are assumed by comparing other existing binary cycle power plant specifications in the world. Working fluid selection is one of the most critical considerations in Organic Ranking Cycle (ORC) design (Valdimarsson, 2017; Rowshanzadeh, 2010). For working fluid selection, several criteria are considered such as environmental sustainability, ozone depletion potential, global warming potential (GWP), safety (non-flammable, non-toxic, and non-corrosive), and the vapor pressure in the boiler, critical temperature, and thermal stability. Working fluids have lower critical pressure and temperature than water. Isopentane was selected as the working fluid for this research design with low vaporizer pressure and at a comparatively lower price.

6.1 Life Cycle Cost Analysis

Geothermal capital costs are relatively low since geothermal energy projects usually require less land compared to wind or solar energy projects. Due to the lack of certain parameters in the geothermal field, Geothermal Electricity Technologies Evaluation Model (GETEM) is used to do the cost analysis of the study. Electrical power generation is the sole geothermal use considered by GETEM and does not provide assessment capabilities for geothermal direct-use or geothermal heat pumps. The model evaluates either a Hydrothermal or an EGS resource type, and then either a flash-steam or binary power plant based on specific resource parameters.

Input parameters to GETEM are reservoir temperature, depth, and power. The reservoir temperature of 157°C, the depth of the reservoir is 3km and the estimated power is taken as 3.1 MW to 8.3 MW. According to GETEM direct and indirect costs are tabulated in Table 5 for the 3.1 MW to 8.3 MW estimated capacity

Table 5 Levelized Cost of Energy for estimated generation capacity

Reinjection Temperature (ºC)	Power capacity (MW)	Levelized Cost of Energy LCOE (₡/kWh)	Levelized Cost of Energy LCOE (Rs/kWh)
130	3.1	40.19	72.34
120	4.0	33.644	60.56
110	4.8	30.06	54.108
100	5.6	27.46	49.428
90	6.5	25.276	45.49
80	7.3	23.768	42.78
70	8.3	22.276	40.09

6.2 Environmental Impact

Binary cycle geothermal power plants are relatively small and require little land to produce the same amount of energy as other common power generation systems. And the amount of land required by a geothermal plant varies depending on the properties of the resource reservoir, the amount of power capacity, the type of energy conversion system, the type of cooling system, the arrangement of wells and piping systems, and the substation and auxiliary building needs.

Geothermal power provides many environmental advantages over fossil fuel power sources in terms of air emissions because geothermal energy production releases no nitrogen oxides, no sulfur dioxide, and much less carbon CO2 than fossil fuel power. For the Kapurella area, a binary cycle power plant is proposed and Binary plants have no CO2 emissions.

7 DISCUSSION

Since Sri Lanka is unfamiliar with geothermal energy, a literature survey for worldwide projects and geothermal resources in Sri Lanka was a compulsory critical step to finding the feasibility of electricity generation.

The biggest challenge was to find the input parameter values (data) relevant to the volumetric Equation which is used in Monte Carlo simulation. Reservoir temperatures are directly extracted from geothermometer results in previously done research. Other necessary parameters were also found in previous studies.

Power generation technology and power plant equipment are selected according to estimated power generation capacities, reservoir temperature, and depth. A Basic power plant layout was designed considering a preheater, evaporator, cooling system, and turbine. Due to the limited available parameters of the resources cost analysis was a difficult task. Therefore, Geothermal Electricity Technologies Evaluation Model was used to find the fixed capital costs and operating and maintenance costs to calculate the specific life cycle cost of the power plant.

8 CONCLUSION

By analyzing collected lithological data from the department of geology, University of Peradeniya, Kapurella hot water spring area was selected as the best location to develop a geothermal power plant. Kapurella has an exploitable amount of heat, comparatively closer to the surface, at about 3 to 4 km depth. Geothermometer results point out that the average temperature of a geothermal reservoir of the Kapurella hot water springs is about 157oC. To find an optimal value, a Monte Carlo simulation was done for eight different values of reference temperatures, and eight power generation capacity values are estimated. The results of the Monte Carlo simulation point out that the reservoir (10 km2 Area) could produce 3.1 MW to 8.3 MW of power for 130ºC to 70ºC reinjection temperatures.

The economic analysis points out that the Levelized Cost (LCOE) of energy from proposed power plant lies between 72.34 Rs/kWh to 40.09 Rs/kWh for 130ºC to70ºC reinjection temperatures respectively. Comparing the Levelized cost values of thermal and hydro power which was around 13.68 Rs/kWh and 2.32 Rs/kWh respectively, this feasibility study results, 72.34 to 40.09 Rs/kWh is a higher range, and power generation from geothermal energy is not economically feasible (Annual report_ CEB, 2020).

The results point out that, this study is not economically feasible for a base-load requirement. Therefore, based on the results of the Geothermal Electricity Technologies Evaluation Model, the development of a geothermal power plant in the Kapurella area will be a difficult task. This is largely due to development barriers and risks related to site access and a lack of data indicating the location of a deeper geothermal resource capable of supporting a utility-scale development. Even though there is a technical potential to generate electricity from the existing geothermal reservoir it is not economically feasible.

The gathering of more resource information is highly recommended for future studies. From previous research work, it is concluded that the heat source of the Nelumwewa hot springs is located under the Dimbulagala Mountain as a Hot Dry Rock, and it transfers heat to groundwater through fractures. Therefore, this area may be suitable to develop an Enhanced Geothermal System (EGS). A feasibility study needs to be carried out in this area to find out the capability of electricity generation from an EGS power plant.

9 ACKNOWLEDGEMENTS

The authors greatly appreciate the assistance given by Prof. H.A. Dharmagunawardena, the University of Peradeniya for providing data on geothermal resources in Sri Lanka and for his valuable advices.

REFERENCES

Mangala, P.S. and Wijetilake, S., 2011. The potential of geothermal energy resources in Sri Lanka. *United Nations University, Geothermal Training Programme. Report, 34.*

Bandara, H.M.D.A.H., Sooriyarachchi, N.B., Dissanayake, C.B. and Subasinghe, N.D., Geothermal Energy-Potential Applications in Sri Lanka. In *National Energy Symposium 2019* (p. 161)

Max, K.Z., Romanelli, M., Hussain, C., 2015. Deep Geothermal Energy, Executive Summary.

Moghtaderi, B., Zhou, C. and Doroodchi, E., 2019. Engineered Geothermal Systems. CRC Press LLC

Geothermal Power: Technology Brief, IRENA Annual report-2017, International Renewable Energy Agency, Abu Dhabi

Bertani, R., 2016. Geothermal power generation in the world 2010–2014 update report. *Geothermic*s, *60*, pp.31-43.

Serpen, U., Korkmaz Basel, E.D. and Satman, A., 2008, January. Power generation potentials of major geothermal fields in Turkey. In *Thirty-Third Workshop on Geothermal Reservoir Engineering* (pp. 28-30).

Samaranayake, S.A., De Silva, S.N., Dahanayake, U., Wijewardane, H.O. and Subasingha, D., 2015. Feasibility of Finding Geothermal Sources in Sri Lanka with Reference to the Hot Spring Series and the Dolarite Dykes. Proceedings of the WGC, Melbourne, Australia, pp.19-25.

Suriyaarachchi,N.B, 2017. Mapping geothermal resources in Sri Lanka: Combined use of Magnetotelluric and Transient electromagnetic method.*P.G.I.S.Postgraduate Research Highlight 2018,* Postgraduate Institute of Science (PGIS),University of Peradeniya

Franco, A. and Donatini, F., 2017. Methods for the estimation of the energy stored in geothermal reservoirs. In *Journal of Physics: Conference Series* (Vol. 796, No. 1, p. 012025). IOP Publishing

Kumara, S.M.P.G.S. and Dharmagunawardhane, H.A., 2017. An appropriate deep reservoir temperature estimate for thermal spring systems in the crystalline terrain of Sri Lanka; a comparison of geothermometers. *J. Geol. Soc. Sri Lanka, 18*, pp.45-53

Ekanayake, S.P., Ranawana, K.B., Chandrajith, R., Jayaratna, S. and Karunarathna, S.,2015. Preliminary observations on ecological aspects of Kapurella thermal spring (thermal marsh) at Mahaoya. Sri Lanka Naturalist, 8(1-2)

Kumara, S.M.P.G.S. and Dharmagunawardhane, H.A., 2014. A. geostructural model for the Nelumwewa thermal spring: north central province, Sri Lanka. *Journal of Geological Society of Sri Lanka, 16*, pp.19-27

Hobbs, B.A., Fonseka, G.M., Jones, A.G., De Silva, S.N., Subasinghe, N.D., Dawes, G., Johnson, N., Cooray, T., Wijesundara, D., Suriyaarachchi, N. and Nimalsisri, T., 2013. Geothermal Energy Potential in Sri Lanka: a preliminary magnetotelluric survey of thermal springs. *Journal of Geological Society of Sri Lanka, 15,* pp.69-83..

Muffler, P. and Cataldi, R., 1978. Methods for regional assessment of geothermal resources. *Geothermics*, *7*(2-4), pp.53-89.

Sarmiento, Z.F., Steingrímsson, B. and Axelsson, G., 2013. Volumetric resource assessment. *Proceedings of the Short Course V on Conceptual Modelling of Geothermal Systems, Santa Tecla, El Salvador, 2.*

Trota, A.P., Rodrigues, F.C. and do Álamo de Meneses, J.G., 2019. Insights for the Angra do Heroísmo hydrothermal reservoir conceptual model. *Sustainable Water Resources Management*, 5(1), pp.135-146.

Shah, M., Vaidya, D. and Sircar, A., 2018. Using Monte Carlo simulation to estimate geothermal resource in Dholera geothermal field, Gujarat, India. *Multiscale and Multidisciplinary Modeling, Experiments and Design*, 1(2), pp.83-95.

Mendrinos, D., Kontoleontos, E. and Karytsas, C., 2006. Geothermal binary plants: water or air cooled. *Centre for Renewable Energy Sources*, 19, pp.1-10.

Zhang, L., Geng, S., Kang, J., Chao, J., Yang, L. and Yan, F., 2020. Experimental study on the heat exchange mechanism in a simulated self-circulation wellbore. *Energies*, 13(11), p.2918.

Valdimarsson, P., 2017. Radial inflow turbines for Organic Rankine Cycle systems. In *Organic Rankine Cycle (ORC) Power Systems* (pp. 321-334). Woodhead Publishing.

Rowshanzadeh, R., 2010. Performance and cost evaluation of Organic Rankine Cycle at different technologies. *Master thesis, department of Energy Technology, KTH, Sweden*

Annual Report, Ceylon Electricity Board(CEB), 2020

Tea factory firewood ash as a potential plant nutrient source for higher productivity of mature tea in Matara District of Sri Lanka

S.K.Weerathunga[1], C.S De Silva[2*], T G.P. Gunarathne[1]
[1] Soils and Plant Nutrition Division, Tea Research Institute, Deniyaya, Matara
[2]Department of Agricultural and Plantation Engineering, The Open University of Sri Lanka, Nawala, Nugegoda, Sri Lanka

*Corresponding Author: email: csdes@ou.ac.lk Tele: +94112881323

***Abstract**: Tea industry has waste products such as refuse tea from made tea production while ash from fire wood. There are 705 tea factories located island wide, nearly 35,250 kg of wood ash is being produced every day as approximately 50 kg of wood ash is being produced in a tea factory for a day. Lack of information on wood ash, composition as well as the plant nutrient value of wood ash, have led the application of wood ash to tea plantation is limited. Therefore, the main objective of this study is to investigate the suitability of tea factory wood ash as a plant nutrient source for mature tea. The experiment was conducted in the Field number 1B, Mervillian Division, Kiruwanaganga Estate at Deniyaya in Matara district. The different rates of wood ash (500, 1000 kg ha^{-1} $year^{-1}$) and refuse tea (20t/ha/yr) or compost (20t/ha/yr) were compared with current fertilizer mixture, VPLC 880. Ten experimental plots were marked out for 5 treatments and controlled by current recommended mixture with 200 bushes per each plot as two replicates for each treatment. The soil pH values were measured with distilled water varied significantly among treatments. The higher pH values can be seen in the plots treated with wood ash compared with inorganic mixture applied plots. Soil available phosphorous content did not vary significantly with treatments. Soil available potassium varies significantly among treatments. The concentration of the soil potassium in wood ash applied pots with compost significantly differs with other treatments especially with inorganic mixture applied plots. Soil available Mg varied significantly among treatments. The concentrations of the soil Mg in wood ash applied pots at 1000kg/ha/yr with either compost or refuse tea significantly differ with other treatments especially with inorganic mixture applied plots. Soil available Ca varied significantly among treatments. The concentration of the soil Ca in wood ash applied pots at 1000kg/ha/yr. with either refuse tea or compost significantly differs with other treatments especially with inorganic mixture applied plots. No significant difference in organic carbon content was observed among treatments. The CEC of the soil in wood ash applied pots at refuse tea significantly differ with other treatments especially with inorganic mixture applied plots. Significant difference in N, P and K content in the mother leaves were observed among treatments. Highest value was observed in wood ash applied pots at refuse tea at 1000kg/ha/yr. Wood ash applied plots showed comparable yield with present TRI fertilizer recommendation. The highest made tea yield was obtained in wood ash applied at 1000kg/ha/yr with refuse tea plots. Therefore, wood ash with refuse tea could be used to produce highest yield of made tea.*

***Key words**: Tea, nutrient, soil, wood ash, refuse tea*

1. INRODUCTION

Agriculture is a vital and dynamic component in the economy of Sri Lanka, due to its contribution to country's income, employment, welfare and culture (Gunasekare, 2012). Plantation crops such as Tea, Rubber and Coconut act major role in agriculture sector in Sri Lanka. Out of them tea is very important, because income from the agriculture sector contributes about 19.7% of the total Gross National Production (GNP) of which the contribution from tea is about 70% and tea contributed 1.3% to Gross Domestic Production (GDP) (Annual report of Tea Research Institute, 2011). Tea export earnings reached USD 1.5 Billion in 2011, a historically high value contributing 15% to the nation's foreign exchange and generating 65% of export agriculture revenue and 2 Million employments directly and indirectly. Altogether 10% of the population of Sri Lanka depends on this industry (Samaraweera *et al.,* 2013).

Any industry always has waste products. In tea industry there are waste products such as refuse tea from made tea production and ash from fire wood. Refuse tea commonly used to protein extraction through membrane filtration technique for instant tea production and use as a mulching material and compost for tea plantations (Annual report of Tea Research Institute, 2003).

The manufacture of black tea from green leaf delivered to the factory requires the following stages of processing. They are withering, rolling, roll breaking, fermentation, drying, shifting, grading and packaging. Wood ash is being released through the drying stage which is an expensive component in processing of tea. A large quantity of hot air is required for this purpose. Common energy sources used in the tea industry are fuel and firewood.

Firewood is the low-cost energy source and it releases minimum undesirable sulfur containing gases respect to the fuel. Withering also required hot air from furnace where firewood is used. Wood ash is the second highest waste from tea manufacture, does not used in a beneficial way though rarely used to produce compost. Even though, our forefathers used ash as an input to the crops they do not know the value of ash.

As a result of the oxidation processes during combustion the generated wood ash retains the overall composition of the mineral nutrients contained in the firewood with the exception of nitrogen compounds, which are mainly released into the environment as gas. Nutrient elements contained in the form of fixed substances are relatively stable during the burning thermal treatment. These elements are in the same proportions as they were in the structure of the wood piece, which is a prerequisite for a good methods and technologies for use in the chemo dynamic cycle of the elements in the soil systems. Nitrogen compounds from the wood piece in the

combustion process are degraded and released in the atmosphere as a waste gas mainly in the form of oxides (Sène and Gallet, 2001). Therefore, wood ash may be a good source of plant nutrient.

There are so many liming materials that can be incorporated to maintain the soil pH ranges which suitable for specific crop. Tea prefers acidic soil with pH 4.5-5.5. Present of comparatively high levels of Potassium (K), Calcium (Ca), and Magnesium Carbonate ($MgCO_3$) or Oxides in wood ash, which gives the strongly alkaline reaction, can neutralize acid soils. Therefore, it can be used as a low-cost liming material to crops. It is better to study nutrition composition of wood ash, neutralizing power of wood ash and what amount of ash going to be applied to crops as a nutrient source (Anandacoomaraswamy *et al*, 2003).

Although huge amount of wood ash is being removed from tea factories in Sri Lanka, there is still no efficient and proper way to reap the maximum benefit out of wood ash from tea factory. There are 705 tea factories located island wide so nearly 35,250 kg of wood ash is being produced every day as approximately 50 kg of wood ash is being produced in a tea factory for a day (Table 1). (Annual report of Tea Research Institute, 2011)

Lack of information on wood ash composition as well as the plant nutrient value of wood ash, have led the application of wood ash to tea plantation to be limited. Therefore, an in-depth study of wood ash would be able to provide invaluable information to interpret and recommend wood ash more rationally to the stakeholders.

Table .1: Number of tea factories located in Sri Lanka

Regions	**Numbers of factories located**
Up-country	130
Low country	416
Mid-country	093
Uva regions	066
Total	**705**

2. METHODOLOGY

2.1. Location

The experiment was carried out at the Kiruwanaganga Estate at Deniyaya in Matara district

2.2. Soil

According to the soil classification systems, this soil has been classified as Red Yellow Podzolic Great soil group and Weddagala soil series. It is a well-drained soil which having sandy clay loam texture and sub angular blocky soil structure. It is a kind of deep soil.

Table 2: Chemical properties of the soil

Property	**Value/Concentration**
pH	3.48
Organic carbon	1.02
Nitrogen (%)	0.27
Phosphorus (mg/kg)	11
Potassium (mg/kg)	98
Magnesium (mg/kg)	24
Sulphur (mg/kg)	47
Calcium (mg/kg)	78
Manganese (mg/kg)	2.55
Copper(mg/kg)	0.34
Zinc (mg/kg)	2.80
Iron (mg/kg)	4.60
Boron (mg/kg)	0.57

2.3. Experimental design and treatments

A randomized complete block design (RCBD) was used as the experimental design having 10 plots surrounded by guard raw which separated the treated area in order to prevent effects in any adjacent plots to influence the experiment. The five treatments were replicated twice. The treatments used are shown in the Table 3.

Table 3: Treatments details of wood ash trial

Treatments	Details
T1	Wood ash (WA) (500kg/ha/yr) + Compost (20t/ha/yr)
T2	Wood ash (WA) (1000kg/ha/yr) + Compost (20t/ha/yr
T3	Wood ash (WA) (500kg/ha/yr) + Refuse tea (20t/ha/yr)
T4	Wood ash (WA) (1000kg/ha/yr) + Refuse tea (20t/ha/yr)
T5	Current recommendation (VPLC 880)

2.4. The composition of treatment materials

2.4.1. Wood ash

There are so many tree species used as firewood in tea industry of Sri Lanka. Wood ashes were sieved by using 0.5 mm sieve and sieved pure rubber wood ash was used (Table 4).

Table 4: Nutrient composition of rubber wood ash

Parameter	Value/Concentration
pH	13.66
EC	5.58
Organic Carbon (%)	0.16
Total Nitrogen (%)	0.13
Potassium (%)	7.26
Phosphorous (%)	0.78
Sulphur (%)	1.13
Magnesium (%)	2.15
Calcium (%)	24.91
Boron (mg/kg)	1337
Iron (mg/kg)	723
Zinc (mg/kg)	255
Copper(mg/kg)	135
Manganese	1432

2.4.2. VPLC 880 fertilizer mixture

Composition of VPLC 880 mixture is as follows:

Urea	parts	587
ERP	parts	126
MOP	parts	167
		880

The mixture contains approximately 30.7% N, 4.1% P_2O_5 and 11.4% K_2O

2.4.3. Compost

Compost is a very common nutrient supplement in Tea lands. The composition of compost is shown in Table 5.

Table 5: Nutrient composition in compost

Parameter	**Concentration**
Total Carbon content (%)	36.5
Total Nitrogen (%)	3.0
C/N ratio	12.3
Phosphorous (%)	0.4
Potassium (%)	4.4
Calcium (%)	1.01
Magnesium (%)	0.35
Zinc (mg/kg)	81 ppm
Manganese (mg/kg)	551 ppm

2.4.4. Refuse Tea

Tea industry has waste products such as refuse tea coming from made tea production in large quantities. Nutrient composition of refused teas is shown in table 6.

Table 6: Nutrient composition in refuse tea

Compositions	Concentration
Total Nitrogen (%)	3.44
Phosphorous (%)	0.34
Potassium (%)	2.10
Calcium (%)	0.34
Magnesium (%)	0.19
Copper (mg/kg)	28
Manganese (mg/kg)	146
Zinc (mg/kg)	34
Iron (mg/kg)	218

2.5 Sampling procedure

2.5.1. Ground fertilizer application

VPLC 880 ground fertilizer mixture was applied to all plots as TRI recommended amount just after plot marking.

2.5.2. Soil samples

Pre soil sampling was done 3 months after applying the VPLC 880 ground fertilizer mixture. The soil samples were taken from two depths of 0-15 cm and 15-30 cm. The samples were collected randomly and three samples from each plot in Z manner, from the plots after removing the surface litter. The collected samples were air dried and sieved by using 0.5mm and 2mm sieves for total and available nutrient analysis respectively.

2.5.3. Leaf samples

Leaf sampling was done 3 months after ground fertilizer application. Two mother leaves were collected from each bush in the plot to provide a composite sample. The leaves were put into paper bags with the label, and placed in the electric oven and kept overnight at 80˚ C. The dried samples were crushed by hand and a sub sample ground in intermediate mill and passed through a 40-mesh stainless steel sieve. At the time of weighing the powdered sample was thoroughly mixed with a spatula.

2.5.4. Yield recording

Yield recording was started after plot marking and it will continue throughout the experimental period. Yield was recorded at 7-10 days interval. Harvested from each plot was weighed separately using a top loading balance. Only two pluckers were used for plucking each plot to minimize the plucking error.

2.6 Analytical procedures

2.6.1. Soil Analysis

- ***Determination of soil pH using distilled water***

Determination of pH of the soil suspension was done using a pH meter (ORION 550A model, USA) with the Ag/AgCl combined electrode. Prior to determination, the meter was calibrated using commercially available buffer solution of pH 4.0 and 7.0 BDH brand. A 10 g sample of soil was weighed into pH cup. Thereafter, 25ml of distilled water was added into each pH cup and stirred well and kept for 30 minutes. Then stirred again and pH reading was taken by using pH meter.

- ***Determination of Available Potassium, Magnesium, Calcium in soil***

Five grams of soil was weighed into plastic bottle and 25 ml of 1N Ammonium Chloride solution (NH_4Cl) solution was added. Then, it was shaken for 30 minutes. Shaken sample was filtered by 542 Whatman filter paper into a jam bottle. Then 3ml of aliquot were pipetted out into volumetric flask and 2.5ml SrCl2 solution was added to make the volume up to 25ml. Then readings were taken by Atomic Absorption Spectrometer for Magnesium, Calcium and by flame photometer for Potassium.

- ***Determination of D.T.P.A (Die ethylene Triamine Pentaacetate) extractable (Mn) Trace element in soil***

Air dried, sieved (pass through 2mm mesh) 10g of soil was weighed into the shaking bottles. Then 20ml of Di DTPA extracting solution was added into it and shacked for two hours, centrifuge and filter. Filtrate was collected into a jam bottle and Atomic absorption spectrophotometer was used to determine the concentration of each element by using the Holo- cathode lamp for each element.

- ***Determination of Total Nitrogen of soil (Kjeldahl method)***

One gram of finely ground air-dried soil was weighed into a 100 ml digestion tube which has 75 ml graduation mark on its neck and added sufficient water to just moisten the soil completely. Then 2 g of the catalyst was added and carefully and 4 ml con. H_2SO_4 was poured in such a way as to wash down all soil particles adhering to the neck of the tube. Then the contents of the flask were mixed well and started

the digestion in a fume cupboard. The contents were boiled for 1 hour after the digest turns green. When cool down to the room temperature few drops of water was added and mixed well. After that the digesta was transferred quantitatively in to a 1-literKjeldahl flask. Then 25 ml of 40% NaOH was added in such a way that the alkali settles at the bottom of the flask. Then a 200 ml conical flask containing 25 ml 4% boric acid and 2 drops indicator was fitted to the delivery tube of the distillation unit. After that the apparatus was connected to the Kjeldahl bottom flask. The distillation was started and collected about 100ml of distillate. The receiving flask was removed, washed the delivery tube with distilled water and the contents were titrated with 0.10N HCl.

- ***Determination of Cation Exchange Capacity***

Soil samples were air dried and passed through 2mm sieve. From each sample12.5 g of soil was measured and put into the folded filter paper (Whatman 542) in a funnel. Next the funnel was fixed to a 250cm^3 volumetric flask, and the content was leached with 1N NH_4Cl solution until around 250cm^3 was collected. After that the same content was leached with 1/20N NH4Cl solution until around 250cm^3 of the leachate was collected. During these two processes, most of the cations in the soil sample were replaced by NH_4^+ ions. Consequently, leaching the same soil with 1N Sodium Sulphate (Na_2SO_4) solution did the replacement of NH_4^+ ions. This was done until 250 cm^3 leachet was collected. Finally, 25.00cm^3 of the collected solution was steam distilled in the Kjeldahl distillation apparatus (BUCHI B 324 model, Netherlands) and the evolved ammonia was collected in the boric acid solution. Ultimately, the amount of ammonia was determined by titrating with standardized 0.1 NH_4Cl.

- ***Determination of Base Saturation in soil***

Base saturation was calculated using following equation.
Base Saturation= {(Ca) + (Mg) + (K)}/Cation Exchange Capacity*100

- ***Determination of hot water extractable Boron in soil***

Air dried, sieved 2g of soil sample was weighed into a plastic shaking bottle. Then 40 ml of distilled water was added, and it was kept for 6 hours in water bath. Next it was centrifuged, and 1 ml of filtrate put into the silicon flask. The filtrate was added with 10 ml of conc. H2SO4 and 10 ml of Carminic acid and swirled to mix well. Each flask was covered by using watch glass and kept 6 hours for color development. The samples were read against the blank, using 2cm cell in spectrophotometer under the wavelength of 610nm.

2.6.2. Leaf Analysis

- ***Determination of Nitrogen in leaf sample***

Finely grinded 0.2 g of plant material was weighed into digestion tubes. Then 0.4g of leaf catalyst was added into the tube. Tubes were placed on digestion block for one hour after adding 3ml of conc. H_2SO_4 acid. Then two drops of distilled water were added while transferring to the Kjeldahl flasks. Next the double distillation was done in Kjeldahl unit {(25ml of Boric acid (H_3BO_3) and 40ml of Sodium Hydroxide (NaOH). Finally, titration was done against 0.1 N Hydrochloric acid (HCl) until the solution turns to the crimson red colour.

- ***Determination of Total potassium, phosphorus, Magnesium, Sodium, Calcium and trace elements in leaf sample***

Finely grinded 0.2 g of plant material was weighed into digestion tubes. Then it was kept in muffle furnace overnight. Then one drop of distilled water and 0.2 ml of digestion mixture was added and placed on hot plate to evaporate. Next 10 ml of 0.05N HCl acid was added using a pipette. Then cap was covered with parafilm and shaked. Potassium was determined by Flame photo meter. Calcium, Magnesium and Trace elements were determined by using Atomic Absorption Spectrophotometer. Phosphorous in leaf were determined by Vando Molybdate yellow method with UltraViolet Visible Spectrophotometer at 425 nm wavelength.

3. RESULTS AND DISCUSSION

3.1. Effect of application of wood ash on soil pH

The soil pH is shown in Table 7. The soil pH values measured with distilled water varied significantly among treatments. The higher pH values can be seen in the plots treated with wood ash compared with inorganic mixture applied plots, it was due to the liming effects of wood ash. In contrast that inorganic fertilizer applied plots showed lowest pH values because of acidity created by nitrification of NH_4^+ ions from urea hydrolyses (Weaver, *et al*., 2004). Any ammonium fertilizer when nitrified by nitrifying bacteria releases H+ ions to the soil solution as follows.

$$CO(NH_2)_2 + H_2O \longrightarrow NH_4COONH_4$$
$$NH_4COONH_4 + H_2O \longrightarrow (NH_4)_2CO_3$$
$$(NH_4)_2CO_3 \longrightarrow 2NH_4^+ + CO_3^{--}$$
$$CO_3^{--} + H_2O \longrightarrow H_2CO_3 + 2OH^-$$
$$2NH_4^+ + 6\,(O) \longrightarrow 2NO_2^- + 2H_2O + 4H^+$$
$$2NO_2^- + (O) \longrightarrow 2NO_3^-$$

Net acidity $2H^+$ per urea molecule i.e. $1H^+$ per N atom.

Table 7: Effect of treatments on soil pH

Treatments	**Soil pH** (water)	**Soil pH** (CaCl2)
Wood ash (WA) (500kg/ha/yr) + Compost (20t/ha/yr)	4.64[b]	4.20[a]
Wood ash (WA) (1000kg/ha/yr) + Compost (20t/ha/yr)	5.40[a]	4.39[a]
Wood ash (WA) (500kg/ha/yr) + Refuse tea (20t/ha/yr)	4.50[b]	4.05[a]
Wood ash (WA) (1000kg/ha/yr) + Refuse tea (20t/ha/yr)	4.35[b]	4.06[a]
Current recommendation (VPLC880)	4.10[b]	3.89[a]
LSD	0.711	0.515
CV%	5.575	4.491

Any process that leads to the release of H+ ions to the soil acidifies the soil because the soil pH which determines the degree of soil acidity is dependent on the concentration of H+ ions in soil solution, if not well buffered.

$$pH = -\log_{10}[H^+]$$

Where H+ is the concentration of hydrogen ions expressed in moles per liter (Wickremasinghe, 1986).

3.2. Effect of application of wood ash on soil available P and K

The soil available P and K are shown in Table 8. Soil available phosphorous content did not vary significantly with treatments. However, higher values were observed wood ash applied plots with refuse tea, the sufficiency level of phosphorus content in the soil should be ≥ 20ppm.

Soil available potassium varies significantly among treatments. The concentration of the soil potassium in wood ash applied pots with compost significantly differs with other treatments especially with inorganic mixture applied plots. Zimmermann and Frey (2002) also showed that wood ash usually presents a relatively high concentration of potassium. The optimum level of soil available K for better growth of tea plant should be greater than 100 mg /kg K of soil. Therefore, K requirement can be fulfilled by application of 500 kg/ha/year of wood ash per hectare per annum with compost.

Table 8: Effect of treatments on soil available P and K

Treatments	**Soil P (mg/kg)**	**Soil K (mg/kg)**
Wood ash (WA) (500kg/ha/yr) + Compost (20t/ha/yr)	25[a]	237[a]
Wood ash (WA) (1000kg/ha/yr) + Compost (20t/ha/yr)	31[a]	231[a]
Wood ash (WA) (500kg/ha/yr) + Refuse tea (20t/ha/yr)	72[a]	78[b]
Wood ash (WA) (1000kg/ha/yr) + Refuse tea (20t/ha/yr)	55[a]	72[b]
Current recommendation (VPLC880)	29[a]	62[b]
LSD	52.43	29.06
CV%	44.57	7.69

3.3. Effect of application of wood ash on soil available Mg and Ca

The soil available Mg and Ca are shown in table 9. Soil available Mg varies significantly among treatments. The concentrations of the soil Mg in wood ash applied pots at 1000kg/ha/yr with either compost or refuse tea significantly differ with other treatments especially with inorganic mixture applied plots. Soil available Ca varies significantly among treatments. The concentration of the soil Ca in wood ash applied pots at 1000kg/ha/yr with either refuse tea significantly differs with other treatments especially with inorganic mixture applied plots. Rigau (1960) also stated that calcium and magnesium carbonate or oxides are present in comparatively large quantities in the wood ash. The optimum level of soil available Mg for better growth of tea plant should be greater than 60 mg /kg Mg of soil.

3.4. Effect of application of wood ash on soil Organic carbon content and CEC

The soil organic carbon content and soil CEC are shown in table 10. Not significant difference ($p \leq 0.05$) in organic carbon content was observed among treatments. Wood ash incorporation with either compost or refuse tea applied pots showed higher values. It may be due to soluble organic compounds in refuse tea. In the tea growing districts of Sri Lanka, the organic matter in general is reported to vary with elevation, between 1.5 to 2.0 percent carbon at low elevation and 3.0 to 6.0 percent carbon at high elevations (Krishnarajah, 1984). Therefore, application of wood ash with organic matter will be the best solution for improvement of organic matter content in soils in low and mid elevation of Sri Lanka.

Table 9: Effect of treatments on soil available Mg and Ca

Treatments	**Soil Mg mg/kg)**	**Soil Ca (mg/kg)**
Wood ash (WA) (500kg/ha/yr) + Compost (20t/ha/yr)	24^{ab}	126^{b}
Wood ash (WA) (1000kg/ha/yr) + Compost (20t/ha/yr)	34^{a}	183^{b}
Wood ash (WA) (500kg/ha/yr) + Refuse tea (20t/ha/yr)	33^{a}	351^{a}
Wood ash (WA) (1000kg/ha/yr) + Refuse tea (20t/ha/yr)	23^{ab}	190^{b}
Current recommendation (VPLC880)	17b	145b
LSD	3.217	103.20
CV%	18.16	18.73

Table 10: Effect of treatments on soil Organic carbon content and CEC

Treatments	Soil O.C %	Soil CEC (meq/100g)
Wood ash (WA) (500kg/ha/yr) + Compost (20t/ha/yr)	2.69[a]	19.7[b]
Wood ash (WA) (1000kg/ha/yr) + Compost (20t/ha/yr)	2.76[a]	20.1[b]
Wood ash (WA) (500kg/ha/yr) + Refuse tea (20t/ha/yr)	2.62[a]	21.8a
Wood ash (WA) (1000kg/ha/yr) + Refuse tea (20t/ha/yr)	2.76[a]	22.1[a]
Current recommendation (VPLC880)	2.25[b]	18.0[c]
LSD	0.231	1.528
CV%	3.18	2.69

The CEC of the soil in wood ash applied pots at refuse tea significantly differ with other treatments especially with inorganic mixture applied plots. Almost all tea growing soils in Sri Lanka belong to soil order Ultisols and Inceptisols (Mapa *et al*., 1999) hence the presence of active clay fraction is poor throughout the profile. Mineralogical analysis performed for Ultisols and Inceptisols of the wet and intermediate zones indicates the dominance of kaolinite which comprised 80-90% and 40% among the total clay fraction respectively (Indraratne, 2009). Therefore, one of the major governing factors of the CEC of such soil is organic carbon content which is mostly pH dependent. Consequently, organic carbon has a higher influence on the CEC thereby to the pH buffering capacity.

3.5. Effect of application of wood ash on leaf N, P and K concentration

The N, P and K, content in mature leaf is shown in Table 11. Significant difference ($p \geq 0.05$) in N, P and K content in the mother leaves were observed among treatments. Wood ash incorporation with either compost or refuse tea applied pots showed higher values compared with inorganic fertilizer applied plots.

Table 11: Effect of treatments on leaf N, P and K concentrations

Treatments	Leaf N %	Leaf P %	Leaf K %
Wood ash (WA) (500kg/ha/yr) + Compost (20t/ha/yr)	1.42[ab]	0.220[b]	1.42[b]
Wood ash (WA) (1000kg/ha/yr) + Compost (20t/ha/yr)	1.38[ab]	0.225[ab]	1.38[ab]

Wood ash (WA) (500kg/ha/yr) + Refuse tea (20t/ha/yr)	1.49[a]	0.260[a]	1.49[a]
Wood ash (WA) (1000kg/ha/yr) + Refuse tea (20t/ha/yr)	1.36[ab]	0.235[ab]	1.36[ab]
Current recommendation (VPLC880)	1.32[b]	0.240[ab]	1.32[b]
LSD	0.137	0.037	0.137
CV%	3.564	5.763	3.564

The literature on wood ash application to tea is limited. However, similar effects have been reported from a long-term field experiments conducted with different rates of N, K and dolomite to assess growth, soil-plant nutrient status and yield of tea (Sandanam *et al,* 1980).

3.6. Effect of application of wood ash on leaf Mg and Ca concentration

The Mg and Ca content in mature leaf are shown in Table 12. Significant difference ($p \geq 0.05$) in Mg content in the mother leaves were observed among treatments. Highest value was observed in wood ash 1000kg/ha/yr applied pots with refuse tea.

Table 12: Effect of treatments on leaf Mg and Ca concentrations

Treatments	**Leaf Mg %**	**Leaf Ca %**
Wood ash (WA) (500kg/ha/yr) + Compost (20t/ha/yr)	0.145[b]	1.46[a]
Wood ash (WA) (1000kg/ha/yr) + Compost (20t/ha/yr)	0.150[b]	1.49[a]
Wood ash (WA) (500kg/ha/yr) + Refuse tea (20t/ha/yr)	0.140[b]	1.44[a]
Wood ash (WA) (1000kg/ha/yr) + Refuse tea (20t/ha/yr)	0.180[a]	1.46[a]
Current recommendation (VPLC880)	0.180[a]	1.61[a]
LSD	0.029	0.396
CV%	6.596	5.526

3.7. Effect of application of wood ash on made tea yield

The variations of tea yield in relation to different treatments are shown in Table 13. Significant difference in yield was observed among treatments. Wood ash applied plots showed comparable yield with present TRI fertilizer recommendation. The highest made tea yield was obtained in wood ash applied pots at 1000kg/ha/yr with refuse tea.

Greenhouse studies at the University of Wisconsin-River Falls show alfalfa and barley yields from wood ash applications of 5-20 tons per acre to be significantly greater than those from commercial lime and fertilizer applied at rates recommended by soil test (Anon, 2013).

Table 13: Effect of treatments on made tea yield

Treatments	**Made Tea Yield (kg/ha)**
Wood ash (WA) (500kg/ha/yr) + Compost (20t/ha/yr)	2994^{b}
Wood ash (WA) (1000kg/ha/yr) + Compost (20t/ha/yr)	3117^{ab}
Wood ash (WA) (500kg/ha/yr) + Refuse tea (20t/ha/yr)	3127^{ab}
Wood ash (WA) (1000kg/ha/yr) + Refuse tea (20t/ha/yr)	3358^{a}
Current recommendation (VPLC880)	3026^{b}
LSD	289.1
CV%	3.332

4. CONCLUSION

Huge amount of wood ash is being removed from tea factories in Sri Lanka; there is still no efficient and proper way to reap the maximum benefit out of wood ash from tea factory. Therefore, the main objective of this study was to investigate the suitability of tea factory wood ash as a plant nutrient source for mature tea. According to the results obtained there is soil, leaf nutrient levels and yield improvement by the application of tea factory wood ash at 1000 kg/ha with refuse tea at 20t/ha/yr.

5.REFERENCES

Anon, (2013). UGACooperative Extension Bulletin1142, pp-105-130.

Anandacumaraswamy, A., Amerasekera, A.R., De Silva, M.S.D.L. and Abeysekera, U.P., (2003). Soil management in tea lands. *Twentieth Century Tea Research Institute in Sri Lanka*, pp.55-62.

Gunasekare, M.T.K., (2012). Tea plant (Camellia sinensis) breeding in Sri Lanka. In *Global Tea Breeding*. Springer Berlin Heidelberg. pp. 125-176.

Indraratne, S . (2009). Principals and applications of soil mineralogy. IRQUE Project, Faculty of Agriculture, University of Peradeniya. pp. 64-66.

Krishnarajah, P. (1984). Soil erosion control measures for tea land in Sri Lanka. Proceedings of International Workshop on Soil Erosion and its Counter Measures.Chianmai, Thailand. pp 56-59

Mapa R B, Somasiri S and Nagarajah S (1999). Soils of wet zone of Sri Lanka: Morphology, characterization and classification. Special publication No. 1, Soil science society of Sri Lanka. Pp78-90.

Samaraweera, G.C., Ping, Q. and Yanjun, L. (2013). Promoting tea business in the tea smallholding sector in developing countries through efficient technology transfer system: Special reference to Sri Lanka. *African Journal of Business Management*, *7*(22), p.2186.

Sandanam, S., Sivasubramanium, S. and Rajasingham, C.C., (1980). Response of seedling tea to forms and levels of nitrogenous fertilizers, levels of potassium and liming in the country tea growing districts of Sri Lanka. Tea Quarterly, 49: 20-29.

Sène, M., Doré, T. and Gallet, C., (2001). Relationships between biomass and phenolic production in grain sorghum grown under different conditions. *Agronomy Journal*, *93*(1):49-54.

Tea Research Institute of Sri Lanka (2011). Agro-ecological regions of Sri Lanka, Annual report-2011, Tea Research Institute of Sri Lanka, Talawakelle.

Tea Research Institute of Sri Lanka (2003). Annual report-2003, Tea Research Institute of Sri Lanka, Talawakelle.

Weaver, A.R., Kissel, D.E., Chen, F., West, L.T., Adkins, W., Rickman, D. and Luvall, J.C., (2004). Mapping soil pH buffering capacity of selected fields in the coastal plain. *Soil Science Society of America Journal*, *68*(2):662-668.

Zimmermann, S. and Frey, B. (2002). Soil respiration and microbial properties in an acid forest soil: effects of wood ash. Soil Biology. Biochemistry. 34:105-123

Journal of Engineering and Technology
The Open University of Sri Lanka (JET-OUSL), Vol. 10, No.1, pp. [33-45], 2022

Retrofit Mango Chip Drying Plant for High Productivity

K.M.L.S. Senarathna*, R.J. Wimalasiri

Department of Mechanical Engineering, The Open University of Sri Lanka, Nawala, Nugegoda, Sri Lanka.

*Corresponding Author: email: sanjaya761@gmail.com, Tele: +94718989064

Abstract – *Dryer is an equipment widely used to remove the moisture from products/materials. This study is focused on an industrial cabinet/tray type dryer which used to dry mango chips. The dryer is designed to operate by steam or electricity and due to the prevailing capabilities and limitations of the factory the electricity has been used to run the dryer. This research is focused on reducing the drying time of the dried chip production process. The reduction of the drying time will reduce the cost and increase the productivity. Initially the total production process was evaluated, and the drying stage parameters were identified. Then a comprehensive literature survey was conducted to theoretically recognize the parameters related to drying, and to identify the possible modifications which can be introduced to minimize the drying time. It was identified that the controlling the level of relative humidity would appropriately affect the drying time. The existing drying plant was retrofitted to reduce the relative humidity of air to optimize the dying time and it was carefully conducted in cost-effective manner. A designed and developed unit mainly consists with heat exchangers were introduced to the existing dryer. The two most important process parameters, moisture content and the water-activity, were continuously monitored and kept within the limits. After the introduction of the unit, the total process was reassessed. A 3.26% reduction of the drying time with an energy saving of 12.65% was recorded. Hence the productivity of the plant is improved. Even considering the reduction in energy consumption, the capital cost can be recovered within less than 2 ½ month which is further shortened if taken the productivity improvement into account. The findings of this research could be applied to similar cabinet/tray type dryers to optimize the drying process thereby to shorten the drying time to enhance the productivity.*

***Keywords**: Cabinet Dryer, Energy Saving, Productivity, Relative Humidity, Tray Dryer*

Nomenclature

Kcv - Drying rate for constant rate period ($kgm^{-2}s^{-1}$)
Td - Dry bulb temperature of air (˚C)
Tw - Wet bulb temperature of air (˚C)
h - Convective heat transfer coefficient ($Wm^{-2}K^{-1}$)
b - 14.31 (Constant for SI unit)
G - Air flow rate (kgs^{-1})
W - Initial moisture content in dry basis
Wc - Critical moisture content
Wi - Final moisture content in dry basis
t - Theoretical drying time ($sm^{-2}kg^{-1}$)
T - Total drying time (min)
X - Relative humidity x 100
A - Constant for drying process

Greek Letters
λ - Latent heat of vaporization at temperature Tw ($kJkg^{-1}$)

Subscripts
c - critical
i - final
d - dry bulb
w - wet bulb

1 INTRODUCTION

One of the leading industries in Sri Lanka which produces food-based items for both local and international markets, has recently started a new venture which is to produce dry-mango-chips. These chips which consume as a snack, are totally exported to Europe and Middle East. The mango chip processing method and the recipe is not yet exposed by other producers. The venture had to conduct a fair bit of R&D to finalize a process which could adapt to reform the wet mango chips to dry chips while maintaining the anticipated quality standards.

Productivity is a key factor, and any productivity improvement not only benefits the employers but also to the employees in different ways, such as salary increments, bonus, health insurance, annual get-togethers, etc. Hence this study is focused on productivity improvement of the mango chip drying plant by refining the drying process. Optimization of the energy usage is also another aspect that the study was focused on.

The production process (Earle, 2004) of dry mango chips is consists with different stages (Fig.1). Starting from washing, the total process takes about 52 *hours* per cycle. Approximately 800 *kg* of wet mango chips are processed in one cycle.

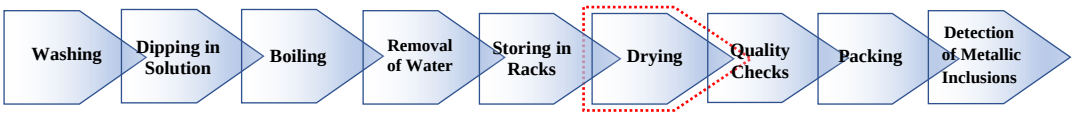

Fig. 1. Production process of dried mango chips

The time study confirmed that the drying stage is the highest time-consuming stage of the entire production process which takes about 24 hours. That is about 46% of the total time per cycle (Fig.2). Stages such as 'dipping in the solution' and 'boiling' must be performed for the specific time (pre-determined according to the quality requirement of final product) which cannot be modified. 'Washing', 'storing on racks', 'quality checking' and 'packing' are manual processes and if required, the time could be reduced by assigning more labor force which is a trade-off where more wages must be paid. But it is obvious that the reduction of time other than 'drying' stage will not significantly improve the productivity of the entire process. So, a reduction in time-consumption for drying would affect the productivity of the entire process.

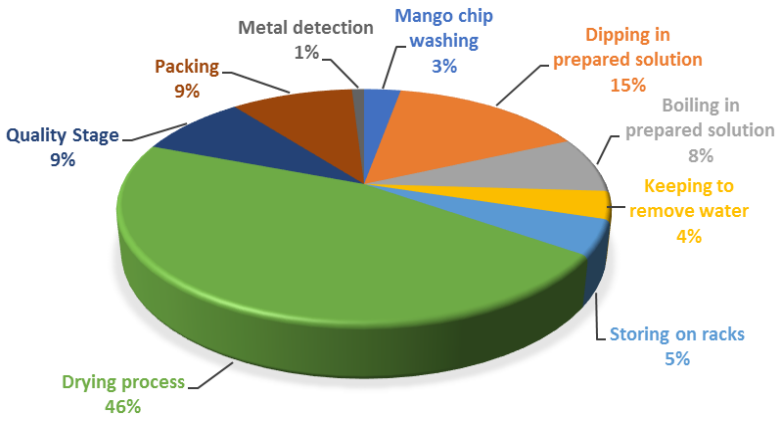

Fig. 2. Time consumption percentage of each production stage

The top management of the industry is also interested in analyzing the possibilities of improving the drying process and given their blessings to incorporate modifications to reduce the drying time. The wet mango chips at 'water removing stage' and 'stored in racks for drying' are shown in Fig.3 *a* and *b* respectively.

a. Chips at water removing stage **b. Wet chips on racks before send to dryer**

Fig. 3. Wet mango chips used for ongoing production process

Changes to any stage of the process must be done without affecting the quality standards of the end-product. The main aim is to propose suitable modification to reduce the drying time of mango chip production process. The total process needed to be studied and must identify the parameters related to ongoing drying process. After the proposed modification is implemented, the improvements are assessed and justified.

2 METHODOLOGY

A time study was carried out (average value of randomly selected five production cycles over a time span of two weeks were considered) and identified that the most effective way to increase the productivity is by reducing drying time. Hence drying stage was further studied. Specifications, controlled parameters, working ranges of the existing dryer were identified. Dryers, working principles of dryers, controllable factors, and efficiency of drying etc., were studied under literature review.

Two modifications were proposed, and experiments were conducted to select the effectiveness of each. A mathematical model was developed and the variation of the theoretical drying time with the relative humidity was studied. Results of these analysis were used to propose feasible and cost-effective method which could reduce the drying time and thereby to improve the productivity. Finally, the proposed modification was implemented and evaluated.

2.1. Drying Process, Parameters and Quality Requirements

The existing dryer (length-3.5 *m*, width-2 *m*, height-2.4 *m*) manufactured in India, is shown in Fig.4. It can operate by steam or electricity. To obtain the dried chips in acceptable standards, the parameters such as drying temperature, duration, set after conducting extensive R&D work. Any parametric changes should be done after careful investigation. Initially, the drying temperature is set at 70˚C for 2 *hours* and thereafter, it is set to 60˚C until the drying completes. This drying plant is electrically operated to accommodate easy change in temperature. If steam is used, the heated air temperature cannot be varied.

Quality inspections are conducted within the drying stage and after the drying stage. Within the drying stage the moisture value of the product is measured several times to verify the product's moisture content, which is the most critical quality parameter.

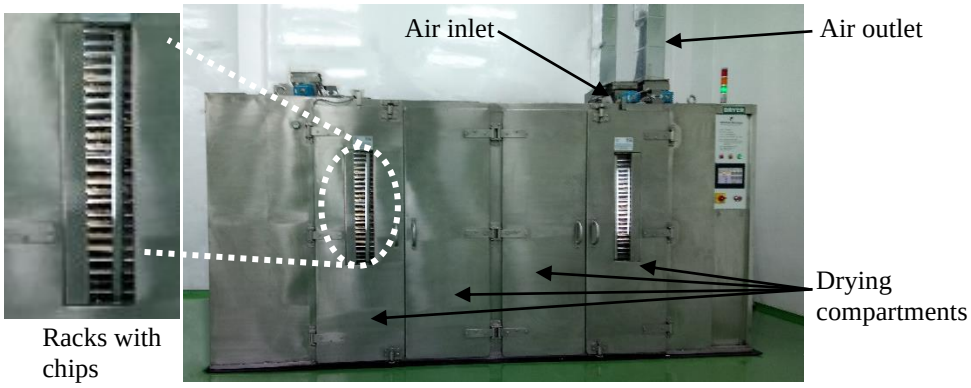

Fig. 4. Dryer used for the production process of dried mango chips

Moisture content was initially measured after 2 *hours* and then once in every 4 *hours* until the value comes down to 20%. Once the moisture content becomes below 20%, hourly measurements were taken to verify the specific dryness of the chips. The moisture content should be less than 14% to minimize the activeness of microorganisms (Parikh, 2014). At the end of drying water-activity was also checked. The water activity must be maintained below 0.7 to prevent the growth of microorganisms (FDA, 2014). The limiting values and measurement intervals are indicated in Table 1. After meeting the required levels of moisture content and water-activity, the drying stage completes. The dried mango chips will be sorted out by color and the size before packaging.

Table 1 Summery of controlled parameters and their ranges

Set temperature	***Duration***	***Moisture Checking Interval***
70 ˚*C*	Initial 2 *hours*	After 2 *hours*
60 ˚*C*	2hrs - Until drying complete	Every 4 hours; till moisture reading gets down to 20%
		Every hour when moisture reaches below 20%
Limiting values of Moisture and Water Activity		
Parameter		***Limit***
Moisture		Below 14%
Water activity		Below 0.7

2.2. Existing Air Path of Dryer

The current configuration of the dryer is shown in Fig.5. The ambient air is directly fed into the dryer and the humid air release to the atmosphere from the exhaust.

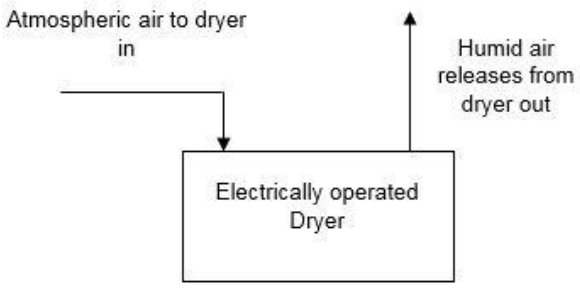

Fig. 5. Schematic diagram of existing configuration of the air path of dryer

2.3. Experiments

The concept behind the 'condensing dehumidifiers' (Jessica Lamond, 2011) was used to develop the experimental model. Two locally made finned heat exchanges with appropriate dimensions (14" x 18") were used to cool the air-in. Since the dryer has its own heating elements it could be used to perform the role of the condenser of the dehumidifier. Chilled water was used as the cooling media. Considering the following two scenarios, experiments were conducted to evaluate the performance.

1. Effect on the drying time by reducing the humidity of ambient air which directs to the dryer.
2. Effect on the drying time by recycling the outlet air back into the dryer after reducing its humidity.

The appropriately equipped experimental model (dehumidification unit) in Fig.6, is made of stainless steel well-sealed housing enabling following assumptions to be made; the heat loss to the surrounding is negligible, kinetic and potential energy changes of the air flow is negligible, pressure drop through the heat exchanger is negligible, air flow is equally distributed over the heat exchanger, heat exchanger tube surface area is negligible, parameters such as air properties, initial product moisture, unit inlet air temperature, cooling water inlet temperature, air flow rate and cooling water flow rate remain constant throughout the experiment and a complete heat transfer occurs through the process.

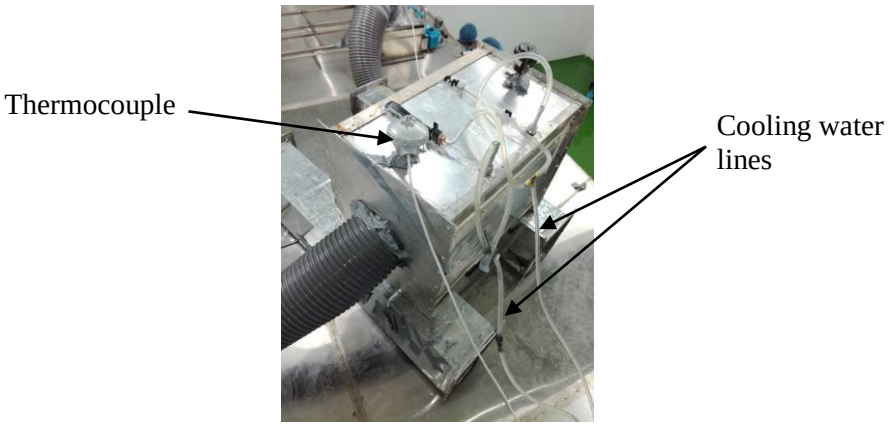

Fig. 6. Model unit used for experiments

Experiment 1

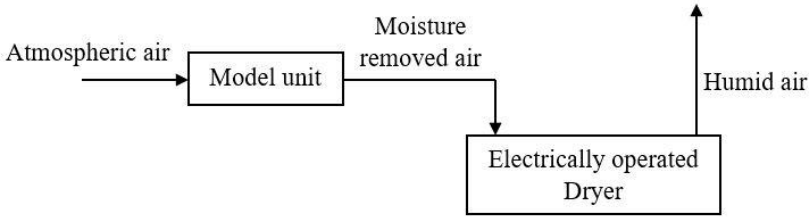

Fig. 7. Setup of Experiment 01

The relative humidity of the ambient air was reduced by the unit (Fig.7) and it was maintained until the experimental cycle is finished. The total drying time and outlet temperatures was measured. The dryer energy consumption was also noted with the product qualities. The measured parameters are;

Calculated dew point - 25.17 ˚C
Avg. unit out air Temp. - 25.67 ˚C
The drying time - 23 hrs 46 min
Product moisture - 13%
Water activity - 0.65
Power Consumption - 1028.6 kWh

Experiment 2

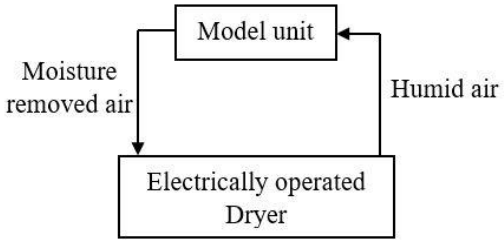

Fig. 8. Setup of Experiment 02

This was done by connecting the dryer exhaust into the inlet of the unit (Fig.8) and procedure and observations were similar to the Experiment 01. The measured parameters are;

Calculated dew point - 55.6 ˚C
Avg. unit out air Temp. - 46.0 ˚C
Total drying time - 20 hrs 13 min
Product moisture - 11.78%
Water activity - 0.6
Power Consumption - 815.4 kWh

Results of experiments

In experiment 1 it was difficult to achieve model unit outlet air temperature below to the dew point temperature. There was no considerable variation of the drying times, and it increases the energy consumption of the dryer. In experiment 2, model unit air temperature goes below to the dew point temperature and drying time was considerably reduced. The power consumption was also reduced.

2.4. Mathematical Model

Water can only evaporate from an object if the air around it can absorb more water (Ahrens, 2006). This could be measured by the relative humidity. A mathematical model was developed to verify the effect of the relative humidity to the drying process. Fig.9 illustrate the overview of the mathematical model.

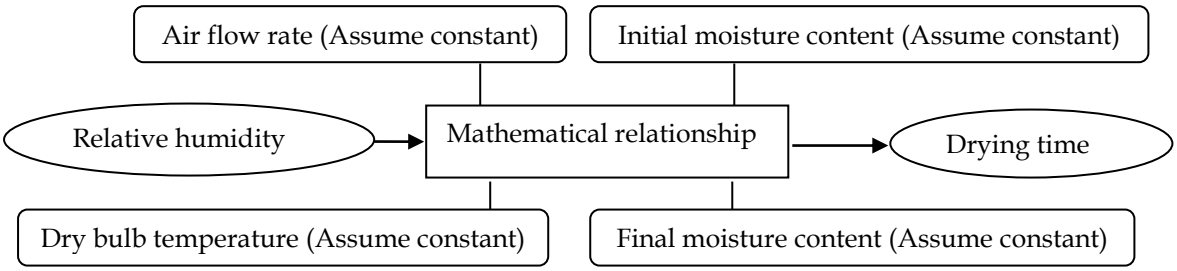

Fig. 9. Overview of the mathematical model

The relationship of drying rate at constant rate period (Perry, 1997) is given by equation (1).

$$Kcv = \frac{bG^{0.8}(Td - Tw)}{\lambda} \quad (1)$$

The total drying time of a material is a combination of constant rate drying and the falling rate drying (IASRI, 2012). The relationship of total drying time is given in equation (2).

$$t = \frac{(W - Wc)}{Kcv} + \frac{Wc}{Kcv \times \ln \frac{Wc}{Wi}} \quad (2)$$

At a certain moisture level of a material, it tends to fall the drying rate. This moisture level is called as the critical moisture level. This is occurred due to the limited moisture content of the material. Critical moisture content for a material needs to find through lengthy experiments. Hence assumed that the total drying time occurs at constant drying region. An equation for the theoretical drying time (t) derived using equations (1) & (2),

$$t = \frac{\lambda K}{bG^{0.8}(Td - Tw)} \quad (3)$$

Considering the constant parameters of the process, assigning a constant factor 'K',

$$t = \frac{\lambda K}{(Td - Tw)} \quad (4)$$

According to equation (4), the total drying time is depending on the dry bulb temperature of the air (T_d), wet bulb temperature of the air (T_w) and latent heat of vaporization (λ) at temperature T_w. The dry bulb and wet bulb temperatures depends on relative humidity. Latent heat of vaporization is depending on the temperature.

Based on the second scenario of the experiments, consider the dry bulb temperature as 60˚C for calculations for several relative humidity values. Wet bulb temperature for the relative humidity is taken from an online calculator (Knight, 2006). The latent heat of vaporization (λ) is taken from an online calculator (EngineeringToolBox, 2010). The constant factor (K) assumed as '1' for the calculation and plotted a scatterplot to identify the theoretical drying time variation with relative humidity (Fig.10) for 60˚C dry bulb temperature. In the practical case, the 'K' having a value specified to the production process.

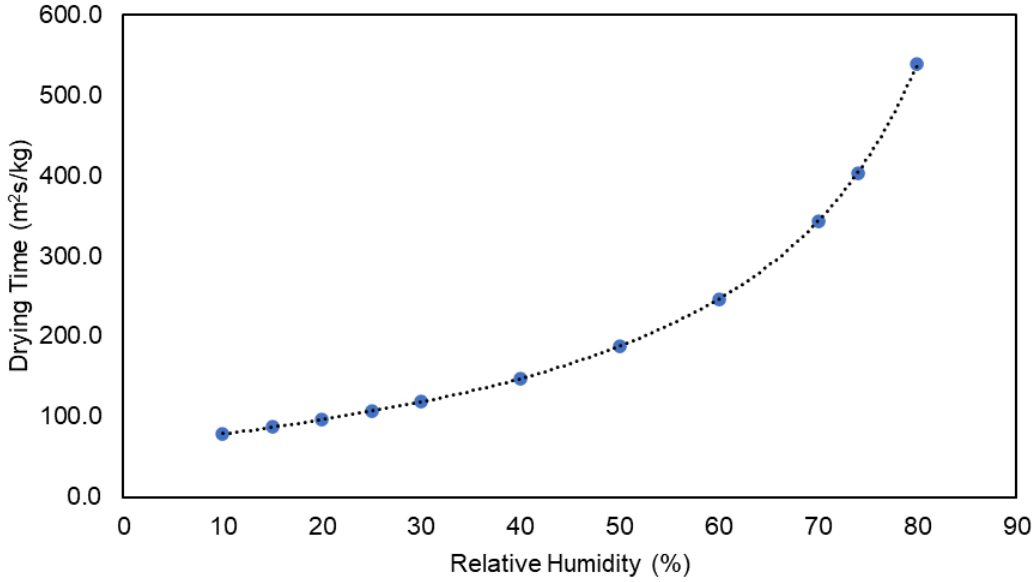

Fig. 10. Theoretical drying time variation with dryer inlet air relative humidity for 60˚C dry bulb temperature

Fig.10 confirmed that the reduction of relative humidity direct to reduce the drying time.

Equation (4) does not include the relative humidity directly. Hence, a higher polynomial equation is generated from Microsoft excel based on the curve of Fig.10 as the modified mathematical model. Equation for the total drying time (T) against relative humidity for 60 ˚C,

$$T = (2\times10^{-8}X^{6}) - (4.35\times10^{-6}X^{5}) + (3.8516\times10^{-4}X^{4}) - (168.1113\times10^{-4}X^{3}) + (3975.9582\times10^{-4}X^{2}) - (2.90311755X) + 81.2726042 \quad (5)$$

This equation gives the total drying time in square meter seconds per kilogram (m^2s/kg). Hence another constant 'A' assigned to the equation to get drying time in seconds related to current drying process. This constant aligns the equation with the mango chip drying process. The unit of the constant is kilograms per square meters (kg/m^2).

$$T = A\{(2\times10^{-8}X^{6}) - (4.35\times10^{-6}X^{5}) + (3.8516\times10^{-4}X^{4}) - (168.1113\times10^{-4}X^{3}) + (3975.9582\times10^{-4}X^{2}) - (2.90311755X) + 81.2726042\} \quad (6)$$

Drying Time and Constant 'A'

The constant 'A' is estimated by observing the drying time for several relative humidity levels. Experiment 2 was done again to observe the drying time and the relative humidity. This was done by throttling the chilled water flow of the experimental unit to change the heat transfer. Due to the practical limitations, only 3 trials were done (Table 2).

Table 2 Theoretical and experimental drying times of mango chips

Relative humidity (%)	Theoretical drying time from mathematical model (m^2s/kg)	Experimental drying time (min)	Constant 'A' (kg/m^2)
65	291.5	1396	287
63	273.0	1322	291
57	228.0	1213	319

Comparing observed drying time with mathematically observed time, the constant 'A' for 3 cases found as 287, 291 and 319. Therefore, as fair value the average of above 3 is taken as the constant for the equation to set up the equation for the current process.

$$\text{Constant 'A'} = \frac{(287+291+319)}{3}$$
$$= 299\ kg/m^2$$

2.5. Comparison of the Results from Experiments and Mathematical Model

The experimental drying time is much higher than the theoretical drying time obtained through the mathematical model. The mathematical model was formed using few constants and assumptions. But in the practical scenario it is difficult to control all these parameters constantly without minor changes. The experimental value is higher than to the theoretical value. A multiplication constant 'A' to the mathematical model was considered to minimize the effect of such assumptions. By the experimental data the constant 'A' was calculated. Practically it is not possible to operate every cycle with similar/constant parameters (e.g., Initial moisture content of the mango chips, slice thickness, constant surface area etc.). Hence it changes the 'A' value from one cycle to another. Due to the practical limitations, the constant 'A' was defined considering only three cases. It can be further correct by increasing the number of trials.

3 PROPOSED DESIGN

Since the critical temperature limits are known, Logarithmic Mean Temperature Difference (LMTD) method is used to design the heat exchangers (Ezgi, 2016), The proposed modification is to install an external unit to the dryer inlet air path to reduce the relative humidity of the of the air which sends into the dryer (Fig.11). Prior tests were carried out to check and optimize the operational parameters.

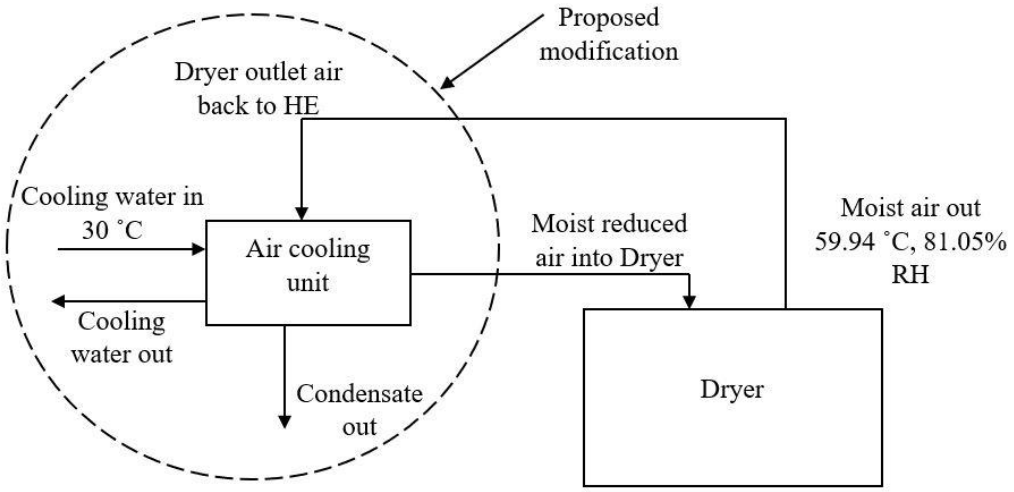

Fig. 11. Schematic diagram of the proposed arrangement

Considering the cost factor and feasibility, raw water (30˚C) is proposed to use as cooling media since the expected temperature difference can be achived. Along with the humidity reduction, the energy can also be saved due to the re-circulation of the air.

4 RESULTS AND DISCUSSION

The outer 3D view and the internal arrangement of the unit is illusrated in Fig.12 (a) and (b). A picture of the total drying unit with the intruduction of the new unit is shown in the Fig.13.

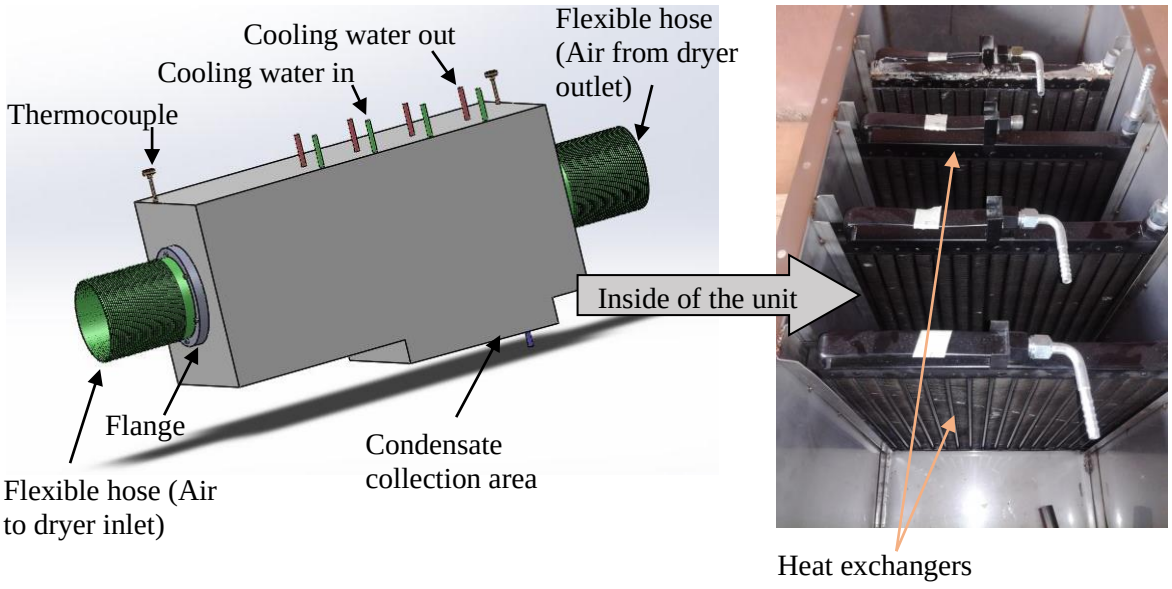

a. Details of the unit **b. Inside of the unit**

Fig. 12. Designed unit

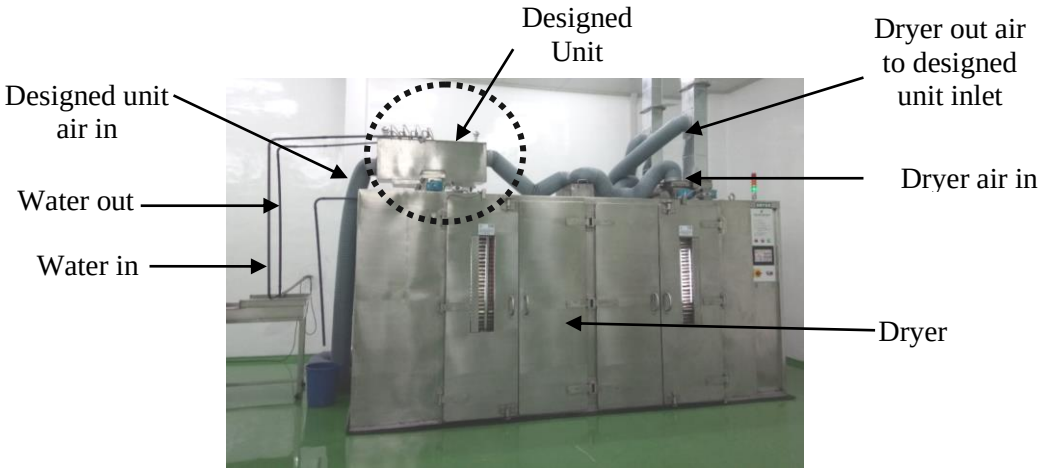

Fig. 13. Introduction of the new unit to the dryer for testing

The retrofitted dryer was tested for 3 production cycles and results were observed (Table 3). From the observed data, the average temperature at unit outlet and the average relative humidity at dryer inlet were calculated.

Table 3 Comparison of test results before and after the modification

Observation	Total Drying Time (min)	Product Moisture (%)	Water Activity	Avg. Temperature at Unit Outlet (˚C)	Avg. Relative Humidity Dryer inlet (%)	Power Consumption (kWh)
1	1383	11.69	0.62	53.5	65	834.3
2	1404	11.58	0.64	55.08	67.25	839.1
3	1392	11.36	0.61	53	64.1	836.6
Before modification	1440.7	11.21	0.61	-	86.4	957.93

Samples were taken from the batches prior and after the modification. The taste is the key factor of the final product as this is a snack. Considering the taste of the chips, no one who involved in taste testing trials (20 people were used) were able to distinguish a taste different in any sample.

The capital cost for the proposed modification is evaluated as around Rs. 109,000.00. Considering only the 'energy saving' aspect this capital cost could be recovered withing 2 ½ months. If the 'increment of profit' due to upsurge of the productivity, the payback period will be reduced further.

5 CONCLUSION

After implementing the proposed modification, the drying time was reduced, and the productivity of the total mango chip manufacturing process was increased by a considerable margin. A significant reduction of power consumption has also been achieved. A saving of 3.26% drying time per one batch was observed. Since the

production process runs continuously, this reduction saves a time for nearly extra one batch for a month, i.e., it allowed to process additional one batch (800 kg) of wet mango chips per month with current facilities. Taking it to consideration a 3.26% increment of the productivity could be achieved. Also, a considerable reduction of 12.65% energy usage per batch is obtained. The capital cost for the proposed modification is Rs. 109000.00. Considering the savings only due to reduction in energy consumption, this capital cost can be recovered within less than 2 ½ month and this payback period could be further reduced by accounting productivity improvement.

Based on the outcome of the project, the humidity reduction of the dryer exhaust air and recirculating the air back to the dryer have improved the productivity of the plant. This improvement can be further enhanced by reducing the relative humidity of the air (proves by the mathematical model). This is be achieved by reducing the temperature (or by using chilled water) of the cooling media. But it needs a continuous supply of chilled water which incur an additional cost and needed to be done in a controlled manner, otherwise the power consumption of the dryer will be increased. This modification can be adapted to any organization who used cabinet dryer/tray dryer for food drying purpose to improve the productivity while reducing the energy consumption.

6 ACKNOWLEDGEMENTS

Sincere gratitude will be given to the venture for giving the opportunity to conduct this project and for the given financial support.

REFERENCES

Ahrens, C. D., 2006. Atmospheric Moisture. In: *Meteorology Today*. 8 ed. s.l.:Cengage Learning, Thomsan Higher Education, pp. 89-91.

Earle, R. L., 2004. Drying. In: *Unit Operations in Food Processing, Web Edition.* s.l.:The New Zealand Institute of Food Science & Technology (Inc.).

EngineeringToolBox, 2010. *Water - Heat of Vaporization.* [Online]
Available at: https://www.engineeringtoolbox.com/water-properties-d_1573.html
[Accessed 03 January 2020].

Ezgi, C., 2016. *Basic Design Methods of Heat Exchanger.* [Online]
Available at: https://www.intechopen.com/books/heat-exchangers-design-experiment-and-simulation/basic-design-methods-of-heat-exchanger
[Accessed 16 January 2020].

FDA, E. o., 2014. *Water activity in Foods.* [Online]
Available at: https://www.fda.gov/inspections-compliance-enforcement-and-criminal-investigations/inspection-technical-guides/water-activity-aw-foods
[Accessed 01 November 2019].

IASRI, 2012. *Food Engineering.* [Online]
Available at: http://ecoursesonline.iasri.res.in/mod/page/view.php?id=3463
[Accessed 28 December 2019].

Jessica Lamond, C. B. F. H. D. P., 2011. A Practical Guide to Drying a Water Damaged Dwelling. In: *Flood Hazards: Impacts and Responses for the Built Environment.* s.l.:CRC Press, p. 106.

Knight, J., 2006. *Psychrometric Calculator.* [Online]
Available at: https://www.kwangu.com/work/psychrometric.htm
[Accessed 03 January 2020].

Parikh, D. M., 2014. *Solids drying: Basics and applications.* [Online]
Available at: https://www.chemengonline.com/solids-drying-basics-and-applications/?printmode=1
[Accessed 17 September 2019].

Perry, R. H., 1997. *Perry's Chemical Engineers' Handbook.* 7th ed. s.l.:McGraw-Hill.

Journal of Engineering and Technology
The Open University of Sri Lanka (JET-OUSL), Vol. 10, No.1, pp. [46-62], 2022

Reliability Improvement of the Medium Voltage Distribution Network Owned by Lanka Electricity Company: A Case Study in Kalutara Area

A.P. Wadduwage[1*], L.A. Samaliarachchi[2]

[1]Department of Electrical and Computer Engineering, The Open University of Sri Lanka, Nawala, Nugegoda, Sri Lanka.

*Corresponding Author: email: amilapradeep18@gmail.com, Tele: +94719537425

Abstract – *This paper presents the reliability and quality improvement of the medium voltage (MV) electricity distribution network owned, operated and maintained by Lanka Electric Company (LECO) in Kalutara area. MV distribution network established in Kalutara area is found to be rapidly growing owing to the load growth and hence a reliable and quality distribution network is required to meet the challenges in upcoming years 2022-2025. Therefore, modern technical evaluation methods are used to carry out the required study to reach techno-economically attractive optimal solution. An Artificial Neural Network based short term load forecasting method is used to predict the demand followed by Monti-Carlo simulation approach to ascertain the most appropriate distribution reliability model. Thereafter, OpenDSS software package in association with MATLAB based randomized load flow analysis is carried out to check the system performances of the proposed network configurations. Finally, the Cost of Energy Not Served (ENS) is used to evaluate the optimal network configuration.*

Keywords*: Medium Voltage Distribution, Artificial Neural Network, Distribution Reliability, Monti-Carlo simulation, Randomized load flow, Energy Not Served*

Nomenclature

ANN - Artificial Neural Network
MC - Monti Carlo
SAIDI - System Average Interruption Duration Index
SAIFI - System Average Interruption Frequency Index
ENS - Energy Not Served

1 INTRODUCTION

Sri Lanka has faced an economic collapse in the years 2019–21 and worsened the situation owing to the locally affected Easter Sunday attack and globally affected corona pandemic. Subsequent effects have slackened the expansion of electrical distribution networks to meet the growing power and energy demand at medium voltage distribution levels. Under the circumstances, forecasting power and energy demand, which enables to maintain existing distribution networks and future expansions while minimizing the forced outages and network losses, in the upcoming era will be a major challenge that must be thoroughly examined. Moreover, the changes that must be made to improve the network performance should be more economically attractive as well. This research study carried out to improve the existing medium voltage (MV) distribution network reliability and quality in Kalutara area of LECO franchise as a case study, using the system elements currently in use or to

add an optimum number of new elements if there is any, that yield towards a better techno-economical solution. MV distribution network in Kalutara owned/maintained by LECO covers many urban and critical areas. Reliability of the said network is considered as an important factor owing to compaction of commercial buildings, district government offices and industrial consumers. MV network consists of three Primary Substations (PS). Molligoda PS emanate three feeders: Pirivena Road (PVR), Pothupitiya (POP) and Wadduwa (WAD). Kalutara North PS emanate three feeders: Hotel (HOT), Nagas Junction (NAG) and Waskaduwa (WAS). Fullerton PS emanate four feeders: Hillside (HIS), Kalutara North (KTN), AMW and Payagala (PAG). Payagala (PAG) feeder is not considered in this study since PAG feeder is owned by Payagala Customer Service Center (CSC). Study focuses on developing an ANN short term load forecast model and subsequently a reliability model to improve reliability and quality of the distribution network. Initial investigation consists of observing the system performance of existing electrical distribution network and thereafter remedial measures are proposed with an intension to improve the same.

2 LOAD FORECAST

Initially, a short-term load forecast is carried out to identify the maximum demands of each distribution feeder. In here, multi regression statistical analysis and artificial neural network methods are used. IBM Statistical Package for the Social Sciences (SPSS) software is used for multi regression analysis whereas MATLAB 2018Ra software is used for ANN method as depicted in Figure 1.

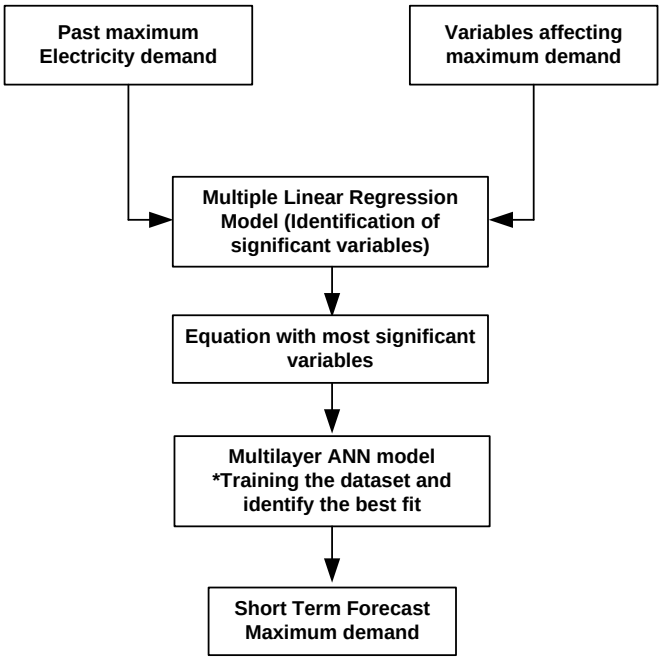

Fig. 1. Flow Chart showing demand forecasting method

MATLAB ANN toolbox is used for demand forecasting with Multilayer Feed Forward Neural Network structure. The multi-layer ANN model as shown in Figure 2 is used to construct the most appropriate architecture for ANN. Gross Domestic Product (GDP), Gross Domestic Product Per Capita (GDPPC), Population, Total number of consumers, Tourist Arrivals, Average Temperature (TMP) and Average Relative Humidity (RH) data are used as dependent variables to construct the ANN model. GDP and GDPPC forecast and historical data are taken from the International Monitory Fund database. TMP and RH

data are taken from the Department of Meteorology. Population and consumer count are taken from the Department of Census and Statistics and LECO database. The consumer count is statically forecasted with combination of population growth. Further World Tourism Organization forecasts are taken to modify the tourist arrival data.

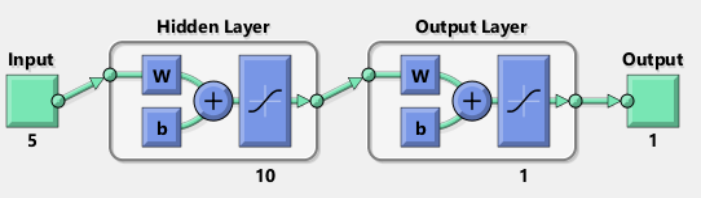

Fig. 2. Multilayer ANN model

Table 1 ANN structure

Description	ANN structure
No of hidden layers	1
No of Hidden neurons	10-13 varies for feeders
Activation function of hidden layer	Tan sigmoid
Activation function of output layer	Pure linear
No of neurons in the output layer	1
Training function	Trainbr

Kalutara Hotel, Molligoda Wadduwa, Molligoda Pirivena Road and Fullerton AMW feeders are forecasted with ANN. Kalutara Waskaduwa and Molligoda Pothupitiya feeders are observed as small feeder sections with saturated peak loads and cannot be forecasted with ANN. Fullerton Hill Street, Fullerton KTN and Kalutara Nagas junction feeder data are severely fluctuated owing to re configuration after 2018 and 2019 years. Therefore, those feeders are not forecasted with ANN and the load growth is separately modified with other feeder ANN forecast growth and statistical growth of the same feeder. Moreover, the correlation coefficients between distribution feeders are calculated up to 2019 and 2021 years separately. Growth of the network demand is observed to be changed after 2020 year owing to pandemic situation and economic crisis. Variables which have strong positive correlation coefficient up to the year 2021 are used by regression analysis while ANN utilized all the strong positive variables until 2019. Correlation coefficients of the variables with respect to all the feeders are shown in Table 2.

Table 2 Correlation coefficients of variables with respect to the feeders

Dependent variable	Variables	Correlation Coefficient							
		Hotel Feeder		AMW Feeder		Wadduwa Feeder		Pirivena Road Feeder	
		Up to 2019	Up to 2021	Up to 2019	Up to 2021	Up to 2019	Up to 2021	Up to 2019	Up to 2021
Maximum demand (Amps)	GDP	0.914	0.825	0.981	0.963	0.911	0.901	0.935	0.841
	GDPPC	0.838	0.836	0.944	0.935	0.840	0.769	0.864	0.628
	Population	0.982	0.444	0.932	0.615	0.970	0.811	0.987	0.953
	Total consumers	0.988	0.427	-	-	0.973	0.800	0.990	0.946
	Tourist arrivals	0.926	0.787	-	-	-	-	-	-
	TMP_ average	0.681	0.283	0.453	0.233	0.543	0.506	0.551	0.666
	RH_ average	-0.274	-0.178	-0.234	-0.149	-0.135	-0.183	-0.200	-0.309

2.1 Kalutara PS to Hotel feeder maximum current demand forecast

GDP, GDPPC, Population, Total consumers and Tourist arrivals data are used for ANN and GDP, GDPPC and Tourist Arrival data are used for Regression analysis respectively. Demand forecast is as shown in Figure 3. Table 3 shows the tested Mean Square Error.

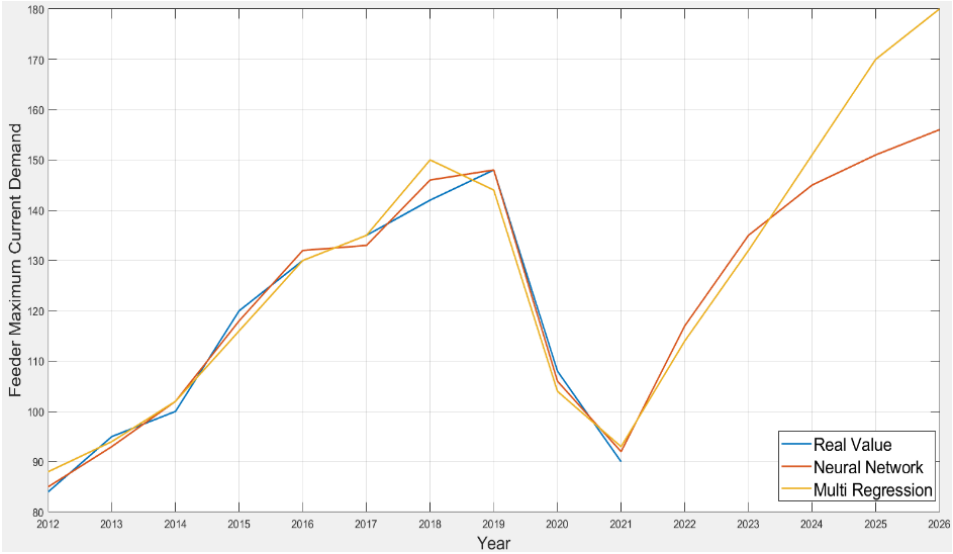

Fig. 3. Hotel feeder maximum current (Amps) demand forecast

Table 3 Tested mean square error

Hidden Layers	MSE (ANN)	MSE (Multi Regression)
13	4.71	13.99

2.2 Fullarton to AMW feeder maximum current demand forecast

GDP, GDPPC and Population data are used for ANN forecast. Only GDP and GDPPC data are used for Regression analysis. This is shown in Figure 4. Table 4 shows the tested Mean Square Error.

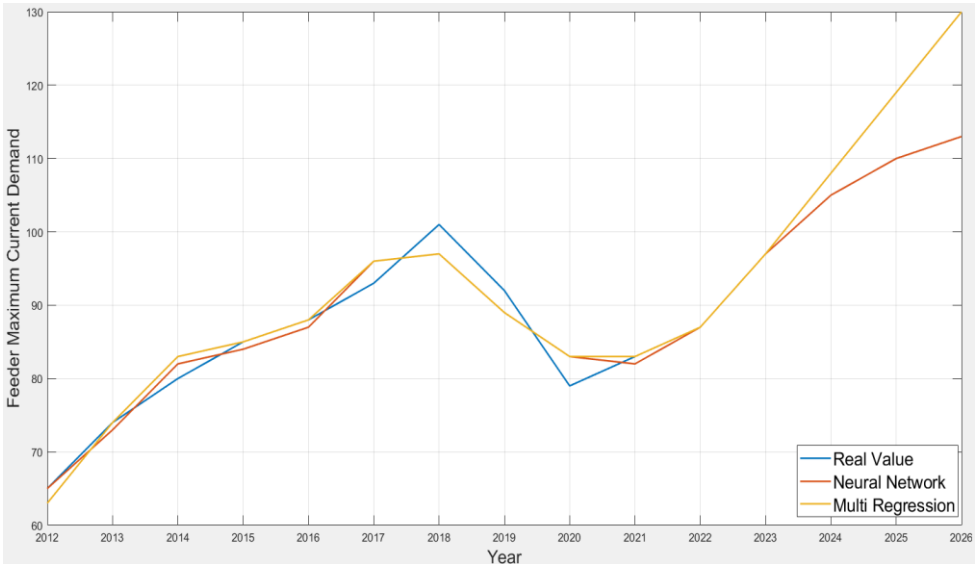

Fig. 4. AMW feeder maximum current (Amps) demand forecast

Table 4 Tested mean square error

Hidden Layers	MSE (ANN)	MSE (Multi Regression)
10	5.57	6.43

2.3 Molligoda to Wadduwa feeder maximum current demand forecast

GDP, GDPPC, Population and Total consumer count data are used for ANN forecast. GDP, Population and Total consumer count data are used for Regression analysis. This is shown in Figure 5. Table 5 shows the tested Mean Square Error.

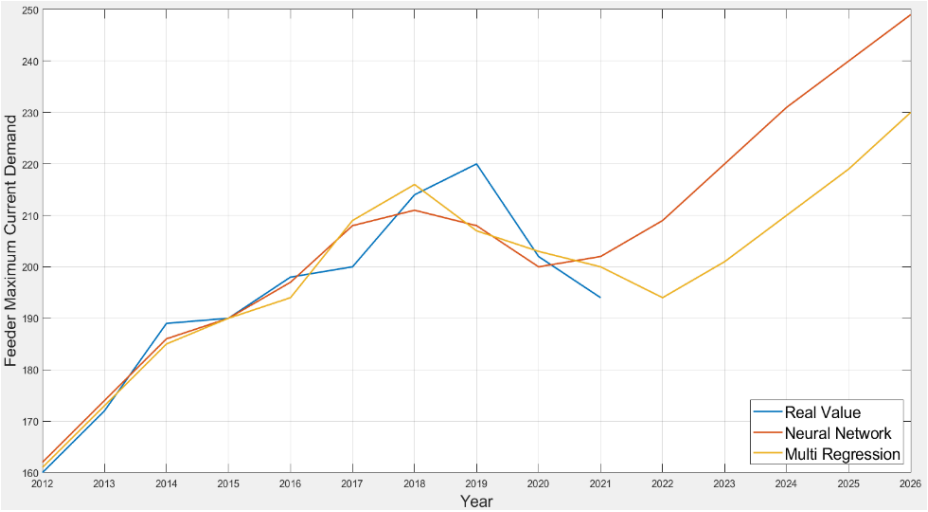

Fig. 5. Wadduwa feeder maximum current (Amps) demand forecast

Table 5 Tested mean square error

Hidden Layers	MSE (ANN)	MSE (Multi Regression)
15	30.84	32.38

2.4 Molligoda to Pirivena road feeder maximum current demand forecast

GDP, GDPPC, Population data and Total consumer count data are used for ANN forecast. GDP, Population data and Total consumer count data are used for Regression analysis. This is shown in Figure 6. Table 6 shows the tested Mean Square Error.

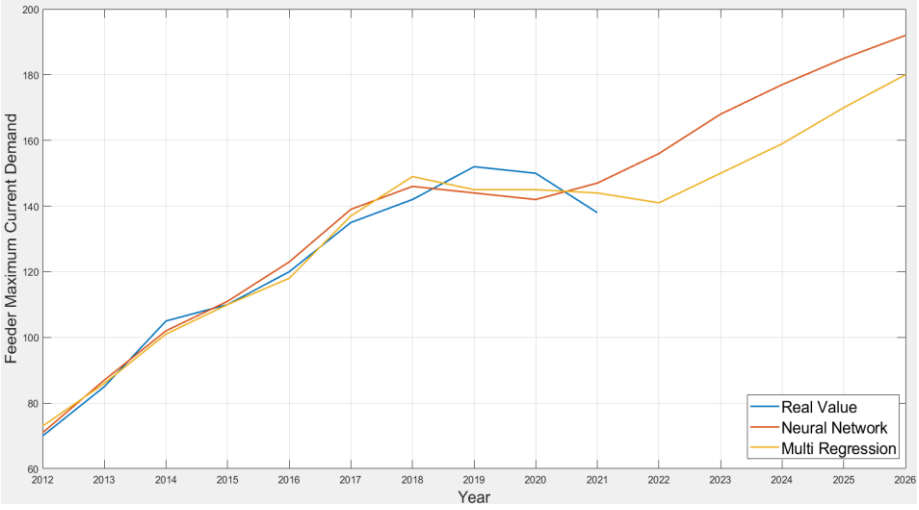

Fig. 6. Pirivena road feeder maximum current (Amps) demand forecast

Table 6 Tested mean square error

Hidden Layers	MSE (ANN)	MSE (Multi Regression)
10	25.69	20.47

3 QUANTITATIVE ANALYSES

OpenDSS Version 9.3.0.1 distribution analysis software package supported by MATLAB 2018Ra is deployed to carry out load flow simulations to arrive at technically feasible solution. In here, load points are randomly varied to catch the maximum feeder current. As such, two thousand (2000) randomizations of loads followed by associated load flow simulations are carried out for a single network configuration. Variation of load demand is randomized between 20-40% of maximum demand and the feeder maximum demand. The planning criteria applied to verify and reach the best network configuration is:

- Voltage at loads should not be greater or less than 4% of its rated operating voltage
- Line losses should not be greater than 1% of the total delivery
- Lines are not overloaded (not more than 50% the thermal rating)
- Primary Substation should not be overloaded (not more than 60% of its rated capacity)

OpenDSS and MATLAB-Com interfaces are used to establish connection between MATLAB and OpenDSS. Figure 7 shows data feeding from MATLAB through Com interface and data returning from OpenDSS.

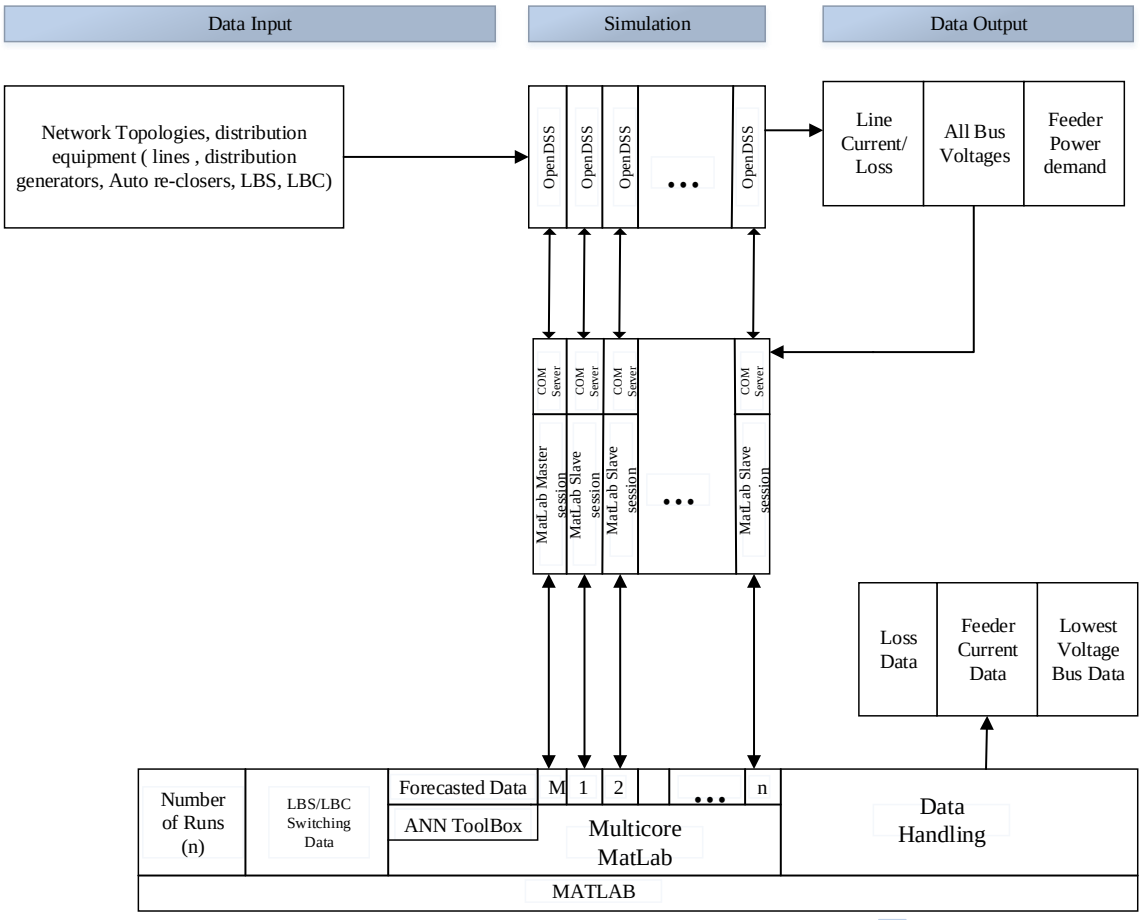

Fig. 7. OpenDSS and MATLAB interfacing

Flowchart showing the load randomization algorithm and load flow simulation handling is as shown in Figure 8. Two thousand randomized loads are generated for each node and feed to OpenDSS to get results in this process.

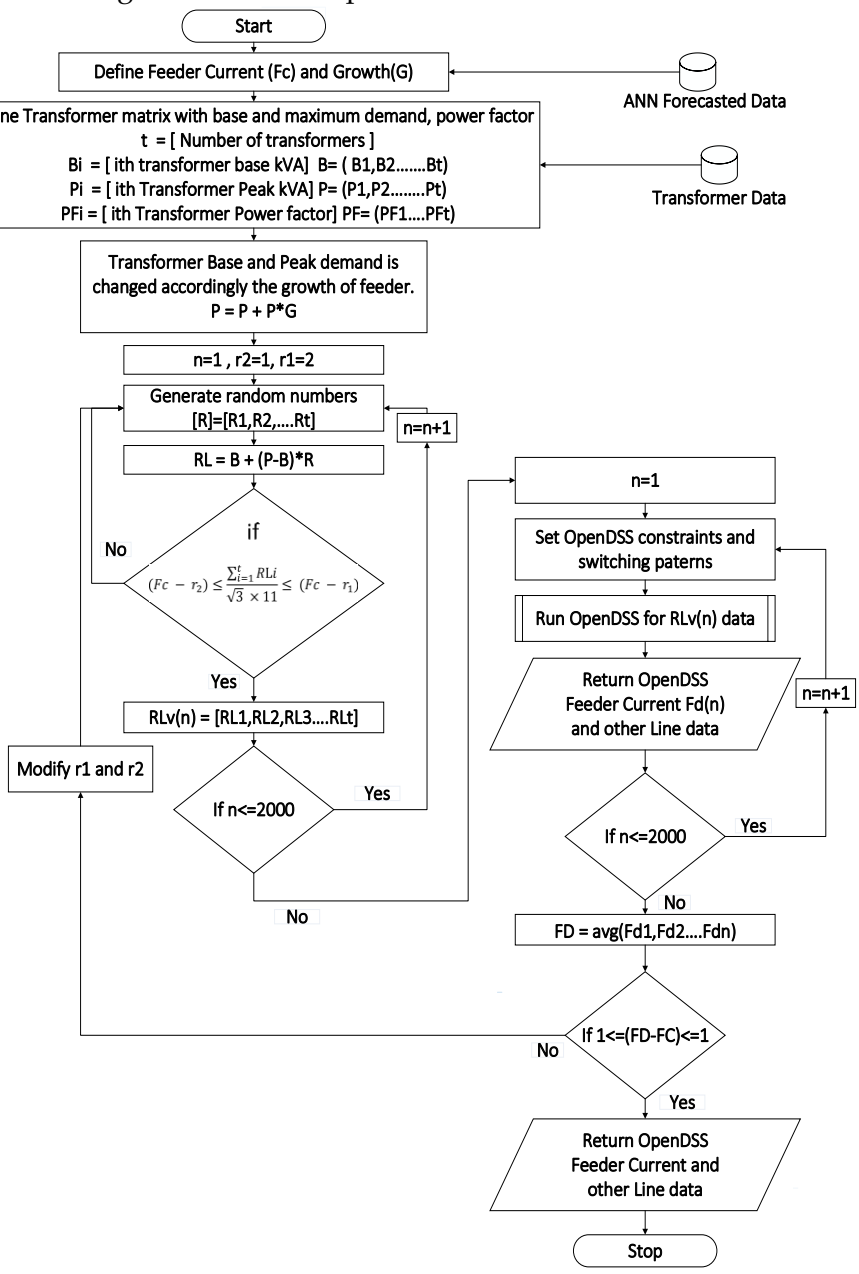

Fig. 8. Load randomization and load flow handling flowchart

1. Start
2. ANN forecasted data and growth data is taken. *(Feeder Current-Fc, Year Growth-G)*
3. Transformer base load and peak loads are defined. Transformer power factor and unique numbers are defined.

t = number of transformers	*Bi = i^{th} transformer base demand kVA*
B = [B1, B2, B3…....Bt]	*Pi = i^{th} transformer peak demand kVA*
P = [P1, P2, P3……. Pt]	*PFi = i^{th} transformer power factor*
PF = [PF1, PF2, PF3,….PFt]	*Ri = Random number between 0-1 for a node i*

4. Set n = 1 and r1=1, r2=2

5. Peak load is modified according to yearly growth for next year.

$$P = P + P*G$$

6. Generate random numbers between 0 and 1

$$R = [R1, R2, R3\ldots\ldots Rt]$$

7. Node loads are randomized $RLi = Bi + [Pi-Bi] *Ri$ & $RL = [RL1, RL2, RL3,\ldots\ldots RLt]$

8. Check loads are in between feeder current. Set variation in between Fc-r1 and Fc-r2.

$$\text{If } (Fc - r_2) \leq \frac{\sum_{i=1}^{t} Ri}{\sqrt{3} \times 11} \leq (Fc - r_1) \text{ go to step 9.} \quad \text{Else go to step 6}$$

9. Update the matrix with all randomized loads (RLv) with RL data $RLv(n) = RL$

10. If n<2000 go to step 6 by incrementing n by 1. Else go to step 11

11. Set n =1

12. Set OpenDSS constraints and run OpenDSS for RLv(n) data

13. Return OpenDSS feeder current (Fdn) and other line data

14. If n<2000 got to step 12 by incrementing 1, else go to step 15.

15. Compute OpenDSS feeder current Average

$$FD = avg(F_{d1}, F_{d2}\ldots F_{dn})$$

16. If OpenDSS average feeder current (FD) and actual feeder current (FC) variation is greater than 1, move to step 6 by modifying r_1 and r_2. Else move to step 17.

17. Return OpenDSS feeder current and other line data.

Load flow studies are carried out for the year 2022 with the existing network condition and the study results are shown in Table 7. The system performance for the years 2022 and 2026 with the required modifications to the network to alleviate the limitations are shown in Table 8 and Table 9 respectively. Further, the developed load flow model is validated with the LECO load flow studies for better clarification.

Table 7 Load flow results for the existing network condition-Year 2022

Primary Sub Station	Feeder (ID)	Current (Amps)	OpenDSS-Load Flow Results						Planning Criteria (Violations)			
			Feeder (MVA)	Feeder Loss (kW)	Feeder Loss (%)	Lowest Voltage (pu)	PS Loading (Diversified) (MVA)	PS Loading (%)	Line Loss (<1%)	Bus Voltage 0.96<V<1.04	Feeder Loading (<50%)	PS Loading (<60%)
Kalutara 2×5 MVA	HOT	117.38	2.23	6.97	0.36	0.99						
	NAG	170.23	3.27	47.17	1.62	0.97			x			
	WAS	17.69	0.34	0.17	0.06	0.99						
							5.52	55.2				
Molligoda 2×5 MVA	POP	48.64	0.92	1.25	0.15	0.99						
	PVR	156.35	2.98	23.62	0.87	0.98						
	WAD	209.09	3.98	59.00	1.69	0.97			x		x	
							7.49	74.9				x
Fullerton 2×10 MVA	HS	221.08	0.93	1.21	0.14	0.99					x	
	KTN	93.96	1.79	11.63	0.69	0.98						
	AMW	87.34	1.66	3.9	0.27	0.99						
	PAG	105.01	2.00									
							9.18	45.9				
x = values exceeding the limits												

Table 8 Load flow results after network modification-Year 2022

Primary Sub Station	Feeder (ID)	Current (Amps)	OpenDSS-Load Flow Results						Planning Criteria (Violations)			
			Feeder (MVA)	Feeder Loss (kW)	Feeder Loss (%)	Lowest Voltage (pu)	PS Loading (Diversified) (MVA)	PS Loading (%)	Line Loss (<1%)	Bus Voltage 0.96<V<1.04	Feeder Loading (<50%)	PS Loading (<60%)
Kalutara 2×5MVA	HOT	117.38	2.23	6.97	0.36	0.99						
	NAG	57.06	1.09	2.61	0.26	0.99						
	WAS	17.69	0.34	0.17	0.06	1.00						
							3.48	34.8				
Molligoda 2×5MVA	POP	48.64	0.92	1.25	0.15	1.00						
	PVR	156.35	2.98	23.62	0.87	0.98						
	WAD	101.79	1.94	13.97	0.82	0.98						
							5.55	55.5				
Fullerton 2×10MVA	HS	133.70	2.55	18.97	0.83	0.98						
	KTN	122.83	2.34	21.47	0.99	0.98						
	AMW	87.34	1.66	3.9	0.27	0.99						
	PAG	105.01	2.00									
							8.12	40.6				
EUR 1×5MVA	EUR T	163.11	3.10	14.2	0.53	0.99	3.10	62.0				

Table 9 Load flow results after network modification-Year 2026

Primary Sub Station	Feeder (ID)	Current (Amps)	OpenDSS-Load Flow Results						Planning Criteria (Violations)			
			Feeder (MVA)	Feeder Loss (kW)	Feeder Loss (%)	Lowest Voltage (pu)	PS Loading (Diversified)	PS Loading (%)	Line Loss (<1%)	Bus Voltage 0.96<V<1.04	Feeder Loading (<50%)	PS Loading (<60%)
Kalutara 2×5MVA	HOT	156	2.96	12.42	0.48	0.98						
	NAG	64.33	1.23	3.30	0.29	0.99						
	WAS	21	0.41	0.25	0.07	0.99						
							4.37	40.37				
Molligoda 2×5MVA	POP	59	1.12	1.85	0.18	0.99						
	PVR	192	3.66	35.35	1.06	0.97						
	WAD	122.56	2.33	19.89	0.97	0.98						
							6.76	67.6				68
Fullerton 2×10MVA	HS	161.07	3.07	28.19	1.03	0.97						
	KTN	148.25	2.82	31.14	1.18	0.97			1.2			
	AMW	113	2.15	6.60	0.36	0.99						
	PAG	127	2.42									
							9.94	49.7				
EUR 1×5MVA	EUR T	212	4.04	24.2	0.70	0.99	4.04	80.8				

4 SIMULATION STUDY FOR RELIABILITY ASSESMENT

4.1 Reliability indices and Monte Carlo simulation

Three basic parameters are defined for components such as Transformers, Auto reclosers, Load break switch, Load break cut outs etc. connected in series for reliability studies in distribution planning and they are: the failure rate λ (interruptions/year), the interruption duration r (hours/interruption), and the unavailability U (hours/year).

$$\lambda = \sum_{i=1}^{N} \lambda_i \quad (1)$$

$$U = \sum_{i=1}^{N} \lambda_i r_i \quad (2)$$

$$r = \frac{U}{\lambda} \quad (3)$$

Where N = Total number of components in the system and i = Index of the node.

The reliability indices considered for distribution planning in this research study are SAIFI, SAIDI and ENS and can be expressed as:

1) System average interruption frequency index: $SAIFI = \frac{\sum_i \lambda_i N_i}{\sum_i N_i}$ (4)
2) System average interruption duration index: $SAIDI = \frac{\sum_i U_i N_i}{\sum_i N_i}$ (5)
   where N_i is the number of customers at load point i.
3) Energy not supplied: ENS (kWh/yr.) $ENS = \sum L_{a(i)} U_i$ (6)
   where $L_{a(i)}$ is the average load (kW) at node i

In here, N is the number of customers connected to the i^{th} node

The Monte Carlo (MC) method simulates the distribution system faulty situations in random manner. Probabilistic technique is used by MC simulation method to predict the behavior of the distribution system components. Sequential down status and up status of the components in distribution system can be simulated through MC simulation method. The time to failure (TTF) which is identified as time taken for a component to fail is randomly predicted by MC simulation as described in equation (7).

$TTF = -\frac{1}{\lambda} \ln(u)$ (7) where u is a uniformly distributed random number (0 to 1).

The time to repair (TTR) is defined as the time required to repair the failed component.

TTR is also estimated randomly using equation (8)

$TTR = -\frac{1}{\mu} \ln(u)$ (8) where μ is the repair rate of the component.

The behavioral pattern for a single component is as shown in Figure 9.

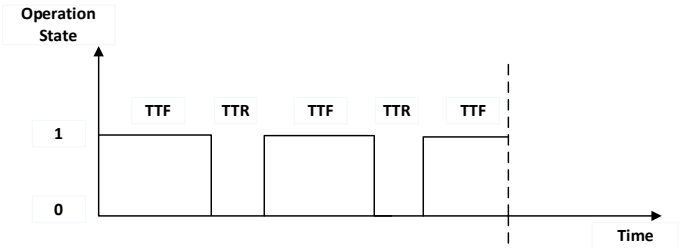

Fig. 9. A single component behavioral pattern

The time to switch (TTS) is separately modified for each feeder. A constant value is assumed for this figure after carefully observing historical outages. Both TTF and TTR are derived using exponential distribution. TTF and TTR for each component is created for one-year simulation period in sequential order. For better achievement of the results, MC simulation should be carried out for considerable number of simulation years, as such 5000 simulation years are considered in this research study.

4.2 Outages considered for MC simulation

There are three types of forced outages identified in LECO distribution system.

1. Repairable and Switchable outages (RS): Repair time and switching time are separately identified for those outages. In this case, section wise outages are modeled using components concentrated to one section.

2. Non repairable and non-switchable outages (NRS): Outages do not belong to RS are categorized under this section. Unknown cases and PS tripped cases are majorly found here. Those faults are factorized according to the affected consumer count to reach accurate reliability index.

3. Primary substation loss (PSL): Outage of the power supply connected to the PS are considered under this category and all the feeders connected to PS are on outage state.

In this research study, only the Repairable and Switchable cases are considered for system performance improvement and MC simulation. The rest of the two cases are considered to verify the results with historical data. NRS outages are factorized with the affected customers to build up the model for NRS outages. Finally, all the outages are simulated with the help of developed model and verified with historically recorded LECO data as shown in Figure 11,12 and 13.

4.3 Reliability data

Required basic reliability parameters for the system components and distribution lines obtained from 2015-2019 LECO outage report are depicted in Table 10 and Table 11 respectively.

Table 10 Reliability data for components

Fault type	Fault Type	Component No	Failures/yr.	Down Time /yr.	Failures/yr./unit	Down time/failure
Kalutara PS		1	73	43.90	73	0.6
Fullerton PS		1	43.4	14.23	43.4	0.33
Molligoda PS		1	74.6	32.24	74.6	0.43
AR	Faulty AR	23	2	7.29	0.0869	3.64
LBS	Faulty LBS	915	12	23.41	0.0131	1.95
LBC	Faulty LBC	586	4.20	2.85	0.0071	0.68
TF	Faulty TF	4387	18.4	21.53	0.0041	1.17
Arrestor	Burnt Arrester	13161	18.8	53.64	0.0014	2.85
DDLO		13161	21.2	16.08	0.0016	0.76

AR - Auto Recloser LBS - Load Break Switch LBC - Load Break Cutout TF - Transformer DDLO - Drop Down Lift Off

Table 11 Reliability data for distribution lines

Feeder name	Fault type	Length (km)	Failures/yr.	Failures/yr. /km	Mean Repair Time (hr.)	Mean Switch Time (hr.)
Fullerton to Hillside	RS	4.48	13.20	2.94	0.87	0.5
	NRS	-	78.59	-	0.42	-
Fullerton to Kalutara North	RS	12.54	21.4	1.70	0.79	0.5
	NRS	-	75.40	-	0.45	-
Kalutara North to Hotel	RS	6.295	11	1.74	0.40	0.2
	NRS	-	17.54	-	0.39	-
Kalutara North to Nagas junction	RS	4.72	24.60	5.21	0.54	0.3
	NRS	-	35.37	-	0.38	-
Kalutara North to Waskaduwa	RS	1.75	3.80	2.17	0.58	0.3
	NRS	-	10.60	-	0.45	-
Molligoda to Pothupitiya	RS	2.38	7.60	3.19	0.53	0.5
	NRS	-	24.40	-	0.48	-
Molligoda to Pirivena	RS	11.02	22.40	2.03	0.70	0.5
	NRS	-	45.26	-	0.41	-
Molligoda to Wadduwa	RS	7.77	12	1.54	0.75	0.5
	NRS	-	28.43	-	0.44	-

* RS = Repairable and switchable outages * NRS = Non-Repairable and Non switchable outage

Components concentrated to one section is considered as one component in MC simulation. As an example, Table 12 shows the components concentrated in a single section between two Load Break Switches BT359 and BT824. Section which can be isolated though LBS or LBC is identified as one single component for MC simulation.

Table 11 Components concentrated in a section for MC simulation

Components concentrated between Load break switches BT359-BT824					
	km or #of Unit	**Failures/yr./km or Failures/yr./unit**	**r repair time hours**	**λ failures/yr.**	**U Unavailability hours**
Line	3.23	2.94	0.87	9.50	8.27
LBS	2	0.0131	1.9508	0.0262	0.0511
DDLO	21	0.0016	0.7588	0.0338	0.0256
LBC	4	0.0071	0.6785	0.0286	0.0194
Arrestor	21	0.0014	2.8535	0.0299	0.0855
TF	7	0.0041	1.1701	0.0293	0.0343
			0.8795	9.6478	8.4859

4.3 Fault isolation and restoration procedure

1. After Identifying the faulty component, the fault section is isolated using $n \times r$ matrix to store failed nodes. (n: faulty components, r: nodes effected)

2. Thereafter, observe the switching matrix. Nodes which can be switched on to restore power are stored here. It requires $n \times s$ matrix to store switchable nodes. (n: faulty components s: nodes switchable)

3. After restoration of the fault as described in 1 & 2, normal operational matrix is restored.

4.4 Monti Carlo simulation procedure. [algorithm & flowchart]

Time sequential Monte Carlo simulation algorithm is used to develop the MATLAB program for the determination of distribution system reliability and is as follows:

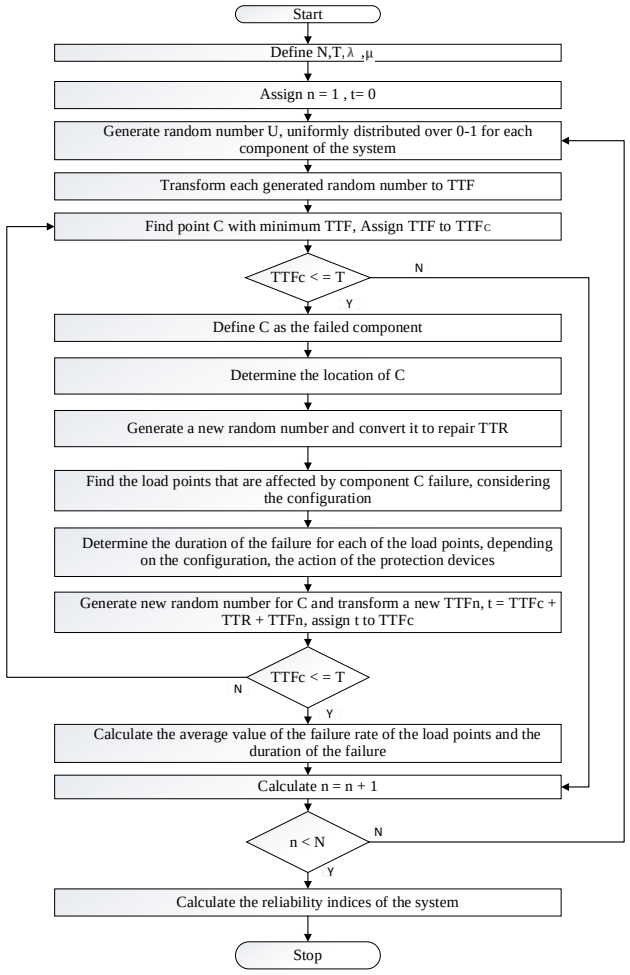

Fig. 10. Flow chart showing time sequential Monte Carlo simulation

Step 1: Define the system variables. Failure rate λ, repair rate μ of each component. Number of sample years (N), simulation period (T).
Step 2: Simulation starts, n = 1, t = 0.
Step 3: Generate random number [0-1] for each component of the network and compute TTF (time to failure) for each component.
Step 4: Find the component with minimum TTF and set it as TTFc
Step 5: Generate random number and convert it to TTR (Time to Repair) of failed component.
Step 6: Find the load points that are affected by the failure of this element considering the configuration and status of breakers, disconnects, fuses and alternate supply and record a failure for each of these load points.
Step 7: Find the switching time by considering affected components.
Step 8: Determine the failure duration depending upon the configuration and status of breakers, disconnects, fuses and alternate supply and record the outage duration for each failed load point.
Step 9: Generate a random number and convert it to TTFn. t = TTFn + TTFc + TTR.
Step 10: Go to Step 4 if the simulation time is < mission time. Else go to step 11.

Step 11: Calculate the average value of the load point failure rate and failure duration for the sample years

Step 12: Calculate the system indices for the sample years

Step 13: Return to Step 3 if the simulation time is less than the total simulation period. Otherwise, print the results

4.5 Verification of the results obtained from the model with historical data

Comparison of recorded SAIFI, SAIDI values for feeders by LECO and simulated results for the same in this research study are shown in Figure 11,12 and 13 respectively.

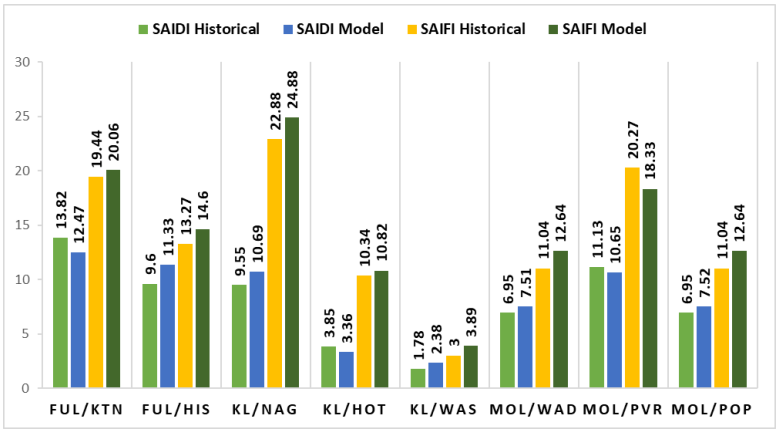

Fig. 11. Reliability Indices for the repairable and switchable outages

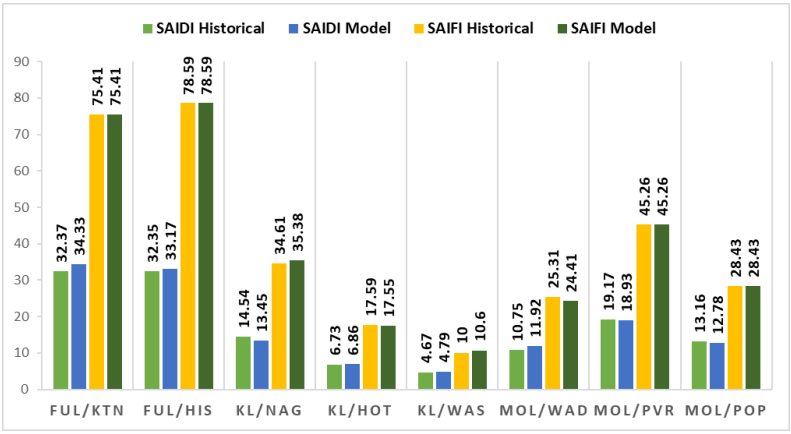

Fig. 12. Reliability Indices for the non-repairable and non-switchable outages

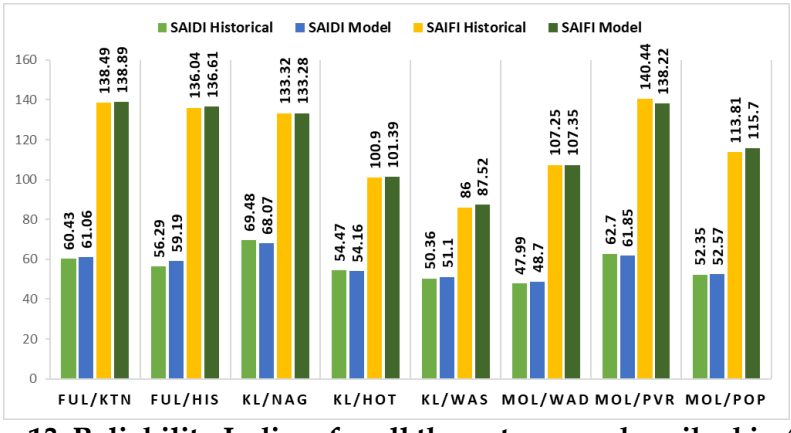

Fig. 13. Reliability Indices for all the outages as described in 4.2

4.6 Modified system reliability indices

Modification to the distribution system is done to achieve the maximum reliability indices by adding new LBSs, moving the existing LBSs to new position, adding new LBCs and reconfiguring the existing 11kV lines. Repairable and switchable outages are reduced through the modification done to the system. Figure 14 shows the repairable and switchable outage reliability indices before and after modifications done to the system.

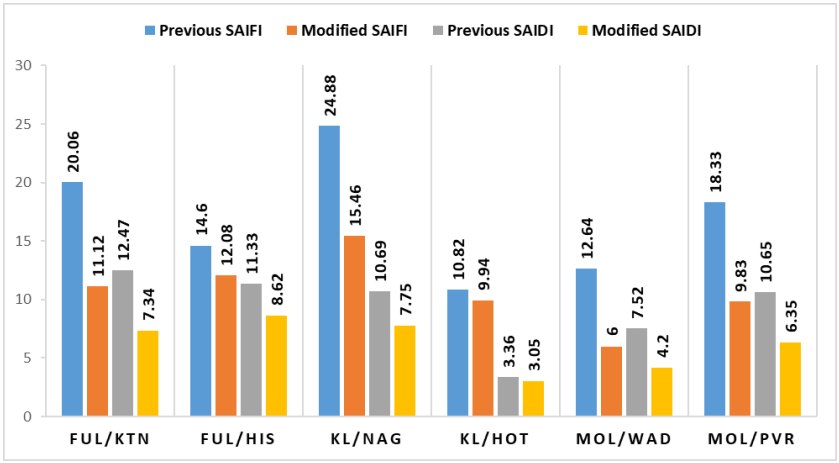

Fig. 14. Modified vs previous system reliability indices

4.7 Cost of energy not served and budget for modification

ENS (Energy Not Served) is calculated by using the mean value of node unavailability. Standard deviation of the data is checked further to verify the variation of taken mean value. Energy usage of single node cannot be found from the current system. So that whole feeder mean energy is taken for calculating ENS. Six-month average monthly energy demand is used for the calculation.

Total Energy Not Served = Mean unavailability of feeder × Mean energy demand of feeder. Cost of the energy is taken as 0.782USD/kWh which is already being used by LECO. 1USD = 202LKR rate is used for the calculations because LECO cost manual is published in first half of the 2022 year. Saved ENS and saved cost of ENS for modified system is tabulated under Table 13 and table 14 for budget of the purposed system. Simply the budget used for the modification of the system can be recovered within a 2.5-year period.

Table 12 Reduction of cost of energy not served by network modification

Primary	Feeder	Previous ENS (kWh)	Modified ENS (kWh)	Saved Cost of ENS (LKR)
Fullerton	HS	5496.03	5315.92	28450.17
	KTN	11696.13	7894.65	600481.78
	EUR_T	12799.98	1725.84	1749271.15
Molligoda	PVR	13567.71	8418.51	813367.63
	WAD	10229.86	6095.23	653106.15
	POP	1991.34	-	-
Kalutara North	NAG	13223.92	10090.59	494940.80
	HOT	6974.85	6427.80	86412.01
	WAS	961.91	-	-
Total Saved Cost of Energy Not Served				**4426029.69**

Table 13 Capital budget required for the modification

Primary	Feeder	LBS (New)	LBC (New)	LBS (Move)	AR (New)	Total Cost
Kalutara	NAG	1	-	-	-	1,749,833
	HOT	-	1	-	-	122,180
	WAS	-	-	-	-	-
Molligoda	PVR	-	-	2	-	273566
	WAD	-	-	-	1	2091770
Fullerton	HIS & Eur-Tec	-	2	1	1	5,728,219
	KTN	-	6	1	-	809863
Total Cost (LKR)						10,775,431

5 CONCLUSIONS

A reliable and quality electrical distribution network is one of the essential requirements to slacken the current economic crisis in Sri Lanka to a certain extent. This research, as a case study, found many technical drawbacks and limitations pertaining to the prevailing distribution network owned and operated by LECO in Kalutara area. Subsequently, by applying novel methods and technologies such as Monti Carlo simulation for network modification associated with OpenDSS and MATLAB load flow studies, considerable improvement to the said network is observed. The study revealed that the proposed network modification required only simple payback period of 2.5 years based on energy not served reliability improvement. It is also noted that in this research study, ANN method of demand forecasting produced better results compared to other statistical forecasting methods too.

6 ACKNOWLEDGEMENTS

The authors would like to offer their appreciation to Dr. Narendra De Silva (General Manager), Eng. Gayan Wijendrasiri (System Development Department), Eng. Ajith Amarasinghe (Branch Engineer), Eng. (Mrs.) Udeni Wijeratne (Construction Engineer) and Mr. Upul Kumara (Technical Officer) attached to LECO for the assistance given to carry out this research work.

REFERENCES

Buddhika De Silva,L Samaliarachchi, 2013. Peak Electricity Demand Prediction Model for Sri Lanka Power System. *Journal of the Institution of Engineers, Sri Lanka,* 46(04), pp. 53-60.

DC Hapuarachchi; KTMU Hemapala; AGBP Jayasekara, 2018. Long Term Annual Electricity Demand Forecasting in Sri Lanka by Artificial Neural Networks. Kota Kinabalu, Malaysia, *IEEE PES Asia-Pacific Power and Energy Engineering Conference (APPEEC).* Available at: https://doi.org/10.1109/appeec.2018.8566586

International Monetary Fund, 2021. *Sri Lanka and the IMF.* [Online]
Available at: https://www.imf.org/en/Countries/LKA
[Accessed 12 May 2021].

Juan A. Martinez-Velasco , Gerardo Guerra, 2016. Reliability Analysis of Distribution Systems with Photovoltaic Generation Using a Power Flow Simulator and a Parallel Monte Carlo Approach. *Energies,* 13 July, 9(7), pp. 537-558.

Lanka Electricity Company , 2019. *2019-2026 Medium Voltage Development Plan,* Colombo: Lanka Electricity Company PVT LTD Sri Lanka.

Ming Dong,L.S.Grumbach, 2020. A Hybrid Distribution Feeder Long-Term Load Forecasting Method Based on Sequence Prediction. *IEEE Transactions on Smart Grid ,* 11(1), pp. 470 - 482.

Supriya M D, Chandra Shekhar Reddy Atla, K R Mohan, T M Vasanth Kumara, 2014. Distribution System Reliability Evaluation using Time Sequential Monte Carlo Simulation. *ITSI Transactions on Electrical and Electronics Engineering,* 2(1), pp. 24-30.

Visanousanh Thepmahavong, Pirat Khunkitti, Chayada Surawanitkun, Apirat Siritaratiwat, and Rongrit Chatthaworn, 2019. Optimal Placement of Auto Reclosers for Distribution System Considering Reliability in Attapeu Province Laos PDR. *The Engineering Access,* 5(1), pp. 33-42.

Journal of Engineering and Technology
The Open University of Sri Lanka (JET-OUSL), Vol. 10, No.1, pp. [63-72], 2022

A Defect Detection System for Logos Print on Elastic Materials Using Image Processing Techniques

R.M.D.K Rathnayaka, D.S Wickramasinghe *

Department of Electrical and Computer Engineering, The Open University of Sri Lanka, Nawala, Nugeoda, Sri Lanka.

*Corresponding Author: email: dswic@ou.ac.lk, Tele: +94718568047

Abstract – *Quality control in the elastic manufacturing industry is crucial for ensuring the integrity of printed logos. However, current methods for evaluating the quality of these prints rely on manual assessment, which is time-consuming, costly, and prone to errors. In this study, we propose an automated image processing-based technique for quality control in elastic logo printing. Our approach uses morphological transformation and normalized correlation to extract features of the logo and identify defects. We demonstrate that our algorithm can inspect a logo in approximately 8 seconds, with an accuracy of 99% in software simulations and 97% in a real-time hardware prototype. This technique has the potential to significantly improve the efficiency and accuracy of quality control in elastic logo printing, while reducing the workload and stress on workers.*

Keywords*: Image processing, Morphological Transformation, Normalize correlation, Quality control systems*

1 INTRODUCTION

In the production line, automation is necessary to reduce human errors and improve customer satisfaction by providing non-defective products. Currently, plant managers rely on a round-robin system of workers to manually inspect defects on the printing line, which is costly, time-consuming, and prone to errors. This method can also lead to worker fatigue and missed defects. In elastic printing, accurate and timely detection of defects during the quality control process is critical for maintaining high standards and minimizing waste. This paper presents an automated defect detection system for improving the quality of logo prints in the manufacturing process and an automated defect identification and tagging system. This system is designed to seamlessly integrate with the current conveyor system and operate in sync with the conveyor timing. The current logo printing and quality control system is shown in Figure 1.

2 RELATED WORK

Several systems are currently used for fabric defect detection using image processing. These systems mainly focus on identifying defects in the raw material used in the textile industry. The fiber scan inspection system is related to elastic defect detection on elastic texture. Logo print on elastic is named as a value addition to the raw elastic, and research on defects in value addition of elastic is more vulnerable for the field of textile

manufacturing. Some systems currently used to identify defects in fabrics are explained subsequently.

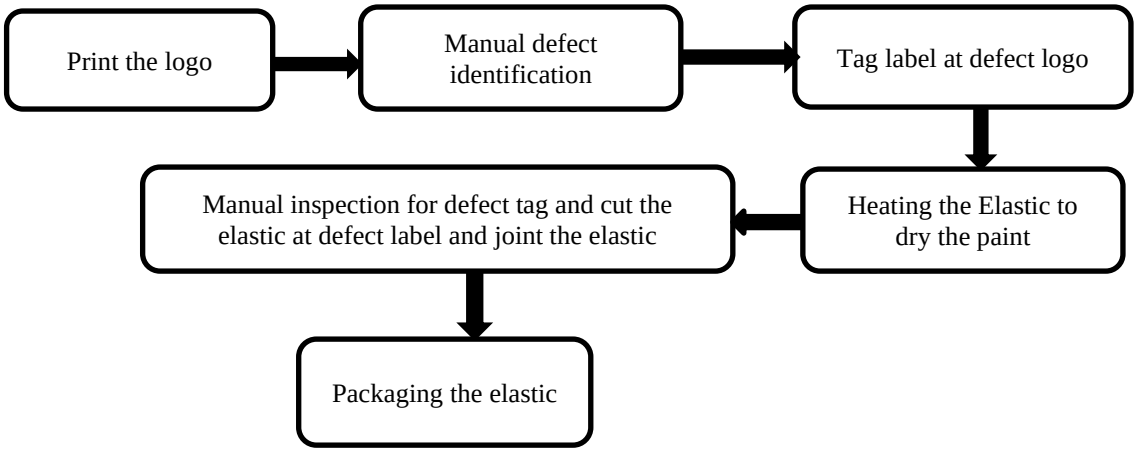

Fig. 1. Existing elastic printing and quality control system

2.1. On loom surface inspection systems for narrow fabrics

The patented system (SARI-SARRAF, 2001)algorithm is based on Wavelet transform, and the correlation is on the loom inspection system. This system inspects narrow fabric, such as woven loom state fabric, such as seat belts, lashing straps, tapes, and lifting and load securing belts. This system is used to capture defects of uniform textured fabrics. The automatic inspection system detects weft defects, warp defects, missed picks, and other deviations.

2.2. Wise Eye fabric defect detection system

This system is used to detect defects in fabric rolls. The CCD camera captures the total length of fabric by using a moving arm. Then analyze the image using the algorithm and find defects. This system can reduce 90% (Wong, 2019) of the loss and wastage in the fabric manufacturing process.

2.3. Fabre scan inspection system

This system applies to the elastic industry. It has the ability to inspect elastic texture at a speed of 280m/min (Anon., 2017). It also provides a tension mechanism to avoid fiber crease. However, that speed can be reached only for regular elastics. Usually, this defect detection system uses in elastic manufacturing process to avoid defective elastic coming to the logo print process.

3. PROBLEM STATEMENT

One major challenge in the elastic value-addition process is the difficulty of accurately detecting defects through manual inspection. This can be time-consuming and costly for manufacturers, who often need to re-inspect entire lots or even reject them due to low quality prints. In order to maintain the quality of their products and retain their export business, manufacturers must ensure early detection of defect prints and prevent the shipment of defective elastic.

Elastic print defect happened due to, Defect in the screen-printing template, Misalignment of blades, Conveyor belt timing issue, and Stretching of elastics.

Defects in elastic prints can occur due to issues such as defects in the screen-printing template, misalignment of blades, conveyor belt timing issues, and stretching of the elastic. Quality control and defect detection are performed after the screen-printing process, at which point workers manually tag any defects using a label tagging gun. However, this manual inspection process is prone to errors and does not allow for the identification and correction of repeated errors. Therefore, automation is necessary to improve the efficiency and accuracy of defect detection and minimize elastic waste.

4. METHODOLOGY

Fig. 2 illustrates the proposed system design for defect detection, which involves a series of operations on images captured by a camera. In the first stage, the image is cropped using a morphological transformation to remove the unwanted areas and isolate the letters. The image is then resized and denoised to improve its quality for comparison with a template. Finally, the test image is compared to a set of reference images using normalized correlation in OpenCV to identify defects.

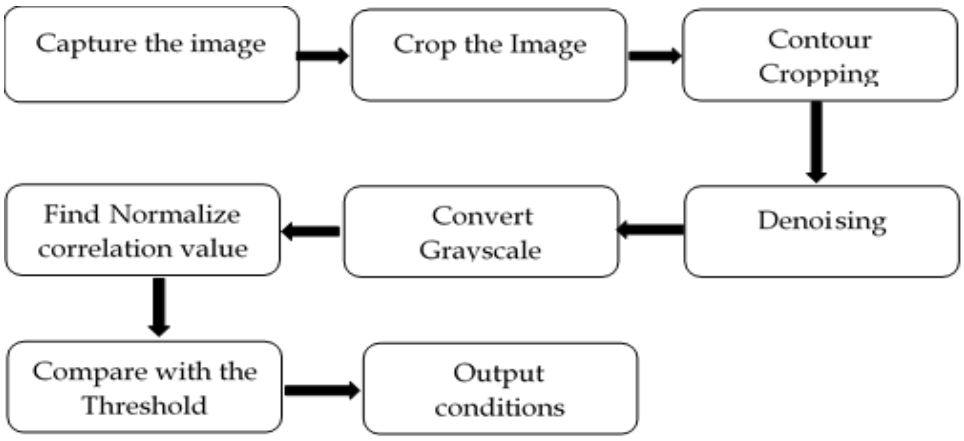

Fig. 2. Flow diagram of the proposed system

4.1 Block diagram of the system

The proposed system operates as follows: the conveyor belt feeds the elastic into a chamber where an image is captured by a camera and sent to a raspberry pi for processing. A rotary encoder provides feedback to the system, which uses a L298 motor driver to position the motor for image capture. If the system detects a defect in the logo, a relay driver activates and a solenoid operates to tag the defect. In cases of repeated errors, the conveyor stops automatically to prevent further waste.

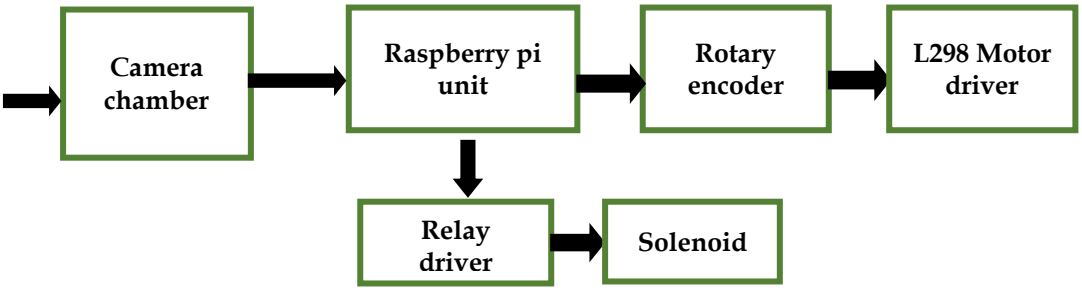

Fig. 3. Overview of the machine

4.2 Algorithms

4.2.1 Image Capturing and Preprocessing

Input – Captured image
Output- Contour cropped denoising image
Steps:

- Capture image
- Cropped image to the predefined size to remove unwanted data
- Crop along the contour of the letter using Morphological Transformation.
- Resized image to the predefined pixel value
- Denoising the image

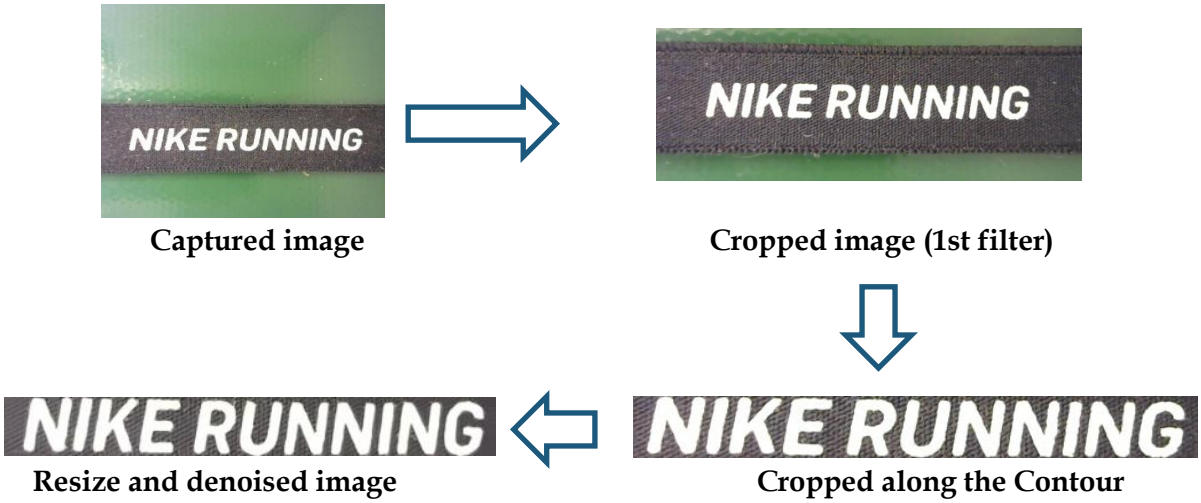

Captured image **Cropped image (1st filter)**

Resize and denoised image **Cropped along the Contour**

Fig. 4. Image Processing Steps

4.2.2 Normalized Correlation Matching

Input: denoised image
Output: matching coefficient
Steps:

- Convert image to grayscale
- Perform match operation using corresponding method (Normalize correlation)

These methods multiplicatively match the template against the image so that a perfect match will be prominent and deficient matches will be small.

$$R_{ccorr}(x,y) = \sum(x',y') \ [T(x',y').I(x+x',y+y')]^2 \quad (1)$$

To reduce the effect of lighting differences between the template and input image, the normalized correlation method (Feng Zhao, 2006), is shown below.

$$R_{ccorr\_norm}(x,y) \quad = \frac{R_{ccorr}(x,y)}{Z(x,y)} \qquad (2)$$

Where ,

R_{ccorr} - Correlation Result

T – Template

I - Image

Z- Zero mean normalized correlation

4.2.3 Histogram Matching

$$d(H1,H2) = \frac{\Sigma I\left(H1(I)-\bar{H}1\right)\left(H2(I)-\bar{H}2\right)}{\sqrt{\Sigma I\left(H1(I)-\bar{H}1\right)^2\left(H2(I)-\bar{H}2\right)^2}} \qquad (3)$$

Where, $\bar{H}k = \frac{1}{N}\sum_j Hk(J)$

Two histograms ($H1$ and $H2$)

N is the total number of histogram bins.

5 GUI IMPLEMENTATION

Tkinter, or "Tk interface," is a Python module that provides an interface to the Tk GUI toolkit, which was developed using TCL (Tool Command Language) and is supported on multiple platforms, including Linux, macOS, and Windows (Anon., 2021). Tkinter is used to implement a user-friendly graphical user interface (GUI) for the operator of the system. GUI design is shown in Fig.5.

6 RESULTS AND DISCUSSION

Each template captures a slight deviation of the image inside the camera chamber to normalize the template. The comparison result of good images with each template is shown is show in Fig.6 and Fig.7. Normalize correlation method used to find matching coefficient.

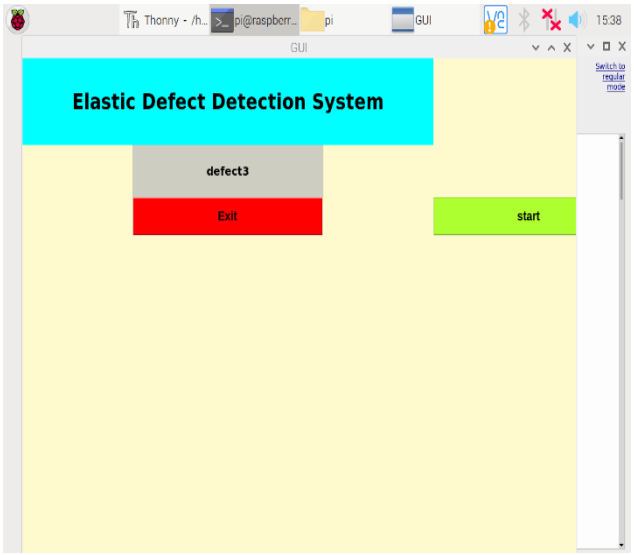

Fig. 5. GUI window

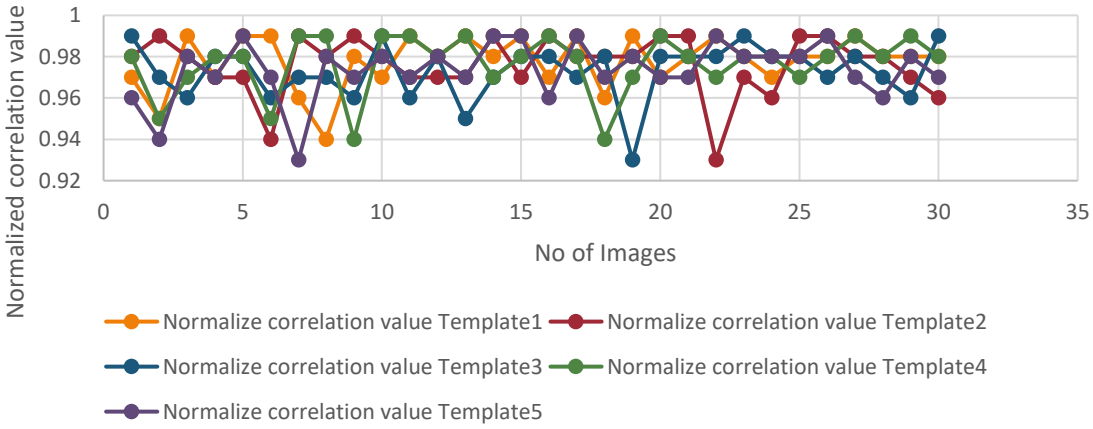

Fig. 6. Normalize the correlation value of the non-defect Logo with each template

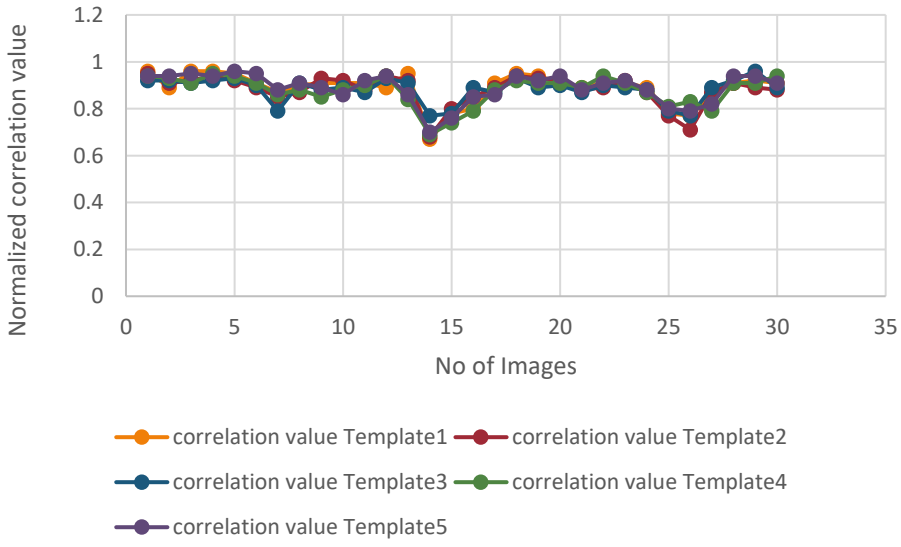

Fig. 7. Normalize the correlation value of the defect logo with each template

The same analysis is carried out with the histogram comparison method. Results are shown in Fig.8 and 9.

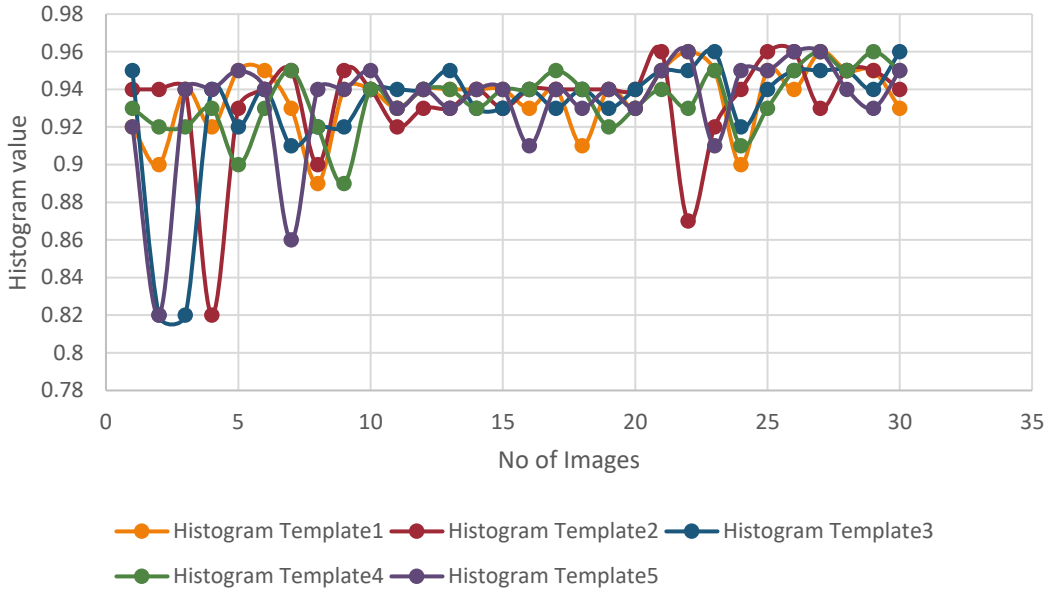

Fig. 8. Histogram comparison value of Non-defect logos with each template

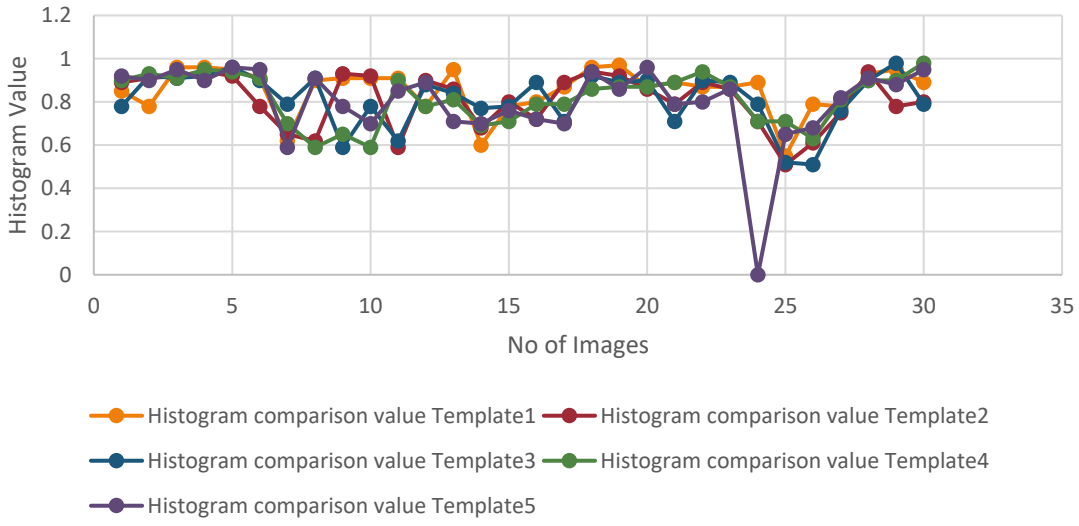

Fig. 9. Histogram comparison value of defect logos with each template

6.1 Mean value of each scenario

30 samples from non-defect and defect images were expereimented and mean value of different methods are shown in below Table 1.

Table 1- Mean value of results

Scenario	Mean value
Normalize correlation – Non-defect	0.9754
Normalize correlation – defect	0.88
Histogram comparison – Non-defect	0.93
Histogram comparison – defect	0.82

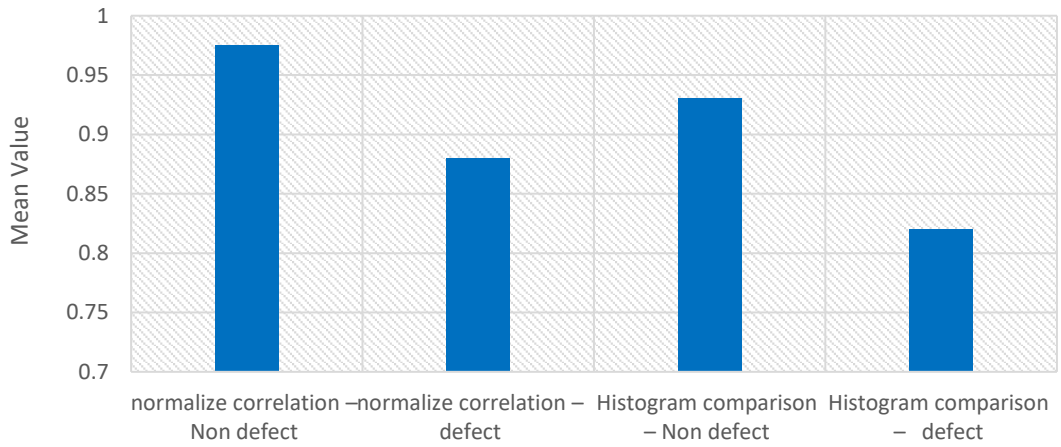

Fig. 10. Mean Value of the results

Our results indicate that normalized correlation is an effective method for detecting defects in elastic logo prints. Using this method, we obtained a matching value of 99% for non-defective images. We set a threshold of 0.98 for identifying good images, and any image below this threshold was considered defective. To confirm the accuracy of our system, we used five templates to check the matching coefficients. If all template values were below 0.98, the image was classified as defective.

This system can accurately detect defects in logos and prevent repeated errors, thanks to a feedback system that helps maintain the proper distance between logos. Normalized correlation is a particularly useful method for analyzing defects because it allows for easy thresholding to compensate for lighting differences between the template and input image. In addition, normalized correlation has minimal variation in values and is fast for comparison.

To improve the torque of the conveyor, we coupled a DC motor with a rotary encoder. A bearing was used to smooth the operation of the roller. One of the main challenges was accurately holding the elastic print in place within the chamber. We initially attempted to use the timing of the belt and physical restraints to hold the print in place, but this proved unreliable as any variations in torque could cause the image to shift by centimeters. To overcome this issue, we implemented a feedback system using a 20-step mini rotary encoder. For even greater accuracy, an industrial-type rotary encoder with micro steps could be used. To further reduce image shifting, we captured five templates with small shifts within the chamber to obtain the normalized result.

7 . CONCLUSION

This study presents an image processing technique and its application for automating inspection and defect detection in the elastic value-addition industry. While various research and automated machines have been developed to identify defects in fabrics and elastics, image processing techniques offer an effective means of automating human inspection in the industry. Our proposed algorithm for detecting defects in logo prints on elastics, tagging defects, and preventing repeated errors has the potential to replace manual inspection in the elastic defect detection process of the production line with suitable industry-level equipment. By implementing this automatic inspection system, we aim to reduce elastic waste and improve the accuracy of printed logos.

In the prototype, we used a roller shutter camera and a conveyor belt to capture images, which introduced a speed limitation. To overcome this limitation, we recommend using a global shutter camera that can capture images on the go. Additionally, the prototype needs to be redesigned and developed according to industry standards. The mechanical structure and label tagging system should be upgraded to meet industrial standards. When deployed in a real-world environment, the system should include an industrial-standard defect tag attachment system.

8. ACKNOWLEDGEMENT

The authors would like to express their gratitude to Mr. Amila Nuwan Amarasinghe, Plant Manager of the Value Addition section at Strechline Pvt Ltd, for providing insights into the real issues and automation needs at the plant.

REFERENCES

Anon., 2013. [Online] Available at: https://opencv-python-tutroals.readthedocs.io/en/latest/py_tutorials/py_imgproc/py_morphological_ops/py_morphological_ops.html.

Anon., 2017. *Fiber Scan.* [Online] Available at: http://www.fibrescan.co.uk
Anon., 2021. *Python interface to Tcl/Tk.* [Online]

Feng Zhao, Q. H. W. G., 2006. IMAGE MATCHING BY NORMALIZED CROSS-CORRELATION. *Acoustics, Speech, and Signal Processing*.

Lutz, M., 2011. *Learning Python.* united state of amaeria: O'Reilly media.

Sanjay Gosh, M. K. W. K. K. S., 2017. *RELAY INTERFACE MODULE FOR A.* Eroupe, Patent No. 9740 429 B2.

SARI-SARRAF, J. G. W. W. H., 2001. *VISION-BASED, ON-LOOM FABRIC INSPECTION SYSTEM.* US, Patent No. 0012381.

Shih-Jeh Wu, P.-C. C. H. L., 2019. Measurement of Elastic Properties of Brittle Materials. *Applied Science*.

SZIGETI, E., 2016. *DIGITAL IMAGE CORRELATION SYSTEM.* USA, Patent No. 0154926 A1.
Wong, P. C., 2019. *Wise eye fabric defect detection,* Hong Kong: PolyU's Communications and Public Affairs Office.

Journal of Engineering and Technology
The Open University of Sri Lanka (JET-OUSL), Vol. 10, No.1, pp. [73-87], 2022

Economic Effects of Saltwater Intrusion for the People at Service Area of Kethhena Intake in Kalu Ganga Lower Basin

D. I. W. Kodithuwakku[1], K. D. N. Kumari[2], C. P. S. Pathirana[2*], and B. C. L. Athapattu[3]

[1] Central Environmental Authority, District Office, Kalutara, Sri Lanka.

[2]Department of Mathematics and Philosophy of Engineering, The Open University of Sri Lanka, Nawala, Nugegoda, Sri Lanka.

[3] Department of Civil Engineering, The Open University of Sri Lanka, Nawala, Nugegoda Sri Lanka.

*Corresponding Author: email: cppat@ou.ac.lk, Tele: +94740137783

Abstract – *Saltwater intrusion can be described as the movement of saline water into freshwater aquifers, which leads to contamination of drinking water sources and other consequences. In the past decades' saltwater intrusion in the Kalu Ganga has increased considerably due to natural disasters and human activities which has become a significant issue in the Kalutara area. This study mainly focused on identifying the social and economic impact faced by the people residing in the Kalutara area where pipe borne water supply by Kethhena water intake due to saltwater intrusion. Furthermore, the economic impact faced by the National Water Supply and Drainage Board (NWS & DB) and sand ferry owners were also focused.*

Preliminary data were collected using a questionnaire which was presented to NW & DB water consumers in Kalutara, Beruwala and Dodangoda Divisional Secretariat Divisions (DSD), where water supply by the Kethhena Water Treatment Plant. A simple random sampling method was used for data collection. To assess the economic impact on sand miners, information was collected from the sand miners and sand ferry is owners in Kalutara, Millaniya and Dodangoda DSDs where the sand ferry located below the Kethhena water intake. GIS mapping was done with GPS Coordination of the data collection area. Data analysis was done using SPSS; 22 and MS Excel. Almost all the people in the area have issues while drinking, cooking, bathing, and washing activities due to saltwater intrusion. Hence, society has to bear the cost of obtaining water. Distributions of fresh water via water bowsers during the saltwater intrusion period incur an additional cost on NWS & DB. Restricting sand mining duration becomes an economic loss to sand miners and the government.

It is revealed that the saltwater intrusion of the Kalu Ganga has a social and economic impact on the society, as well as an economic impact on the government. To minimize these issues, it is recommended that rehabilitate the eroded sand bars at the river mouth, the construction of a salinity barrier and moving water pumping points up in the river about a few kilometers, can be presented. In addition, improvement of water cleaning techniques, control of groundwater extraction and minimizing over pumping by industries, and conducting social awareness programs on the importance of minimizing water wastage, the effect of over pumping and lack of availability freshwater and also about the importance of rainwater harvesting can be suggested.

Keywords*: Kalu Ganga lower basin, Kethhena intake, Saltwater intrusion, Sand mining, Socio-economic effect*

1 INTRODUCTION

Kalutara District is situated in the Western Province and is bounded by Colombo District in the North, Ratnapura District in the East, Galle District in the South and the Ocean in the West. There are three major rivers in the district as the Kalu Ganga, Bolgoda Ganga and Bentara Ganga. The Kalu Ganga is the main source of potable and industrial water to the Colombo south area and coastal belt of Kalutara District from Wadduwa to Aluthgama. There are two water intakes located at Kethhena and Kandana, operated under National Water Supply and Drainage Board (NWS & DB). The service area of the Kethhena scheme includes the western coastal belt stretching over a distance of about 43 km along the Galle Road in the distribution zones Kalutara, Wadduwa, Payagala, Maggona, Beruwala, Darga Town and Aluthgama and hilly areas situated in Mathugama. The other intake and treatment plant is located upstream to the Kethhena intake in Kandana, Horana close to Naragala Bridge which is sufficiently elevated to prevent Saltwater intrusion (SWI).

The Kethhena water intake is located at Kalu Ganga around 17.4 km up stream of the river's outfall. At the present the water extracted from Kethhena water intake fulfill the water need of over 250,000 people using 73,000 water connections and proposals have been made to expand to serve 540,000 people under 130,000 water connections in 2025 in Kalutara District. SWI to Kethhena water intake has become a major problem for NWS & DB. During the dry weather conditions in several months, intake is badly affected by SWI which creates severe operational problem to water supply schemes.

SWI can be described as the movement of saline water into freshwater aquifers, which leads to the contamination of drinking water sources and other consequences. The higher pressure and density of saltwater causes it to move into coastal aquifers in a wedge shape, which protrudes a long way up the estuary below the layer of fresh water. In the absence of any tidal fluctuations this wedge would remain stationary, and it has been shown that the main parameters that determine the length and thickness of the saline wedge are the density difference, the rate of fresh water outflow and the depth of flow in the river. In the presence of a tide, however small, the wedge would no longer be stationary. Instead it would be pushed up and down the estuary by the ebb and flood flow (Nanseer, 2016).

Certain human activities, especially sand mining have increased SWI in many coastal areas and these conditions intensified due to drought. Water extraction points the level of fresh groundwater, reducing its water pressure and allowing saltwater to flow further inland. At the coastal margin, fresh groundwater flowing from inland areas meets with saline groundwater from the ocean. The fresh groundwater flows from inland areas towards the coast where elevation and groundwater levels are lower. Saltwater has a higher content of dissolved salts and minerals. It is denser than fresh water, causing higher hydraulic head than freshwater. Hydraulic head refers to the liquid pressure exerted by a water column and a water column with a higher hydraulic head will move into a water column with a lower hydraulic head, if the columns are connected. Other contributors to SWI include navigation channels or agricultural and drainage channels which provide conduits for saltwater to move inland and sea level rise. SWI can also be worsened by extreme events like hurricane storm surges. SWI has become an ever increasing problem throughout the world. In the Sri Lankan context, mainly western coastal communities are facing several problems due to salinity intrusion such as contamination of water supply and this problem has been recorded during the last few decades. Kelani Ganga; due to salt water intrusion the Ambatale water intakes has been threatened several times by the past (Nanseer, 2016). Benthara Ganga also have been threatened several times in saltwater intrusion. As well as Gin Ganga and Walawe Ganga also has saltwater intrusion in the Southern Province (Ranjan, 2007).

In the past decades SWI in the Kalu Ganga has increased considerably due to natural disasters and human activities which has become a significant issue in the Kalutara area. SWI will affect the lives in the Kalutara area which will result the economical disaster for the people in the Kalutara area. This study mainly focused on to identify economic impact faced by the people residing in the Kalutara area where pipe borne water supply by Kethhena water intake due to saltwater intrusion.

1. METHODOLOGY

2.1. Location

This study was aimed to collect information from the DSDs which NWS & DB distributed water from the Kethhena water intake. There are several overhead water tanks in Kalutara, Beruwala, Aluthgama, Payagala, Wadduwa and Bombuwala areas for *supplying* domestic and industrial uses. These tanks are situated in Kalutara, Beruwala and Dodangoda DSDs and are fed by the Kethhena water treatment plant. The Survey was conducted in those DSDs.

2.2 Sampling Method

A simple random sampling method was used for data collection where DSDs received water from the Kethhena water intake. The sample size was two hundred & fifty-one (251) from the total population at Kalutara, Beruwala and Dodangoda DS divisions. The data collected sample percentage is proportionally equal to *the percentage* of public water supply by NWS & DB through DSDs.

2.3 Data Collection

Preliminary data were collected using a questionnaire which was presented to NWS & DB water consumers in Kalutara, Beruwala and Dodangoda DSDs, where water supply by the Kethhena Water Treatment Plant.

The data were collected through a questionnaire in five main areas: demographic detail, water consumption, saltwater intrusion, salinity problems and economic impact. This was used to demographic data, the water requirement of household level and industry level, a problem arises for the consumer at the period of SWI, consumer's satisfaction of the quality of water obtained from the pipeline during the SWI, issues related to sources of obtaining water for drinking and other activities, and also to identify the economic effect of the SWI. This questionnaire was also used to identify whether the existence of technology for purifying salt water, which supplies through the pipeline during the SWI, at the household level or industrial level.

2.4 Data Analysis

Data analysis was done using SPSS 22 and MS Excel. Presentation of the data includes a pictorial representation of the data by using graphs and charts, which help in adding the visual aspect to data which makes it much more comfortable and easier to understand. The Pearson Chi Square test is used to see the relationship among the variables.

2. RESULTS AND DISCUSSION

3.1 Primary Data Analysis

Primary data has been obtained from 30 GNDs lives within three DSDs of Kaluthara District, where the majority of the respondent (51%) are resident in Kalutara DSD. Beruwala DSD represents 44% and 5% of the sample represents Dodangoda DSD as shown in Fig. 1.

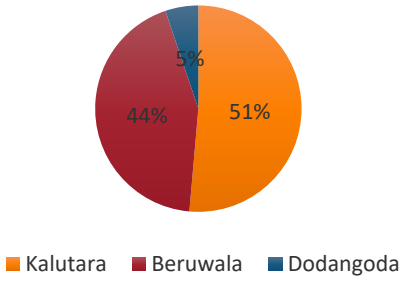

Fig.1: Data Collected Divisional Secretariat Divisions

This sample population and the number of water connections provided by NWS & DB in 2019 are proportionally related within the DSDs. The sample can be divided into two sectors as industrial and domestic households sectors. 90.4% of the respondents are fallen into the households sector. Kalutara and Beruwala DSDs are very popular in the tourism industry because of the coastal area. Hence the sample has included ten hotels and twenty of other different industrial activities and the industrial sector includes 9.6% of the respondents.

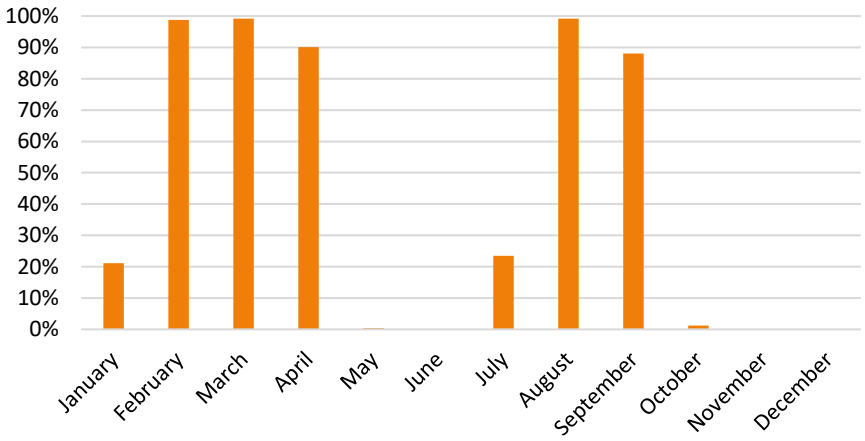

Fig.2: Data Collected Divisional Secretariat Divisions

The majority of the respondents have to face saltwater problem mainly in the months of February, March, April, August and September of the year 2021. Generally, the water flow of the Kalu Ganga is getting low in the months of January, February, March, April, July, August, November and December of the year also. In most of these months, Kalutara district experienced less precipitation during the dry season.

According to the primary data collected from the sample, generally resident and engaging in industrial activities in the area of Kethhena water supplying area use either pipe born water, bottled drinking water, well water and tube well water simultaneously for their drinking purposes as shown in Fig. 3.

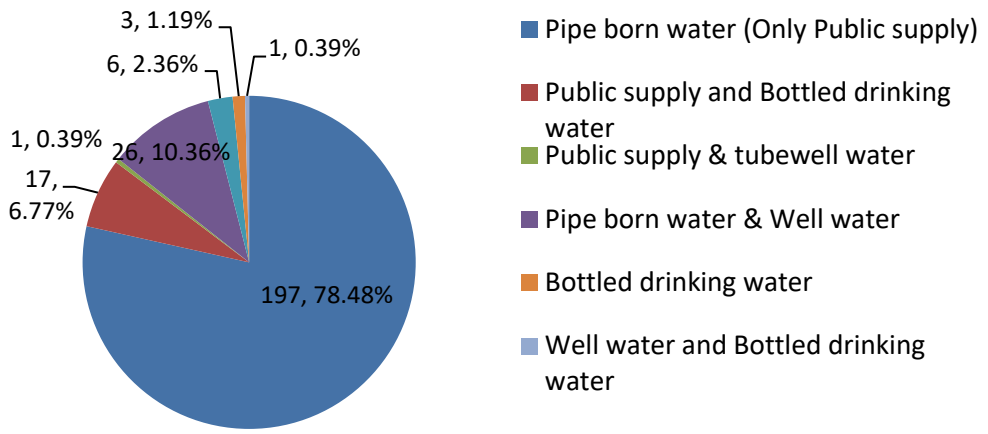

Fig. 3: Ways of Obtaining Drinking Water in Kalutara, Dodangoda and Beruwala DSDs

Therefore, it is revealed that 97% of the population have to face the SWI problem.

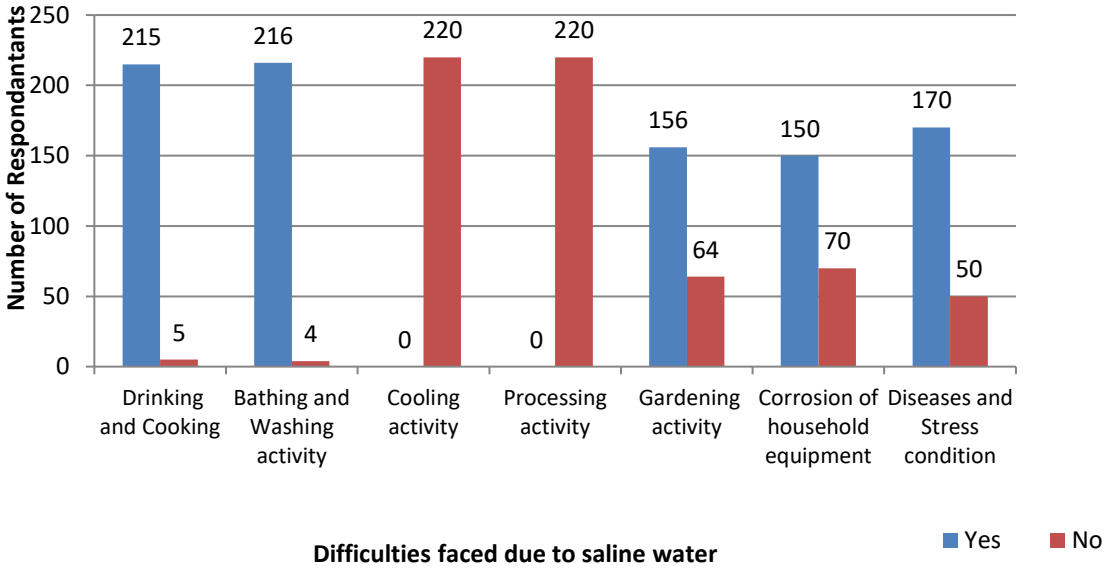

Fig. 4: Major difficulties faced by the domestic level due to saline water

When considering the water usage purposes of the sample population, most of the people use water for household chores such as cooking, bathing, washing and gardening activities other than drinking purposes. However, due to SWI, they have suffered with difficulties such as corrosion of household equipment, diseases and stress condition when they are involved in those activities as shown in Fig. 4. In addition to the above when considering the industrial sector they have to face difficulties in cooling activities and processing activities due to SWI problem.

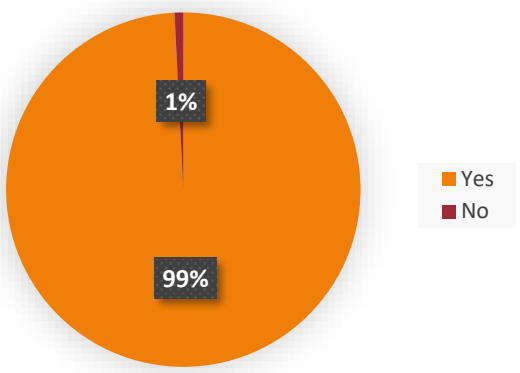

Fig. 5: Face the saltwater intrusion

On the other hand, 99% of respondantants in the area have issues while drinking, cooking, bathing, and washing activities due to SWI. Hence, society has to bear the cost for obtaining water due to dissatisfaction of water quality with the taste, odder, color and solubility of soap in the water at the time of SWI. The vast majority of the population used bottled drinking water or the water supplied by NWS & DB, through tanks placed in the vicinity to meet drinking water requirements at the time of SWI. In percentage term it is 35% and 39% respectively as shown in Fig. 6. Others obtain their drinking water through wells, which are sourced from wells in the surrounding area or far away at the time of SWI.

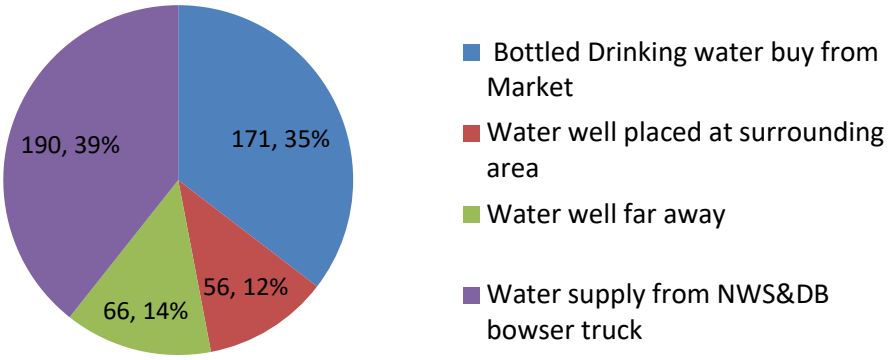

Fig. 6: The way of obtaining drinking water, during saline water supply in Household Level

According to data obtained, fifty percent (50%) of household level respondents use saline water provided by the public supply for activities other than drinking during SWI. Other fifty percent (50%) use water sources placed in the surrounding area or far away collectively at the time of SWI shown as Fig.7.

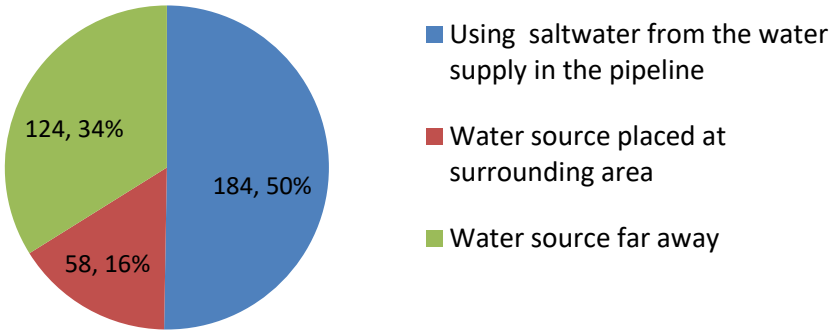

Fig. 7: The way of obtaining water for bathing and washing, during saline water supply in Household Level

At the industrial level, they also have to face the same problems. Instead of household activities, industries have to face problems when carrying out their cooling and processing activities. The majority of the industry (50%) fulfilled their drinking water requirement during the period of SWI by purchasing bottled water from the market. Others use other means to obtain drinking water during the period of SWI. About two percent of the sample indicated that their water requirement was fulfilled by buying an extra water bowser.

When considering about health issues arised during the SWI period, the majority of the people stated that, they did not face any physical health issues. But about 8.76% of the participants responded that they had to face physical illness such as skin rashes, waxy hair etc. as shown in Fig. 8. Although SWI does not affect people's physical health enough to seek medical attention as shown in Fig. 9.

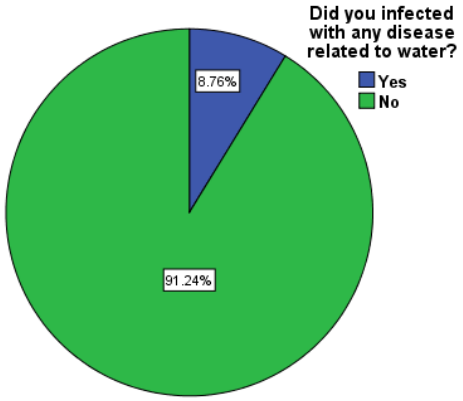

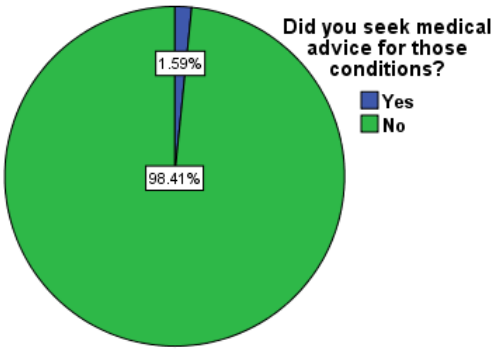

Fig. 8: Health effects due to saline water usage by people

Fig. 9: Seeking medical advice for the health problem

When considering stress development due to SWI, almost all the categories in the population have to face stress conditions as shown in Fig. 10. According to the data collected, the majority of the population is depressed due to SWI, but only 0.4% of them receive medical treatment for stress as shown in Fig. 11.

Considering society, one can conclude that housewives who engage in everyday household chores suffer from salt water problems. Because they are the persons who have to use salt water in activities such as cooking/ food processing, washing clothes ect., However, all individuals in the sample population face stress as they attempt to overcome this SWI problem. Therefore, it shows that SWI causes people to become depressed and have health problems.

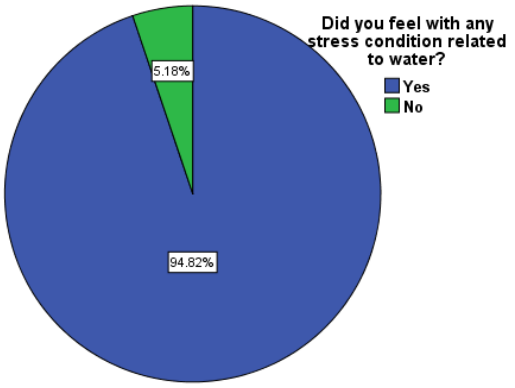

Fig. 10: Experiencing stressful condition

Fig. 11 : Seeking medical advice for stress

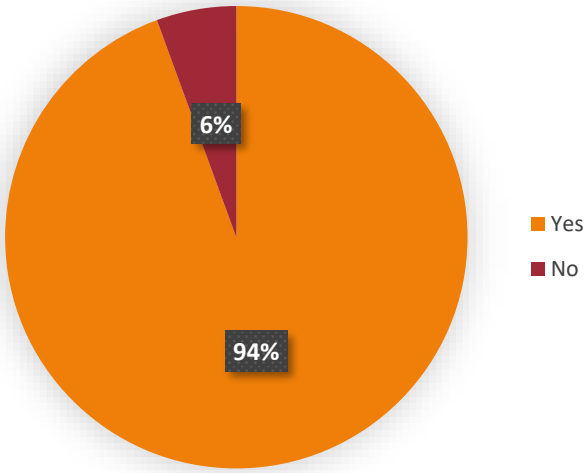

Fig. 12 : SWI cause to increase in monthly expenditure

The majority of the respondents in the household sector (94%) have to increase monthly expenditure due to SWI. From that 82 respondents have to increase their monthly expenditure by the range of Rs.5,000.00-10,000.00 as shown in Fig. 13.

According to the analyzed sample, all the industries (100%) have to face increase in monthly expenditure. The majority of them have to expend additional more than Rs.25,000.00 monthly due to SWI problem as shown in Fig. 14.

The sample has indicated in various reasons for incurring extra expenditure due to SWI such as buying bottled drinking water from the market, using vehicles to collect water, and repairing corrosion equipment which has shown in Fig. 15. Further it indicates that buying extra water bowser and pumping water from another water source will not affect the incurring of extra expenditure due to SWI.

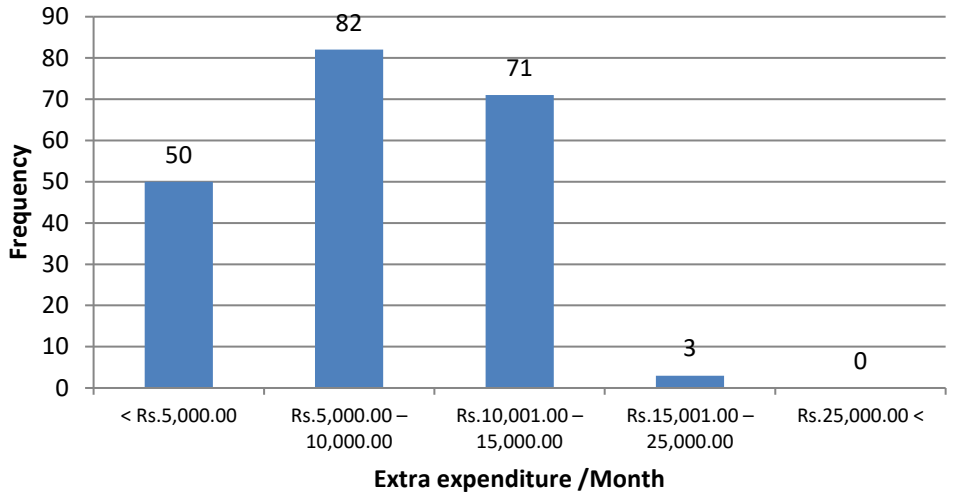

Fig. 13: Extra expenditure incurred per month due to SWI – Domestic Level

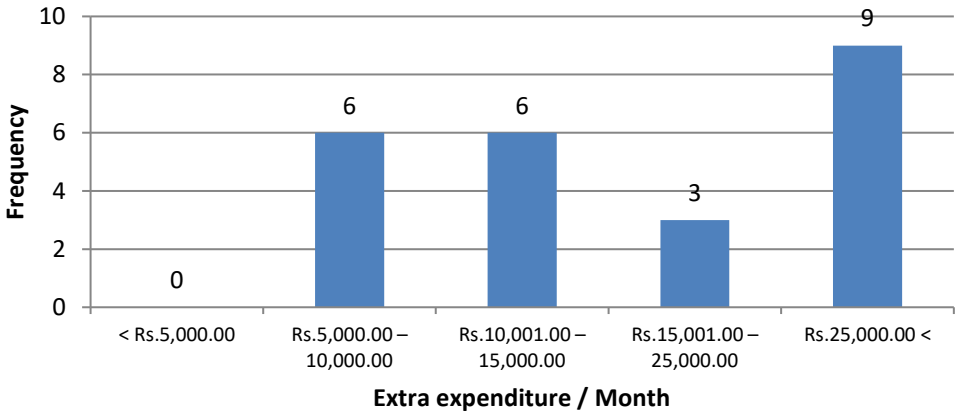

Fig. 14: Extra expenditure incurred per month due to SWI – Industrial Level

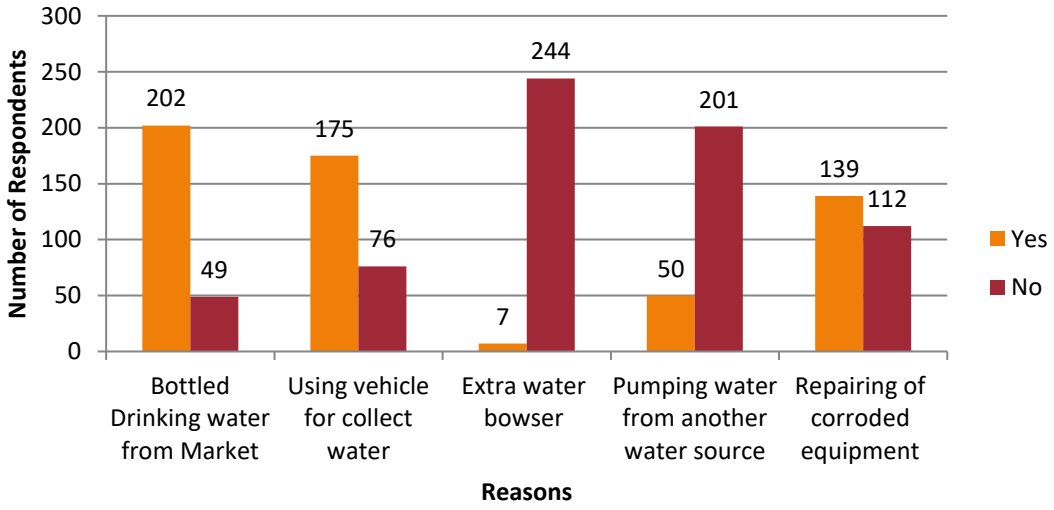

Fig. 15: Reasons for incurring extra expenditure due to saltwater intrusion

3.2 Factors affecting to increase in monthly expenditure due to SWI

In the preliminary analysis, it had observed that several social and economic aspects that the people in the service area of Kethhena intake in Kalu Ganga lower basin face due to SWI. However, it is essentials to see the factors affecting to increase in monthly expenditure due to SWI. Although, Fig. 15 explore the basic reasons for incurring extra expenditure due to SWI, there may be other factors that will increase the monthly expenditure due to SWI.

Pearson Chi-Square Tests

		Cause to increase in monthly expenditure
Member of Family	Chi-square	12.592
	df	4
	Sig.	.013*
Monthly Income Range	Chi-square	42.865
	df	4
	Sig.	.000*

*. The Chi-square statistic is significant at the .05 level.

According to the Pearson Chi- Square tests, the number of members in a family will affect the decision of whether there is an increase in monthly expenditure. Further, the monthly income range also affects the decision on increasement of the monthly expenditure.

Pearson Chi-Square Tests

		Cause to increase in monthly expenditure
the dissatisfied water qualities	Chi-square	66.557
	df	4
	Sig.	.000*

*. The Chi-square statistic is significant at the .05 level.

At the 5% significant level by using the Pearson Chi- square test, it can be observed that the qualities of the water such as Taste, Hardness / Dissolving of soap, Odor or colour that the people were dissatisfies with, at the time of salt water intrusion, will affect the decision whether there is an increase in monthly expenditure due to the SWI.

Pearson Chi-Square Tests

		Cause to increase in monthly expenditure
the difficulties of Drinking and Cooking	Chi-square	11.478
	df	1
	Sig.	.001*
the difficulties of Bathing and Washing activity	Chi-square	11.478
	df	1
	Sig.	.001*
the difficulties of Cooling activity	Chi-square	.240
	df	1
	Sig.	.624
the difficulties of Gardening activity	Chi-square	2.627
	df	1
	Sig.	.105b
the difficulties of Processing activity	Chi-square	.876
	df	1
	Sig.	.349
the difficulties of Gardening activity	Chi-square	2.627
	df	1
	Sig.	.105
the difficulties of Corrosion of household equipment	Chi-square	22.601
	df	1
	Sig.	.000*
the difficulties of Diseases and Stress condition	Chi-square	43.323
	df	1
	Sig.	.000*

*. The Chi-square statistic is significant at the .05 level.

Under the major difficulties faced due to saline water, the difficulties of drinking and cooking, the difficulties of bathing and washing activities, the difficulties of corrosion of household equipment and the difficulties of diseases and stress conditions only will affect the decision of whether the monthly expenditure will increase due to SWI.

In preliminary data analysis it is observed that the reasons for incurring extra expenditure due to SWI are buying bottled drinking water from the market, using vehicles to collect water and repairing of corrosion equipment. With a 5% significant level the Pearson Chi Square test will confirm that the monthly expenditure will increase for buying bottled drinking water from the market, using vehicles to collect water and repairing corrosion equipment.

Pearson Chi-Square Tests

		Cause to increase in monthly expenditure
Extra expenditure for -To buy Bottled Drinking water from Market	Chi-square	61.124
	df	1
	Sig.	.000*
Extra expenditure for - Using vehicles to collect water	Chi-square	34.141
	df	1
	Sig.	.000*
Extra expenditure for - To buy extra water bowser	Chi-square	.425
	df	1
	Sig.	.514
Extra expenditure for - To pump water from another water source	Chi-square	3.688
	df	1
	Sig.	.055
Extra expenditure for - To repair of corrosion equipment	Chi-square	18.401
	df	1
	Sig.	.000*

*. The Chi-square statistic is significant at the .05 level

Pearson Chi-Square Tests

		Cause to increase in monthly expenditure
Buying Bottled Drinking Water from the market,(liters per week)	Chi-square	64.356
	df	5
	Sig.	.000*
Buy extra water bowser for drinking purposes	Chi-square	.425
	df	1
	Sig.	.514
Frequency of filling the nearest water tank per week	Chi-square	15.149
	df	3
	Sig.	.002*,b,c
The distance to the nearest NWS&DB water tank	Chi-square	18.840
	df	4
	Sig.	.001*

*. The Chi-square statistic is significant at the .05 level.

At 05% significant level, it can be said that the buying bottled drinking water from the market, frequency of filling the nearest water tank per week and distance to the nearest NWS&DB water tank will affect the decision on whether there is an increase in monthly expenditure due to SWI or not.

3. CONCLUSION

This study mainly focused to identify economic effects, faced by the people residing in the Kalutara area where the pipe borne water supply by Kethhena water intake due to SWI. People who are living in the area, where the water supply facilitate by the Kethhena water treatment plant have to face the problem of fulfilling their water requirements during the dry season. They also have to face physical and mental health issues due to SWI. Every level of society has to incur an extra expenditure due to SWI.

With the preliminary analysis, it was identified several social impacts on the people residing in the Kalutara area where the pipe borne water supply by Kethhena water intake due to SWI which will course in an extra expenditure for the people. With this study it can be concluded that the number of family members and the average monthly income level will affect the decision that whether there is an increase in monthly excentre due to SWI or not. Further, it was found that the quality aspects of the water will affect the decision of whether there is an increasement in monthly expenditure due to SWI or not. Most of the people in the Kalutara area where the pipe borne water supply by Kethhena water intake, worry about the difficulties of drinking and cooking, the difficulties of bathing and washing activities, the difficulties of corrosion of household equipment and the difficulties of diseases and stress condition due to SWI. Further, it can be confirmed that the monthly expenditure will increase for buying bottled drinking water from the market, using vehicles to collect water and repairing of corrosion equipment.

Finally, it can conclude that the results of the study clearly indicate that the saltwater intrusion of the Kalu Ganga has an economic impact on society.

4. RECOMMENDATIONS

The following recommendations can be implemented to mitigate the social and economic problems arising from the results of this study due to saltwater entering the Kalu Ganga.

After 2017 due to the erosion of the sand reefs, sea out fall has got widened and river directly linked to the sea. Although Kethhena water intake situated about 17.5 km upstream of the Kalu Ganga from the sea outfall, due to the above reasons impact of the SWI has a significant on the Kethhena water intake. Because of that, it can be recommended to move the water pumping points up in the river. It also can be suggested that to rehabilitate eroded sand reefs, to minimize SWI.

Instead of rehabilitateing eroded sand bars at the river mouth, it can be also suggested to build up a brand new sand barrier at the mouth of the river to stop the tidal effect.

The problem can be solved by constructing a salinity barrier in the same manner as a salinity barrier was constructed to minimize the SWI impact of the Kelani River.

It also can be suggested to further minimize or halt the sand mining activity for the period of time, until the coastal sand line and river bed naturally generate to their optimal level.

Most of the catchment area of the Kalu Ganga was covered by cultivations like tea, and rubber but in the recent past rubber cultivation began to replace by introducing palm oil cultivation. It has been revealed that palm oil plants cause to increase depletion of groundwater levels. Hence it can recommend taking actions to discourage palm plantations.

Rainwater can be used to recharge the depleted ground water level. It can be done by constructing water bodies such as ponds and pumping rainwater in to the deep of the ground. Hence it is important to make aware of rainwater harvesting, among the people, especially people that are engaging in industries. And encourage them to harvest the rainwater and construct ponds, to recharge the ground water level.

As per the findings, most industries obtain water for their processing activity by pumping groundwater from wells or tube wells. So it is better to make them aware of the consequences that can arise due to the over pumping of groundwater and the importance of reducing water wastage.

Unauthorized low land, the filling can be also identified as a reason for the depletion of the ground water level which cause to increases in SWI. Because lowlands, wet or marshy land help to recharge the ground water level. So it can be recommended to strengthen the rules and regulations related to unauthorized land fill to discourage low land/wet land filling.

Implementing further research can be also recommended, in the areas such as the Biological effect on the flora and fauna species and fresh water bodies due to SWI in Kalu Ganga, the effect on soil fertility of agricultural area related to Kalu Ganga due to SWI etc,.

An Environmental Impact Assessment (EIA) is required when implementing recommendations such as the construction of salinity barriers, the buildup of sand barriers etc,. It is helpful to identify the environmental condition and implement the best suitable alternative. Awareness programs, relevant research articles, rules and regulations subject to the scope of the relevant government agencies are helping to implement other recommendations.

REFERENCES

Central Environmental Authority (1988). An Environmental Profile of the Kalutara District.

Central Environmental Authority (2014). An Environmental Profile of the Kalutara District.

Central Environmental Authority (2016). Preliminary Perception survey on water safety Kelani River Basin. UNICEF.

Central Environmental Authority (2018). Guideline for Determination of Environmental Flows (E-flows) for Development Projects that Result in Impounding of Water in Streams/Rivers.

Central Environmental Authority (2018). A Study to Identify Environmental and Social Issues of Oil Palm Cultivation in Sri Lanka; Observations and Recommendations; <http://www.cea.lk/web/images/news/2018/katupol/Oil_Palm_Report_28.05.2018_03-ilovepdf-compressed.pdf.>.

Davison, A., Howard, G., Stevens, M., Callan, P., Fewtrell, L., Deere, D. and Bartram, J. (2005). Water Safety Plan, World Health Organization, Geneva.

Department of Census & Statistics (2018). District Statistical Handbook – Kalutara District.

Lanka Hydraulic Institute Ltd. (2017).Environmental Impact Assessment Report (EIAR), Construction of salinity barrier at Kalu Ganga.

Nanseer, N. K. M. and Rajkumar, S. G. G. (2016). Kelani Ganga Conservation Barrage and result of Model studies. DOI: http://doi.org/10.4038/engineer.v39i2.7185., pp. 42–49.

National Water Supply & Drainage Board (2015). The Preparatory Survey on Water Sector

Development Project I(ii) in The Democratic Socialist Republic Of Sri Lanka Final Report.

National Water Supply & Drainage Board (2017). Annual Report, Ratmalana, Sri Lanka.

Panabokke, C. R. and Perera, A. P. G. R. L. (2005). Groundwater Resources of Sri Lanka, Water Resources Board. pp. 3-26.

Ranjan, S. P. (2007). Effect of Climate Change and Land Use Change on Saltwater Intrusion. Journal of Environmental Management 80(1), pp. 25-35.

Ranjan, S. P. (2007). Numerical Modeling of Salinity Intrusion: Case Study from Southern Coastal Aquifer in Sri Lanka.

Ratnayakage, S. M. S., Sasaki, J., Suzuki, T. et al. (2020). On the status and mechanisms of coastal erosion in Marawila Beach, Sri Lanka. Natural Hazards 103, pp. 1261-1289.

Samarasinghea, S. M. J. S., Nandalalb, H. K., Weliwitiyac, D. P., Fowzed, J. S. M., Hazarikad, M. K. and Samarakoon, L. (2010). Application of remote sensing and GIS for flood risk analysis: a case study at Kalu- Ganga river, Sri Lanka. Research journal of Applied Sciences, Engineering and Technology 6(10), pp. 1884-1894.

UNEP (2003).Groundwater and its susceptibility to degradation: A global assessment of the problem and options for management, pp: 46-93.

Wijesundara, K. and Piyadasa, R. U. K. (2013). Saline Water Intrusion along the River Benthera and its Impact on Irrigation Water. pp. 35-45.

Journal of Engineering and Technology of The Open University of Sri Lanka

Volume 10 No. 01 March 2022 ISSN 2279-2627

Desinged by CETMe-OUSL
Prnited by Press OUSL